Proposal of an efficient pyrolysis plant for conversion of microplastic waste to bio fuel

Sakthithasan,T. Limbu,S.Seyam,N.Parikh,R.

Supervisor: Dr. Hadis Zarrin

Ryerson University

Dear Dr. Zarrin,

Enclosed is a proposal of an efficient pyrolysis plant for conversion of microplastic waste and other biomass to biofuel. The objective of this project report is to analyze current recycling and microplastic removal options and design a process suitable for the City of Toronto that can be environmentally and economically beneficial for the local economy.

The scope of this report contains a technology review, process selection, equipment selection, equipment design & sizing, a developed process flow diagram, control system, preliminary process description, mass and energy calculations, environmental impact, risk assessment, and an economic evaluation. It is expected that a preliminary model of a fast pyrolysis plant that could be successfully be built to scale using this report as a conceptual guideline.

Thank-you for the support and guidance you provided to our group throughout the year.

Regards,

Thabina Sakthithasan, Sese Limbu, Nada Seyam, Rushi Parikh

Report Contribution Summary

All four members on this team have contributed equally to the completion of this report. The summary of contributions to this report are as follows:

Contributor	Percent Contributed	Signature
Thabina Sakthithasan	25%	T.S
Sese Limbu	25%	S.L
Nada Seyam	25%	N.S
Rushi Parikh	25%	R.P

Abstract

Environmental pollution and the utilization of fossil fuels has resulted in severe climate change and global warming over the last century. In order to combat these problems and undo some of the environmental damage, a race to find sustainable sources of energy has emerged. Biomass is one of the only renewable carbon containing energy sources capable of being converted into gas, liquid, and solid products. The biofuels derived from biomass are regarded as the only renewable fuels that can partially substitute fossil fuels. In this process, biomass will be created from the pyrolysis of waste collected from Ashbridge's Bay Wastewater Treatment Plant to produce bio-gasoline, bio-naphtha, bio-kerosene, and bio-gasoil through fractional distillation. Screenings will be taken from the preliminary treatment and microplastics will be removed from the effluent using highly efficient rotary disc filters. The process will be able to reduce about 1680 tonnes of waste sent to landfills every year through repurposing preliminary screenings and remove about 9950 kg of microplastics that would otherwise be polluting Lake Ontario every year. There are economic and environmental benefits to creating high-value products from cheap plastic waste. By making cheap plastic valuable, it can provide incentives to governments and organizations to clean up plastic pollution in the environment. This disposal of this solid waste removed during pre-treatment operations accounts for about $357,000/year in fees, and it also contributes a large amount of waste for the City of Toronto, leading to further environmental pollution. This report will discuss the market analysis, detailed equipment selection and design, and the economic real-world benefit of implementing such a process in the City of Toronto. The biofuels generated in this process can replace some of the commercial uses for heating oil, gasoline, and crude oil, generating sustainable energy and reducing environmental damage caused by microplastic pollution and landfill waste.

Contents

Abstract **4**
Abbreviations **11**
Nomenclature **13**
1. Introduction **14**
2. Market Analysis **16**
2.1 Why the City of Toronto 16
2.2 Why Wastewater Treatment Plants 16
3. Raw Material Overview **18**
4. Plant Location **19**
4. Process Description **21**
4.1 Stream Properties in Process Flow Diagram 23
5. Equipment Selection **26**
5.1 Rotary Disc Filters 26
5.2 Conveyor System 27
5.3 Bubbling Fluidized Bed Reactor 28
5.4 Distillation Column 30
5.5 Venturi Scrubber 31
5.5.1 Types of Scrubbers *31*
5.5.2 Selection of Scrubbing Liquid *32*
5.5.3 Venturi Scrubber Process *32*
5.5.4 Composition of Syngas *33*
5.6 Cyclone 34
5.7 Stripping Towers 35
5.8 Heat Exchangers 35
5.9 Compressors 36
5.10 Pumps 37
6. Mass & Energy Balances Summaries **38**
6.1 Approach 38
6.1.1 Mass Balance *38*
6.1.2 Energy Balance *39*
6.2 Mass and Energy Balance Assumptions 39
6.2.1 Disc Filters *39*
6.2.2 Bubbling Fluidized Bed reactor *40*
6.2.3 Distillation Column *41*
6.2.4 Stripping Towers *42*
6.2.5 Venturi Scrubber *42*
6.2.6 Heat Exchangers *42*
6.2.7 Condenser *43*
6.2.8 Summary Chart of Mass and Energy Balances *43*
7. Equipment Design and Sizing **46**
7.1 Rotary Disc Filter 46
7.2 Screw Conveyor 46
7.3 Design of Bubbling Fluidized Bed Reactor 47
7.3.1 Design of Reactor Vessel wall Thickness *49*
7.3.2 Design of Distributor Plate *49*

7.3.4 Superficial velocity (u_s) *50*
7.4.5 Bed Pressure Drop *51*
7.4.6 Diffusion and Mass Transfer Analysis *52*
7.3.7 Chemical Reaction *55*
7.4 Centrifugal Separator Cyclone 55
7.5 Distillation 59
7.5.1 Calculation of Column Trays *60*
7.5.2 Calculation of Column Dimensions *65*
7.6 Stripping Towers 67
7.7 Condenser 68
7.8 Venturi Scrubber 70
7.8.1 Aspen Plus Design *71*
7.9 Cyclone 74
7.9.1 Aspen Plus Simulation *75*
7.9.2 Small Scale Wastewater Treatment system *76*
7.10 Heat Exchanger Design 77
7.11 Pipes and Pumps 78
7.11.1 Piping System Design Codes *78*
7.12 Compressors 86
7.13 Storage Tanks 87
8. Process Control 89
8.1 Disc filter 91
8.2 Bubbling fluidized bed reactor 92
8.3 Cyclone 94
8.4 Distillation Column 95
8.5 Stripping Tower 98
8.6 Condenser 100
8.7 Heat exchangers 101
8.8 Venturi Scrubber 103
9. Safety, Loss Prevention & Environmental Impacts 104
9.1 General Considerations 104
9.2 Reactor Safety 106
9.3 Environmental Impact 106
9.4 Chemical Hazards 107
9.4.1 Methane *107*
9.4.2 Benzene *108*
9.4.3 Carbon Monoxide *109*
9.5 Emissions 111
9.10 Fire & Flammability Assessment 112
9.11 Toxic Dispersion Models 114
10. Risk Assessments 116
10.1 Hazard Assessment Study 117
10.2 Risk Assessment Analysis 121
10.3 Event Trees 121
10.3.1 Syngas Leakage *121*
10.3.2 Over Pressure in Distillation Column *123*
10.3.3 Safety System Failure *124*
10.4 Fault Trees 126
10.4.1 Fault Tree of Syngas Pipeline Leakage *127*
10.4.2 Fault Tree of Over Pressure in Distillation Column *128*

10.4.3 Fault Tree of Explosion *129*
11. Plant Layout **131**
12. Economic Evaluation **133**
12.1 Overview 133
12.2 Total Fixed Capital Costs 133
12.3 Production Cost and Cost Analysis 134
12.4 Cash Flow Analysis 136
13. Conclusions & Recommendations **138**
14. References **139**
15. Appendix **143**
15.1 Elementary Calculation Sample for Stream 25 143
15.1 Mass Balance for Stream *143*
15.1.2 Energy Balance Calculation for Stream *143*
15.2 Elementary Calculations for Fluidized Bed Reactor 144
15.2.1 Mass Balance Fluidized Bed Reactor *144*
15.2.2 Energy Balance Fluidized Bed Reactor *144*
15.3 Elementary Calculations for Distillation Column 144
15.3.1 Mass Balance for Distillation Column *144*
15.3.2 Energy Balance for Distillation Column *145*
15.4 Elementary Calculations for Stripping Towers 147
15.4.1 Mass Balance for Stripping Towers *147*
15.4.2 Energy Balance for Stripping Towers *147*
15.5 Elementary Calculations for Venturi Scrubber 148
15.5.1 Mass Balance for Venturi Scrubber *148*
15.5.2 Energy Balance for Venturi Scrubber *148*
15.6 Condenser Energy Calculations 149
15.7 Heat Exchanger Energy Calculations 149
15.8 Screw Conveyor Power Consumption Calculation 150
15.9 Piping and Pump Design Sample Calculation 150
15.10 Compressor Design Sample Calculation 152
15.11 Fluidized Bed Design Sample Calculations 155
7.3.2 Design of Distributor Plate *155*
7.3.4 Superficial velocity(u_s) *156*
7.4.6 Diffusion and Mass Transfer Analysis *158*
15.12 Distillation and Stripping Design Sample Calculations 160
15.13 Condenser Design Sample Calculations 169
15.14 Storage Tank Design Sample Calculation 176
15.15 Toxic Dispersion Sample Calculation 177
15.15 Risk Assessment Sample Probability Calculations 177
15.16 Economic Evaluation Sample Calculations 177
15.17 Quantification of Microplastics Calculation 178
Ashbridge Bay WWTP Mass Balance: *178*
15.8 True Boiling Point Graphs for Crude Oil 180

List of Figures

Figure 1 Categories of Waste Plastic (Ragert, 2017). 15
Figure 2 Dried Biowaste that is collected from Ashbridge's in December of 2020 17
Figure 3 Ashbridge Landform Project and Proposed Area of Construction (Ashbridges Bay Landform Project 2020) 20
Figure 4 PFD of Microplastic Waste into Fuel Pyrolysis Process 22
Figure 5 Back wash system (Huber, 2014) 26
Figure 6 Different Stages Occurring in the Fluidized Bed Process(Perry et al., 1997) 29
Figure 7 Venturi Scrubber Configuration (Cooper, 2011) 33
Figure 8 General parameters of Compressor Operating ranges (Towler et al.,2013) 37
Figure 9 Representation of Pump Type based on Flow Rate (Towler et al., 2013) 38
Figure 10 Quantity of Fuel Product Distilled based on Temperature (Nelson, 1968) 41
Figure 11 Entrainment of Cyclone 57
Figure 12 Cyclone Dimensions (Towler et al., 2013) 58
Figure 13 Proposed Plan with Dimensions Calculated Cyclone 59
Figure 14 Decomposition Method that enables the use of FUG Equations (Liu, 2002) 62
Figure 15 Comparisons made between Decomposition Method Calculations and HYSYS Modelling (Liu, 2002) 62
Figure 16 TBP Data that was used to Find Number of Trays (Liu, 2012) 63
Figure 17 Number of Actual Plates in the Distillation Column (Nelson, 1968) 64
Figure 18 Collection Efficiency as a Function of Particle Size and Pressure Drop in Venturi Scrubber (Cooper et al.. 2011) 73
Figure 19 Typical Diameter Cut in Relation to Pressure Drop (Cooper et al.. 2011) 73
Figure 20 Pipe Friction Versus Reynolds and Relative Roughness 82
Figure 21 P&ID of Process 90
Figure 22 P&ID of Disc Filters 91
Figure 23 P&ID of Fluidized Bed Reactor 92
Figure 24 P&ID of Cyclone 94
Figure 25 P&ID of Distillation Column 97
Figure 26 P&ID of Stripping Towers 99
Figure 27 P&ID of Condenser 100
Figure 28 P&ID of Heat Exchanger 102
Figure 29 P&ID of Venturi Scrubber 103
Figure 30 Common Acts and Regulations Plants must abide by (Crowl et al., 2002) 105
Figure 31 Failure Rate for Various Process Control Components (Towler et al., 2013) 106
Figure 32 Hazard Identification and Safety Information for Methane (ESPA,2020) 108
Figure 33 Hazard Identification and Safety Information for Benzene (ESPA,2020) 109
Figure 34 Toxicity Data (Towler et al., 2013) 110
Figure 35 General System of Priority for Plant Safety (Towler et al., 2013) 112
Figure 36 Flammability for Methane in Process 113
Figure 37 Event Tree 1 Syngas Leakage 122
Figure 38 Event Tree 2 for Overpressure in Distillation Column 124
Figure 39 Event Tree 3 for Process Control Failures 125
Figure 40 Fault Tree 1- Syngas Pipeline Leakage 128
Figure 41 Fault Tree 2- Overpressure in Distillation Column 129
Figure 42 Fault Tree 3 of Critical Case of an Explosion 130
Figure 43 2D Plant Layout 131
Figure 44 3-D Design of Plant Process 132
Figure 45 Calculated Profitability of Plant for 20 Year Span 137
Figure 46 Specific Heat of Different Crude Based on API and Temperature (Nelson, 1968) 145
Figure 47 Specific Heat Correction Factors of Hydrocarbon based on Specific Gravity (Nelson, 1968) 146
Figure 488 Pipe frction versus Reynolds number and relative roughness (Nelson, 1968) 151
Figure 49 Approximate Polytropic Efficiency (Towler et al., 2013) 153

Figure 50 Compressibility of Gases and Vapors (Towler et al., 2013) *154*
Figure 51 The K1 Values Based on Plate Spacing and Flv (Towler et al., 2013) *162*
Figure 52 Weir Length to Column Diameter Ratio Based on Area % (Towler et al., 2013) *164*
Figure 53 K2 Value for Weeping Based on Weir Length (Towler et al., 2013) *166*
Figure 54 Orifice Coefficient Based on Percent Perforated Area (Towler et al., 2013) *167*
Figure 55 Fractional Entrainment Based on Flv (Towler et al., 2013) *169*
Figure 56 Pitch Values Based on Number of Passes in Condenser *171*
Figure 57 Friction Factor Based Re Number and Baffle Cut for Condenser (Towler et al., 2013) *176*
Figure 57 TBP Data Obtained For Crude oil of API 43 (Treese et al., 2015) *180*
Figure 58 TBP Data For Crude Oil of 41.7 (Liu, 2012). *180*

List of Tables

Table 1 Summary of raw material physical and chemical properties (John Rumble, 2021) *18*
Table 2 Properties of each Stream *23*
Table 3 Comparison Between Belt and Screw Conveyor for Equipment Selection (Towler et al., 2013) *27*
Table 4 Summary of Advantages and Disadvantages of a Distillation Column (Taghipour, 2019) *31*
Table 5 Summary of Comparison between Scrubber Types (Cooper, 2011) *32*
Table 6 Summary of Composition Information in Syngas(Lee, 2019) *34*
Table 7 Summary of Advantages and Disadvantages of Cyclone (Cooper,2011) *34*
Table 8 Summary of Advantages and Disadvantages of Stripping Towers (Perry et al., 1997) *35*
Table 9 Summary of Heat Exchanger Comparisons *36*
Table 10 Comparison Summary of Different Compressors (Towler et al., 2013) *37*
Table 11 Kinematic Reaction (Ranzi, 2008) *40*
Table 12 Summary of Mass and Balance For Process *44*
Table 13 Assumptions Made for Disc Filters(IN-EnkO,2018) *46*
Table 14 Summary Table for Belt Conveyer *47*
Table 15 Summary of Parameter details for the Fluidized Bed Reactor (Towler et al., 2013). *48*
Table 16 Assumed Values and Properties Assumed for Reactor (Towler et al., 2013) *54*
Table 17 Calculated Values for Reactor Design *54*
Table 18 Chemical Composition of BioFeed (Ranzi,2008) *55*
Table 19 Stairmand's method to determine the scaling factor (Towler et al., 2013) *56*
Table 20 Summary of Cyclone Dimensions *58*
Table 21 Component mole fractions used in comparisons Crude Assay (Liu, 2012). *63*
Table 22 Summary Table of Assumptions and Design Calculations for the Distillation Column (Towler et al., 2013) *67*
Table 23 Summary Table of Assumptions and Calculated for Stripping Tower Design *68*
Table 24 Summary Table for Assumptions and Calculations for Design of Condenser *70*
Table 25 Summary of Design Results Obtained for Venturi Scrubber (Cooper et al. 2011) *74*
Table 26 Summary of Design Parameters for Cyclone *76*
Table 27 Calculated Heat Load Summary for Fuel Heat Exchangers *78*
Table 28 Summary of Results Obtained from HYSYS for Heat Exchangers *78*
Table 29 ASME B31.3 Relevant Standards for Fluids (Bhatia, 2016) *80*
Table 30 Equivalent Pipe Diameters for Fitting and Valves *82*
Table 31 Summary of Calculated Piping Parameters *83*
Table 32 Properties Calculated of Pumps *86*
Table 33 Summary for Compressor Design Parameters *87*
Table 34 Summary Table for Storage Design Parameters *88*
Table 35 Summary of Process Control Details for Disc Filters (Perry et al., 1997). *91*
Table 36 Summary of Process Control Details for Fluidized Bed Reactor (Perry et al., 1997). *94*
Table 37 Summary of P&ID Details of Cyclone *95*

Table 38 Summary of P&ID Parameters of Distillation Column *98*
Table 39 Summary of P&ID Parameters for Stripping Towers *100*
Table 40 Summary of P&ID Parameters of Condenser *101*
Table 41 Summary of P&ID Parameters for Heat Exchangers *103*
Table 42 Summary of P&ID Parameters for Venturi Scrubber *104*
Table 43 Effects of Exposure Routes of Carbon Monoxide (Towler et al., 2013) *110*
Table 44 LFL and UFL for Various Elements (Crowl et al, 2002) *113*
Table 45 Summary of Toxic Dispersion Values for Cases *116*
Table 46 Developed Hazard Assessment Guide (HAZOP) (Crowl et al., 2002). *117*
Table 47 HAZOP Study of Processing Units in System *118*
Table 48 Calculated Probability Results for Event Tree 2 ..... *123*
Table 49 Calculated Probability Results for Event Tree 2 ..... *124*
Table 50 Calculated Probability Results of Event Tree 3 ..... *125*
Table 51 Fault Trees Legend (Cooper et al. 2011) *126*
Table 52 Summary of Failure Probabilities for Devices (Crowl et al., 2002) *127*
Table 53 Summary of Equipment Costs *133*
Table 54 Yearly Expenses in Plant Life Time *134*
Table 55 Total Cost for Products *135*
Table 56 Summary of Yearly Expenses and Savings in Long Term *137*
Table 57 Specific Heat Values and Correction Values of Fuel Products *146*
Table 58 Assumptions Used for Reactor Design Calculations *159*
Table 59 Calculated Values for Reactor Design *159*

Abbreviations

Abbreviation	Definition
(L/G)	Liquid-to-gas Ratio
Abbreviations	Definition
ANSI	American National Standardization institute
API	American Petroleum Institute (Oil and Gas Industry)
ASME	American Society of Mechanical Engineers
Aspen EDR	Aspen Exchanger Design & Rating
ASTM	American Society of Testing Materials
BFBR	Bubbling Fluidized Bed Reactor
C10H8	Naphthalene
C2H2O2	Acetylenediol
C2H4O	Vinyl alcohol
C2H4O2	Glycolaldehyde
C3H6O	Allyl alcohol
C6H6O3	Hydroxyquinol
C7H8	Toluene
CELL	Cellulose
CELL	Cellulose (C6H10O5)
CEPA	Canadian Environmental Protection Act
CH4	Methane
CO	Carbon Monoxide
CO2	Carbon Dioxide
DAF	Dissolved Air Flotation
DF	Disc Filter
ECA	Environmental Compliance Approval
EDR	Exchanger Design and Rating
EPA	Environmental Protection Agency
FPA	Focal Plane Array
FT-IR	Fourier transform infrared spectroscopy
FT-NIR	Fourier transform near infrared spectroscopy
FUG	Fenske- Underwood -Gilligand
G{CH2O}	Trapped Formaldehyde
G{CH3OH}	Trapped Methanol
G{CH4}	Trapped Methane
G{CO}	Trapped Carbon Monoxide
G{CO2}	Trapped Carbon Dioxide
G{H2}	Trapped Hydrogen
GCMS	Gas Chromatography Mass Spectrometry
H2	Hydrogen Gas
H2OB	Moisture in feed
HAZOP	Hazard and Operability Study
HCE	Activated Hemicellulose
HCE	Hemicellulose (C5H8O4)
HCE1	Activated Hemicellulose 1 (C5H8O4)
HCE2	Activated Hemicellulose 2 (C5H8O4)
HDPE	High-density polyethylene
HRT	Hydraulic Retention Time
HX1	Heat Exchangers
ID	Induced Drafts
IRR	Internal Rate of Return

KDV	Katalytische Drucklose Verölung
LD50	Lethal Dose 50%
LDPE	low-density polyethylene
LDS	Leak Detection System
MBR	Membrane Bioreactor
MF	Microfiltration
MOECC	Ministry of the Environment and Climate Change
MP	Microplastic
NESHAP	National Emission Standard for Hazardous Air Pollutants
NPDES	National Pollutants Discharge Elimination
NPR	Net Present Value
OHSA	Occupational Safety and Health Act
OPEC	Organization of Petroleum Exporting Countries
PE	polyethylene
PET	Polyethylene terephthalate
PFD	Process Flow Diagram
PM	Particular Matter
PP	polypropylene
PS	Polystyrene
PSM	Process Safety Management
PVC	Polyvinyl Chloride
Py-GCMS	Pyrolysis Gas Chromatography Mass Spectrometry
RMP	Risk Management Plan
RO	Reverse Osmosis
RSF	Rapid Sand Filter
SAL	Small Anthropogenic Little
STR	Solid Retention Time
TBP	True Boiling Point
TED	Thermal Extraction and Desorption
TEMA	Tubular Exchanger Manufacturers Association
TLV-TWA	Threshold Limit Value – Time Weight Average
TSS	Total Suspended Solids
UF	Ultrafiltration
US	United State
UV	Ultraviolet
WHO	World Health Organization
WWTP	Wastewater Treatment Plant

Nomenclature

Symbol	Definition
µm	Micrometers
atm	Atmosphere (Pressure)
cm	Centimeter
gal/ft3	gallon per volume
kPa	Kilo pascal
kW	Kilowatt
m	meters
m/s	Meter per second
mg/L	Milligram per litre
s	Seconds
u	Velocity
Δ P	Pressure Drop
ρ	Density
η	Efficiency
κ	Thermal Conductivity
λ	Latent heat
ϕ	Void Fraction
°C	Degree Celsius
Btu/lb	British thermal unit per pound
Cp	Specific heat
H	Enthalpy
Hp	Horsepower
J	Joule
K	Kelvin
KJ	Kilo joule
KJ/hr	Kilojoule per hour
KJ/mol	Kilojoule per mole
K	Kelvin
Kt/a	Kilo tonnes anually
L	Liter
ML	Mega Liter
Mt	Mega tonnes
N/m2	Newton per meter square
P/L	Particle per Liter
Pa	Pascals
Ppm	Parts Per Million
R	Universal gas constant
ref	Reference
U	Internal Energy

1. Introduction

Since the discovery of plastics in 1930, they have become an essential raw material found in the manufacturing of everyday products due to their relatively low cost and highly versatile capabilities (Anderson et al., 2016). Within the last few decades, people are beginning to study the impacts plastic poses to the aquatic environment, as they are being disposed of carelessly and incorrectly. Microplastics are categorized as being smaller than 5 mm and classified as either primary or secondary (Anderson et al., 2016). Microbeads found in the ingredients of personal care products such as facial scrubs, toothpaste, and cosmetics, are considered primary microplastics. Primary microplastics often remain in their manufactured size and due to microbeads not being able to dissolve after they are rinsed down the drain, makes removing them from lakes even more difficult. Regulations were implemented on July 1, 2018, to prohibit the manufacture and import of all toiletries that contain microbeads in Canadian industries (Weeks, 2016). Secondary microplastics are a result of UV degradation, wear-and-tear, or produced during manufacturing of larger plastic particles. Some examples include line and fibers from laundering, foam from packaging, and tire wear. Microplastics enter the aquatic environment through different routes such as effluent discharged to the lakes from water and wastewater treatment plants that lack in retaining this material. Other ways microplastics end up in waterways is through combined sewage overflow events, industrial processes, and stormwater sewers that wipe away incidental plastic products from roadways and debris (Karapanagioti et al., 2019). Populated urban locations and plastic industries increase the abundance of microplastics in nearby water bodies. Once microplastics wind up in a body of water, there is a great chance that they may be moved by wind and water from land to rivers and lakes to oceans. Currently, between 0.48 and 1.27 million tons of plastic waste enters the ocean annually, and it is expected to double in the next 10 years (Karapanagioti et al., 2019). Due to the polymer's stable carbohydrate bonds characteristics, makes it resistant to decompose in the environment. Common plastic polymers that are typically found in all types of bodies of water include polypropylene (PP), polyethylene (PE), and low-density polyethylene (LDPE).

In a society so heavily dependent on plastic products, whether that be the packaging in food, electronics, or appliances, the use of plastic is exponentially growing. Canada alone was calculated to have consumed 4.6 million tonnes of plastic in the past year and by 2030, it is estimated that plastic consumption will grow to 6 million tonnes (Litchfield, 2020). With all the plastic that gets consumed, it is hard to find alternatives to dispose of it safely. Plastic waste is categorized in two mains sections, which would help to determine how it should be disposed of as shown in Figure 1. The first is post-industrial waste, which is waste that is cleaner, it is a type of plastic product that does not end up with the consumer (Litchfield,

2020). Post-industrial plastic is often a lot easier to sort out and recycle, as it is not mixed with other types of plastics and contains far less contaminants in it (Litchfield, 2020). On the other hand, post-consumer plastic waste is far more difficult to dispose of. This type of plastic often gets mixed with organic contaminants and other waste such as paper or wood. Two disposal methods that are widely used to dispose of plastic waste are through either mechanical or chemical means (Ragaert, 2017).

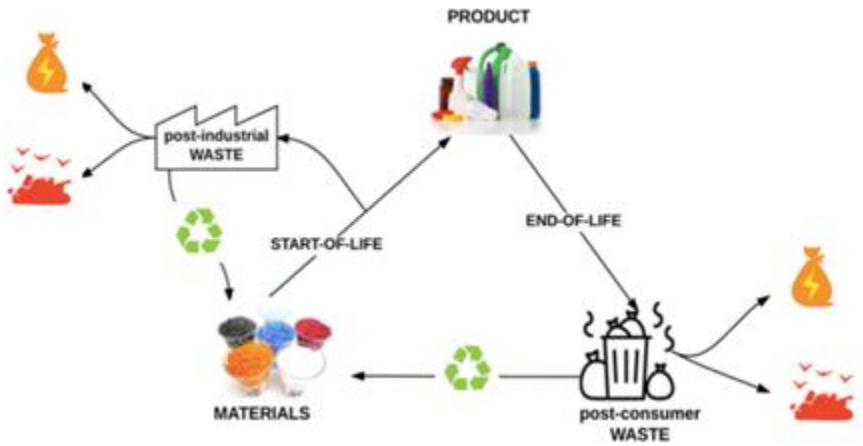

Figure 1 Categories of Waste Plastic (Ragert, 2017).

Mechanical recycling involves technologies that promote sorting, depending on the thermal-mechanical properties of the plastic. It is mainly used for post- industrial waste as it is cleaner to sort through and is often reused by the production company to produce more of that specific plastic product.

However, chemical recycling is much more of an appealing alternative because it can convert plastic waste and other impurities into valuable products that are not heavily dependent on how the plastic is sorted. Most products of chemical recycling are petroleum, and smaller hydrocarbons that can be refined further into bio-oils and biofuels. Chemical recycling differs from the incineration of plastic waste because it does not take part in combustion, where the plastic is eradicated, instead it manipulates the physical properties and converts it into a usable product. The idea and potential of chemical recycling is rising, and it is looking like a more viable option to help reduce and eventually eliminate plastic waste (Ragaert, 2017).

2. Market Analysis

2.1 Why the City of Toronto

Lake Ontario is one of the most polluted bodies of water in Canada; there are around 7 primary urban developments that surround it, all which include; Bay of Quinte, Eighteen Mile Creek, Hamilton Harbor, Metro Toronto, Oswego River, Port Hope Harbor, and the Rochester Embayment. In addition, there are about 85 or more water and wastewater treatment plants that discharge effluent and stormwater into this lake. Although Lake Ontario has been a great freshwater resource, due to the amount of urban development that surrounds the lake, it has become extremely polluted in several areas. The City of Toronto will be the primary municipality that will be targeted for this design project for three main reasons. Firstly, it is one of the most populated cities as the population is reaching more than 3 million, hence more plastic pollution from urban development. Secondly, a hot spot for microplastic accumulation is known to be in the Toronto Humber Bay and Don Valley River area (Costello, 2020). Thirdly, the City of Toronto is already creating strategies to obtain a sustainable energy source, therefore creating another option of making gas and fuel will align with the city's goals.

2.2 Why Wastewater Treatment Plants

Due to the numerous pathways that allow microplastics to enter Lake Ontario, it was difficult to determine the method that would be best for removing it out of the environment. It is extremely challenging and labor intensive to remove microplastics once they enter large bodies of water as the majority end up sinking to the bottom of the lake or ocean floor and it is almost impossible to remove it then. The three main types of pathways that can be controlled is through water treatment plants, wastewater treatment plants, and storm water discharge locations. The best available option is by removing microplastics at the source This can be done by removing microplastics from the final effluent discharge before it enters Lake Ontario as well as taking screenings from the preliminary treatment where most large debris and plastic particles are caught.

Toronto Water has four main wastewater treatment facilities which are Ashbridge's Bay Treatment Plant, Highland Creek Treatment Plant, Humber Treatment Plant and the North York Treatment Plant. These plants collect wastewater from sewage and combined drains and treats the wastewater through preliminary, primary, and secondary treatment stages. A study was conducted with samples of wastewater final effluent collected from the four treatment plants in Toronto and analyzed to conclude 13.3 particles/L

in wastewater effluent that is polluted into Lake Ontario (Grbic, 2020). Moreover, in journals such as, "*Wastewater Treatment Plants as a Source of Microplastics in River Catchments*", thoroughly explains there was an increase in microplastics found downstream in the treatment process. Some of the possibilities as to the increase in microplastics found in the wastewater treatment process include microplastics embedded in the sludge applied for agriculture purposes, release through diffusion of secondary microplastics, and aerial depositions (Kay, 2018). Thus, targeting wastewater effluent is effective as it is easier to manage the discharge locations and allows for the removal of microplastics through a continuous process.

Targeting the preliminary screenings and grit from a water treatment process and re-purposing that waste feed product at site allows for the process to be commercially viable. Disposing of preliminary screenings accounts for a large portion of the operation costs of a waste-water treatment facility. For Ashbridge's Bay, this product amounts to 4.6 tons/days of waste which would need to be disposed of. Figure 2 depicts a picture of the waste feed. As can be seen, through Ashbridge's Bay continuous process, this material is screen, shredded, and dried before entering a large collection bin. The stored waste product will be utilized at this pyrolysis facility, just adjacent to Ashbridge's Bay, and convert it into a biofuel.

Figure 2 Dried Biowaste that is collected from Ashbridge's in December of 2020

Biofuel has many commercial uses; however, the primary use is through using biofuel for one for electricity. The energy created by burning biomass can be directly used for heating buildings and water, for industrial process heat, and for generating electricity in steam turbines and CHP units (U.S. Energy Information Administration 2020). Biofuel can also be further processed and used as transportation fuel for diesel powered vehicles.

3. Raw Material Overview

The major raw materials used in the overall process are as follows: water, steam, biomass, and nitrogen gas. The biomass feed is used for the reactor to produce biogases, bio-oil, and char. The biomass feed goes through thermal decomposition in a pyrolysis process. The screw conveyer is used to feed the reactor with biomass. Steam and nitrogen do not directly participate in the thermal decomposition reaction, they just act as a medium for the fluidizing process to occur. Water is used throughout the various parts of the plant for temperature control processes. The heat exchanger and cooling jacket is the most significant use of water to lower the temperature from the reactor and stripper outlet streams. The steam is also used for controlling the temperature in the distillation column and removing the lighter hydrocarbons from the stripping column while refluxing it back to distillation column. Thus, the steam helps improve the quality of the product.

Table 1 Summary of raw material physical and chemical properties (John Rumble, 2021)

Material	$C_6H_{10}O_5$	H_2O	Steam	N_2
Molecular weight (g/mol)	162	18	18	14
Specific heat capacity (J/kg K)	4.7419	4179.6	1996	1040
H_f (KJ/mol)	-936,000	37.55	40.68	472.435
H_c(KJ/mol)	-2828,000	-	-	-

The composition of the feed is taken from a report with characterization of screening from three municipal wastewater treatment plants. From the report sanitary textile has the most weight percentage making it a category for cellulose. The composition data is collected from the primary mesh screen,

which is our primary source of biomass feed. The composition feed is 76.1% sanitary textile, 13% fine fraction and the others in 10.9% (Barillon. B, 2009).

4. Plant Location

Facility location strongly influences economic feasibility of the fast pyrolysis and hydro-processing pathways. Biorefinery internal rate of return (IRR) and net present value (NPV) are very sensitive to bio-oil yield, feedstock cost, location capital cost factor, and transportation fuel market value (Brown, 2013). An important step when determining the location of a biorefinery plant is to identify and select a location that produce biomass feedstock in enough concentrations and volumes to enable continuous operation of a commercial-scale fast pyrolysis and hydro-processing biorefinery. Choosing Ashbridge's Bay Wastewater Treatment Plant will provide sufficient feedstock from the final effluent and grit screenings to operate the process, while reducing microplastics and waste that end up in lakes, oceans, and landfills (Dau, 2014). While the exact composition of feedstock is difficult to determine, it is important to take into consideration the feedstock type as it significantly affects bio-oil yield.

The wastewater treatment plant of interest is the Ashbridge Bay Treatment Plant for three main reasons, capacity, location, and access to resources. Ashbridge Bay Treatment plant is located near the Don Valley which is an area where a large amount of industrial and consumer debris would make its way to Lake Ontario. Moreover, in a study called "*Microplastics entering northwestern Lake Ontario and diverse and linked to urban sources*" collected samples from both Ashbridge Bay and Humber Bay treatment plants. It pinpointed the types of microplastics being primarily microfibers and silicones from various applications, primarily through washing machines (Grbic, 2020). Ashbridge Bay is also the largest treatment plant in Ontario, it has a maximum capacity of 818000 m^3 of wastewater influent per day (Grbic, 2020).

Preliminary coarse and fine screenings for Ashbridge Bay amounted to 4.6 tons/day in 2019, which was sent to landfill waste (Ashbridge Bay Report, 2019). In addition, 74.7% of this waste is sanitary textile material which is also considered a source of microplastic in the environment (Hyaric et al., 2009). There have been studies that found white microplastic fibers in flushable wipes and other sewage related waste which contains a combination of PET and cellulose (Briain et al., 2020). The proposed process uses pyrolysis technology which can utilize most of this waste as feed material reducing microplastic pollution to the environment and disposal fees for Ashbridge's Bay.

Disposal fees for screenings and grit are one of the largest operational costs for wastewater treatment facilities. The most common methods of disposal are through landfilling or incineration. The City of Toronto enforces a decrease in the amounts of biodegradable organic matter disposed in landfills. Moreover, this waste also contains high water content, often going over the limit for landfills and causing problems in operational conditions for incinerators (Hyaric et al., 2009). Through a discussion with a representative at Ashbridge's Bay, it was determined that the 2020 disposal cost for screenings and grit were $159.03/MT and haulage cost were $50.58/MT, which would cost Ashbridge's Bay about $357,000 per year in disposal fees. These costs are expected to increase year after year as inflation rises and cost of transportation and disposal fees increase. Thus, a demand exists for finding alternate methods of disposing of or re-using this waste.

Moreover, the City of Toronto is currently undertaking the Ashbridge's Bay Landform Project, which will transform the bay of Coastworth Cut and create space for additional projects. Figure 3 depicts the current design projections, expected to complete in 2030. This will allow us to build our plant adjacent to the Ashbridge's Bay facility.

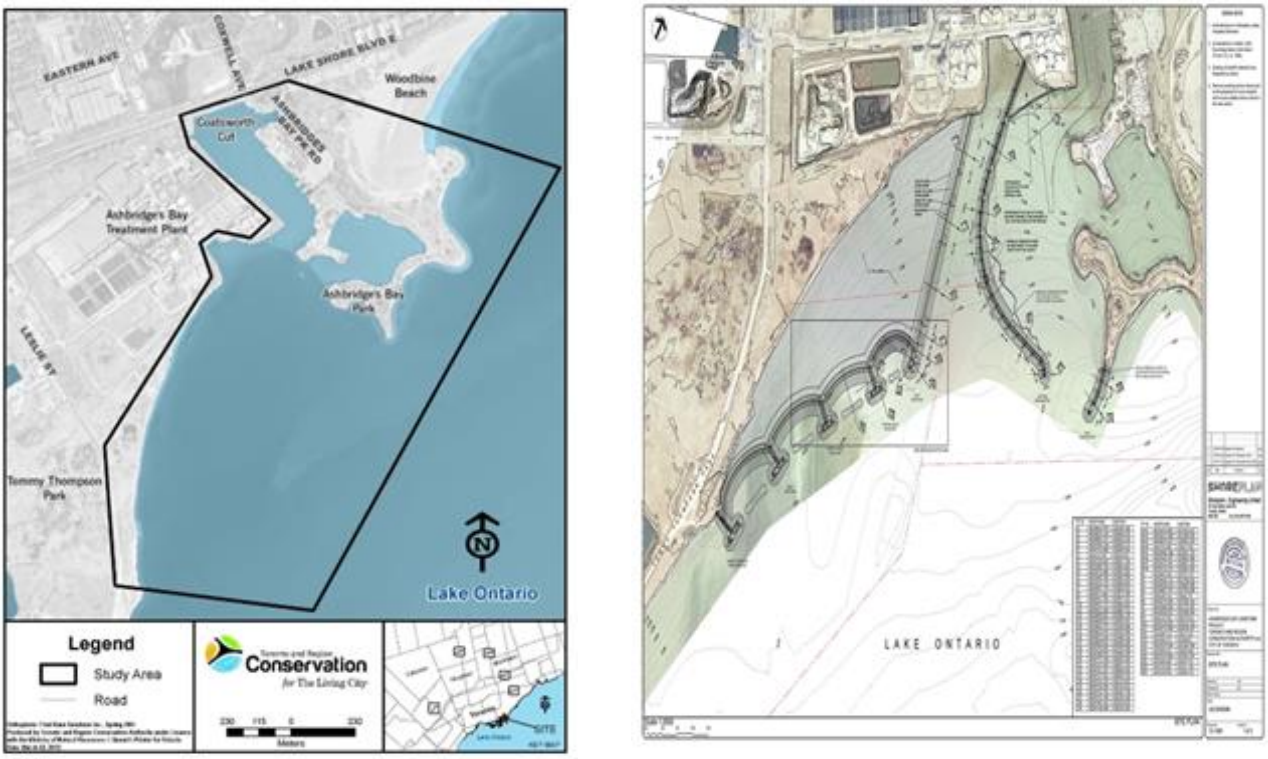

Figure 3 Ashbridge Landform Project and Proposed Area of Construction (Ashbridges Bay Landform Project 2020)

4. Process Description

The objective of this design project will be to reduce the number of microplastics entering Lake Ontario through Ashbridge's Bay wastewater treatment facility. This will create a cost-effective, continuous process that will recycle microplastics and 4.6 tonnes/day of preliminary screenings and waste through a fast pyrolysis reaction to convert the waste into usable biofuel. Figure 4 provides a detailed PFD with all the units and streams entering and leaving each equipment. Firstly, 18 low-cost disc filter set-ups will be used to treat the effluent of the Ashbridge's Bay Wastewater Treatment Plant. This filtration process will remove 9.950 tonnes/year of microplastics and will be combined with 1680 tonnes/year from the grit and screenings to be fed to the Screw Conveyor (SC-1). The screw conveyor will transport all the waste that will be fed to the Bubbling Fluidized Bed Reactor (R-1), where the fast pyrolysis reaction occurs. The products from the reactor are sent to the cyclone to remove any undesired excess char into the char collection tank that will be sent to a flare or used for energy. The solid waste is converted into biogas and syngas where this mixture will be fed into the Distillation Column (DC-1) to separate and purify the products further. Steam fed into the column aids in separating and obtaining the profitable products including bio-gasoline, bio-naphtha, bio-kerosene, and bio-gas oil. The 3 stripping columns are used to remove any final impurities in the oil mixtures and the products are sent to the storage tanks. The distillation column also separates the syngas from the oil and is sent to the Venturi Scrubber (V-1), where the tar in the syngas is removed to obtain a purified gas mixture that is re-circulated back to the reactor. The syngas is used for aid in the combustion process and obtaining a higher yield of products. To further improve the separation between the tar mixture and the clean syngas, the cyclone separates the waste stream and is sent to Ashbridge's Bay to the surcharge program to treat the water before it is sent to the lake as it contains toxins. The legend provides a color code scheme that helps to identify composition of the fluid in different streams.

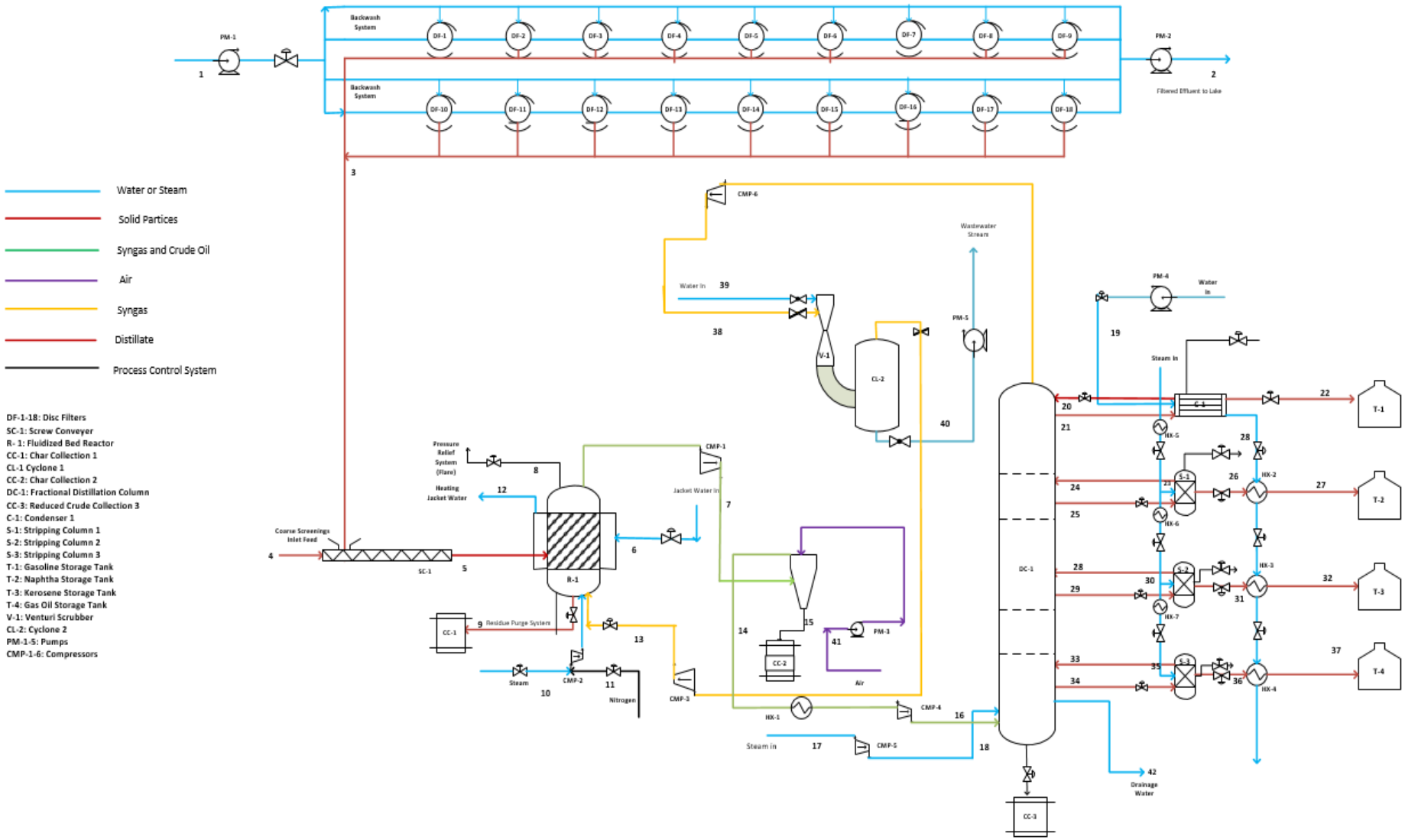

Figure 4 PFD of Microplastic Waste into Fuel Pyrolysis Process

4.1 Stream Properties in Process Flow Diagram

Table 2 Properties of each Stream

Reference #	Stream	Operating Temperature (℃)	Flowrate (kg/day)	Composition (w.t%)	Energy Content
1	Ashbridge's Bay Effluent In	23	1.5×10^6	1.81×10^{-3} % MP 99.99 % water	12560434.44
2	Filtered Effluent Out	23	1.5×10^6	4.44×10^{-4} % MP 99.999% water	12560434.44
3	Solid Filtered MP to Dryer	23	20.64	90% polyester 10% cellulose	36.2538431
4	Coarse Screenings Inlet Feed	23	2468.96	74% cellulose 11% polyester 15% grit	1992.424008
5	Total Biomass Inlet	90	2468.96	74% cellulose 11% polyester 15% grit	1992.424008
6	Jacket Water In	15	3871.52	100% H_2O	-97242.88
7	Bio-Crude Vapor into Cyclone	517	2197.37	76.90% bio-crude vapor 19.75% Syngas 3.66% Char	2902913.39
8	Pressure Relief System	N/A	As Needed	N/A	-
9	Residue Purge System	N/A	As Needed	N/A	-
10+11	Steam In + Nitrogen gas	200	839.76	As Needed	39020.27408
12	Jacket Water Out	350	3871.52	100% H_2O	5332151.44
13	Clean Syngas In	50	339.16	48.6 % CH_4, 11.5 % CO, 6.4 % CO_2, 32% H_2, 1.5% Tar	48493.58 kJ/day
14	Bio-Crude Oil into Heat Exchanger	517	2123.76	79.60 % Bio-Crude oil 20.40% Syngas	3619808.91

15	Char	517	73.61	100% Carbon	16640.99918
16	Bio-crude oil Inlet to Distillation Column	315	2123.76	79.60 % Bio-Crude oil 20.40% Syngas	2145612.53
17	Steam Line	279.4	116524	100% H_2O	2206121
18	Reduced Crude Outlet	265	624.71	100% Reduced Crude	405890.42
19	Water Line into Condenser	15	446.35	100 % H_2O	-11100.572
20	Reflux of Gasoline from Condenser	26.67	90.53	100% Gasoline	1275.71
21	Gasoline going into Condenser	141.11	452.86	100% Gasoline	135182.4
22	Gasoline into Storage Tank	26.67	362.33	100% Gasoline	5105.81
23	Steam going into Naphtha Stripper	132	11.37	100 % H_2O	10145.37
24	Reflux from Naphtha Stripping Tower	145.6	17.08	67% Steam 33%Gasoline	13207.53
25	Naphtha going into Stripping Tower	168.33	95.13	94% Naphtha 6% Gasoline	34247.91
26	Naphtha in Heat Exchanger	68	89.42	100% Naphtha	9677.84
27	Naphtha out Heat Exchanger	30	89.42	100% Naphtha	1853.20
28	Reflux from Kerosene Stripping Tower	192.8	40.45	67% Steam 33% Naphtha	29799.85
29	Kerosene Going into	215.56	337.96	96% Kerosene 4% Naphtha	166101.29

	Stripping Tower				
30	Steam going into Kerosene Stripper	179	26.92	100 % H_2O	34191.39
31	Kerosene in Heat Exchanger	94.6	324.44	100% Kerosene	56986.30
32	Kerosene out Heat Exchanger	40	324.44	100% Kerosene	14711.13
33	Reflux from Gas Oil Stripping Tower	242.77	10.56	66% Steam 34% Kerosene	14439.20
34	Gas Oil Going into Stripping Tower	265.56	179.11	98% Gas Oil 2% Kerosene	144617.78
35	Steam going into Gas Oil Stripper	229	6.97	100 % H_2O	11654.15
36	Gas Oil in Heat Exchanger	252	175.53	100% Gas Oil	100161.02
37	Gas Oil out Heat Exchanger	50	175.53	100% Gas Oil	12574.32
38	Syngas Inlet into Gas Scrubber	60	433.99	23% tar 25% H_2 38% CH_4 9% CO 5% CO_2	92550.54
39	Water Line into Gas Scrubber	15	304.09	100% H_2O	-12727.99
40	Liquid Water Out	24.5	392.93	77.39% water 22.61% tar	-691.75
41	Air	N/A	As Needed	100% Air	
42	Discharge Drain	N/A	116524	100% Steam	2206121

5. Equipment Selection

5.1 Rotary Disc Filters

A disc filter consists of several discs in the rotating system. Each disk has a pie shaped section which acts as a filter where the filtration size can be changed. The disc filter can be operated using either a vacuum pump or pressurized disc filters. It is mostly used in mining and minerals, chemicals, and water treatment plants. Similar to the rotary vacuum drum filter, the disc filter pulls slurry or secondary effluent under the center barrel of the filter. The formed cake inside the membrane is back washed using a smaller nozzle to take out the microplastic as shown in Figure 5(Huber, 2014).

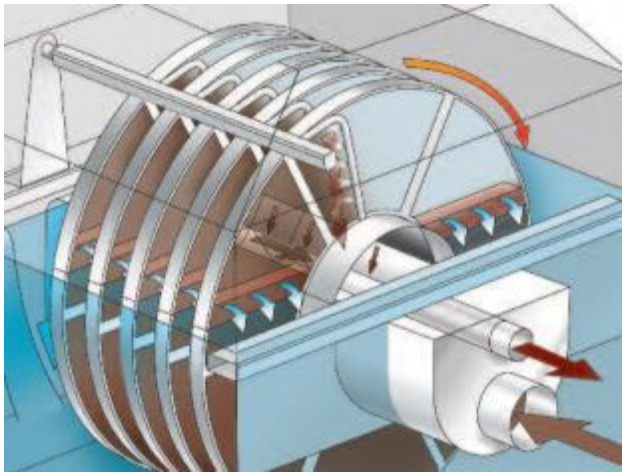

Figure 5 Back wash system (Huber, 2014)

The design of the Huber Disc Filter has the same mechanism as Hydrotech HF2220 disc filter. There have been studies on disc filters being effective for microplastic particle removal of size 10µm (Huber, 2014). There are various research papers on performance of a disk filter. Fourier transform infrared automatic analysis (FTIR) was used to obtain infrared spectra for the various plastic analysis conducted by the report. Wastewater treatment plants in Denmark have used disc filters in the past for removal of microplastics. They reported to have removed 3.8 kg of microplastics per 4.9 kg before filtration, resulting in a 77.6% removal efficiency. Some things to consider when selecting the type of disc filter for the system includes method of operation (batch or continuous), size, method of filtration, and the nature of the substance to be filtered (Solid, 2020). A wide variety of industrial filter equipment were available for continuous filtration processes. Unlike other continuous filers, disc filters have a unique ability to backwash every filter continuously. This means that pressure drop or clogging in the filter membrane is non-existent

(Huber, 2014). Rotary Disc filters is selected for this process as it is simple to construct and operate. The filter operates at an absolute pressure of 1 atm, using ultrafiltration. The rotary disc filter has a capacity of 1500m^3/h and is suitable for continuous processes like the wastewater treatment effluent.

5.2 Conveyor System

A conveyor system is required in the process to transport solids from Ashbridge's Bay to the pyrolysis process in our plant. Conveyor belts and screw conveyors are the most popular ones used in a wide range of applications. Table 3 below summarizes the advantages and disadvantages of belt conveyors and screw conveyors. The choice between belt conveyors versus screw conveyors comes down to what materials that is being conveyed. Shafted screw conveyors are often used in wastewater treatment for dewatered biosolid materials. Since the moisture content is very low, shafted screws are the best option since the feed is too abrasive for shaftless screw liners. Thus, a shafted screw conveyor is the most ideal equipment to transport the effluent microplastics and the biomass from the coarse and screening from Ashbridge's Bay.

Table 3 Comparison Between Belt and Screw Conveyor for Equipment Selection (Towler et al., 2013)

Type	Advantages	Disadvantages
Belt Conveyor	• Uses less power • Best for long distances and high volumes • Simple to design and easy to maintain	• Limitations on incline degrees • Many roller bearings • Costly to enclose
Screw Conveyor	• Completely enclosed (higher safety) • Less bearings • Can convey vertically • Ideal for wide range of feed	• Certain materials may clog or get stuck on shafts or hanger bearings • Shearing action may change feed size

5.3 Bubbling Fluidized Bed Reactor

The fluidized bed reactor has gained wide usage in the petroleum and chemical processing industries. The fluidizing bed reactor design is based on the behavior of the Kunii-Levenspiel bubbling bed model. The Bubbling Fluidized Bed Reactor (BFBR) is cylindrical in shape and contains particles through which gases flow. Sand is used as a catalyst for the reactions. The major concern for a fluidized bed is the velocity of the gas distributed from the disruptor plate that should be sufficiently high enough to suspend or fluidize the sand particles to drastically increase the surface area for the reaction. The fluidized bed reactor is between a small-scale laboratory equipment and industrial large-scale system (Fogler, 2005). The reason bubbling fluidized bed reactor was used for the biomass pyrolysis instead of other reactors was due to following advantages (Jahirul.M, 2012):

1) It involves a simpler design.
2) The cost of design and construction is relatively cheap.
3) Efficient mixing of particles in the reactor
4) Uniform temperature of particles in the reactor
5) Lower operating temperature with higher yield
6) Lower nitrogen feed gas velocity for fluidization
7) This is known to handle municipal waste for pyrolysis process.

The fluidization of the bed occurs when sufficient upward-flowing gas passes through the particle from a porous distributor plate. The upward gas flow gives a drag force that overcomes the gravitational force being exerted on the particles. The drag force is the result of the friction force imposed by the particles when gas passes through it. The particles then impose equal and opposite drag force on the fluidizing gas.

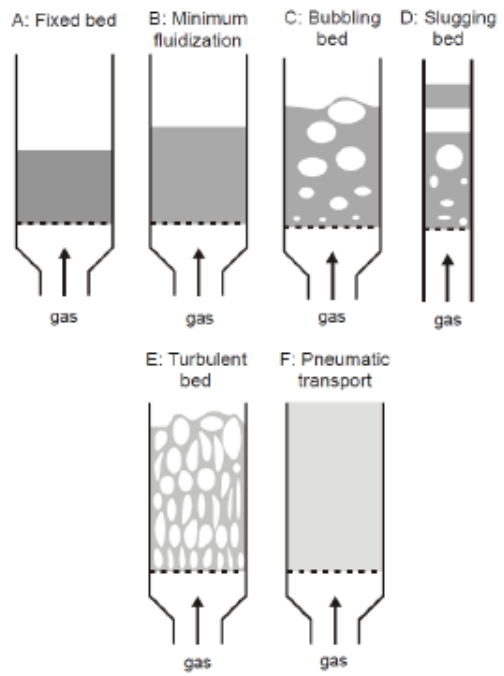

Figure 6 Different Stages Occurring in the Fluidized Bed Process(Perry et al., 1997)

Pyrolysis is a process of chemically decomposing the biomass feed at elevated temperatures in the absence of oxygen, which is typically above 480°C under pressure. The reaction involved is an irreversible, physical phase change and chemical composition change in the system. Some things to consider when selecting the type of reactor for pyrolysis in the system includes method of operation, size, feed for the reactor, type of pyrolysis, reactor design (Jahirul.M, 2012). The reactor is a continuous system where the goal is to maximize the bio crude oil production compared to other char and gas products. Fast pyrolysis was selected for that reason of operation at medium temperature with high heat transfer rate, making it the highest yield for biocrude oil. The bubbling fluidized bed has a large heat storage capacity, very high temperature control, better gas solid contact, and excellent heat transfer characteristics. These biomass materials fed to the system, were assumed to be similar to oak biomass since it had high presence of cellulose in the feed (Ranzi, 2008). Sanitary textile had the highest weight percent in the composition of feed which is a type of cellulose and polyester combined composite. The fluidized bed reactor also has a vast amount of research done among the various reactors for reference and a proven industrial scale use in waste biomass energy production. The fluidized bed reactor used has a capacity of 2467.96 kg/day, which is sufficient for this process.

5.4 Distillation Column

The products that are retrieved from the fluidized bed reactor must be separated in two ways, first the biocrude oil and the gas collected from the reaction and secondly the products that can be extracted out of the bio-crude itself. In most oil refineries, fractional distillation is employed as it effectively separates all the components of the products based on physical characteristics. This section will explore how fractional distillation will be used, why it was chosen as a separation method and Table 4 summarizes the advantages and disadvantages that this separation method provides.

Fractional distillation uses the differences in boiling points to separate components, when the feed enters the distillation tower from the bottom the components with lower boiling points rise to the top of the tower (Taghipour, 2019). The higher the vapor rises the higher purity of product is achieved, as the heavier components in the vapor phase will condense and fall back into liquid stages. Through the study of the properties related to boiling points and the volatility of the components in the crude oil, products such as, reduced crude, gas oil, kerosene, naphtha, and gasoline can be retrieved (Taghipour, 2019). The separation of products from biocrude highly differ with the composition of the biocrude, as studies have shown it contains more than 400 known compounds with ranging boiling points (Taghipour, 2019). Through comparing bio crude with crude oil fed into petroleum refineries, the percentage of the products were assumed. Fractional distillation will have a variable temperature based on the products being distilled, with the temperature coolest at the top and hottest at the bottom.

The temperature of the products leaving the tower are based on the Perry Handbook and petroleum refining textbooks. The temperatures of gas oil, kerosene, and naphtha would be 510°F (265°C), 420°F (216°C), 335°F (168°C), respectively, where the products would primarily be at liquid state with very small portions of vapor (Perry et al., 1997). Gasoline would be at the top of the column retrieved at 296°F (147°C) at a vapor state, and reduced crude at 510°F (265°C) at a completely liquid state (Perry et al., 1997). Unlike a regular distillation column where reboilers often provide heat to the bottom of the tower and help promote a temperature gradient, a distillation tower for crude does not have one. For one, the vaporization usually can be present partly in the feed of the column. The steam and the stripping towers also help to with sustaining the vapor percentage and the temperature in the tower. Moreover, by introducing a reboiler, biocrude oil would require a lot of energy to vaporize.

Table 4 Summary of Advantages and Disadvantages of a Distillation Column (Taghipour, 2019)

Fractional Distillation Column	
Advantages	**Disadvantages**
Does not need a catalyst to separate	Can be cost extensive due to energy
Products can be separated without further processing	Due to ranges in temperature, pressure, various safety measures must be taken
Can create multiple separations from one unit	To be cost effective needs high amount of feed
Usually used in fuel production	
Highly effective and efficient	
Easy to implement	

5.5 Venturi Scrubber

5.5.1 Types of Scrubbers

Cyclonic, spray, and venturi scrubbers are the three main types of scrubbers used in the industry today, that serve as gaseous pollution control systems. Table 5 provides a summary of the pressure drop, liquid-to-gas ratio required, particle size range, and the efficiency of each scrubber. Venturi scrubbers are simple to design and maintain, with the highest efficiency compared to other scrubbers. The high efficiency, however, is at the cost of a high pressure drop and energy consumption (Cooper, 2011). The venturi scrubber was selected for the equipment design that follows the pyrolysis reaction and separation, due to its capability to collect condensing tars. Tar produced from the fluidized bed reactor in the form of vapors, are one of the undesired by-products that is comprised in syngas. Syngas is used as a form of energy for the process, mostly comprising of hydrogen and carbon monoxide (Cooper, 2011). Small concentrations of tar can be found along with the syngas and can pose a threat to the system and cause serious problems at further stages in the pyrolysis process. Tar contaminants can result in pipe malfunctions, filter blockage and deactivation of catalyst's particles. This means that a highly efficient wet scrubber is required for the process to operate effectively and smoothly with other equipment. Thus, a venturi scrubber is the most ideal for this system. Wet scrubbers, also known as gas-liquid separators, use cooling liquid agents in order to condense the tar vapor and divert into a separate stream. The scrubbing liquid to remove contaminants in syngas can be either water or an organic solvent.

Table 5 Summary of Comparison between Scrubber Types (Cooper, 2011)

Scrubber Type	Pressure Drop (in. H_2O)	L/G Ratio gal/1000 acf	Effective Particle Sizes for Scrubber	Efficiency (%)
Venturi	8-60	3-15	0.5 µm and up	98
Cyclonic	4-8	2-10	2 µm and up	95
Spray Tower	1-4	1-20	6 µm and up	90

5.5.2 Selection of Scrubbing Liquid

When selecting the ideal solvent for the scrubber, liquids with high solubility for the solute is preferred. Moreover, the solvent should be affordable, non-volatile, non-corrosive, stable, non-flammable, etc. The loss of solvent in the exiting stream due to evaporation, requires the liquid to be replenished which increases the operating costs. There are usually two main types of solvents used in scrubbing systems: water or organic liquids such as acetone (Cooper, 2011). Water used as the scrubbing liquid for the removal of tar may pose some difficulties due to the low solubility of tar in water, and the resultant pollutant wastewater stream would require further treatment or filtration before disposal. Acetone, on the other hand, has a high solubility of tar which enables for a higher tar removal efficiency. The main drawback for implementing an organic solvent as the scrubbing liquid, is the relatively high cost. Often, low-cost solvents are chosen over more expensive ones of higher solubility to remain cost-effective (Cooper, 2011). For this reason, water was selected over acetone.

5.5.3 Venturi Scrubber Process

The primary collection mechanism for a venturi scrubber involves direct interception and inertial impaction (Cooper, 2011). The collection efficiency of a venturi scrubber is dependent on the throat velocity or pressure drop, the liquid-to-gas ratio, and the chemical nature of the particles. A venturi scrubber consists of a converging and diverging flow channel along the length of the scrubber. The cross-sectional area of the channel decreases then increases around the throat. In the converging section, the decrease in area results in an increased turbulence and velocity of the waste gas. The scrubbing liquid enters the scrubber before the throat or directly into the throat section, where it is atomized by turbulence in the throat, thus, increasing the gas-liquid contact and droplet collection. Once the gas-liquid mixture moves through the diverging section, the gas-liquid velocity decreases where the facilitation of further droplet

collection occurs (Lee, 2019). The liquid droplets are then separated from the gas stream in the cyclone separator as shown in Figure 7. The gas to be cleaned usually enters at a higher temperature than the scrubbing liquid. The temperature of the inlet gas stream can significantly alter the collection efficiency, thus, sometimes a cooling tower is installed before the scrubber to control the inlet gas temperature (Unyaphan et al., 2017). Moreover, the temperature of the spray affects the efficiency of the scrubber. Lower temperature spray liquids improve the condensation process and the overall efficiency of the scrubber.

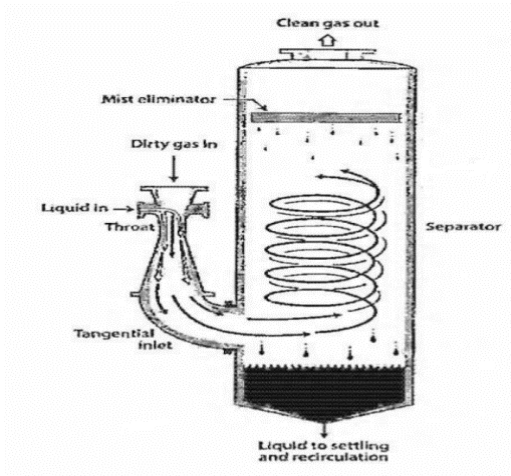

Figure 7 Venturi Scrubber Configuration (Cooper, 2011)

5.5.4 Composition of Syngas

Depending on the pyrolysis process feedstock (plastics, biomass, etc.) and the operating conditions, the tar composition in syngas will vary significantly. Syngas produced from the pyrolysis process is mainly composed of CO_2, H_2, CO, CH_4, and tars. Tars are hydrocarbons that are heavier than benzene, that condense between 200-300°C. In most cases, tar compounds in biomass syngas were found to have similar characterization to naphthalene ($C_{10}H_8$) and toluene (C_7H_8). In this proposal, toluene was chosen to model tar compounds due to its wide acceptance and for the purpose of simplicity when preparing the compositions on Aspen Plus. Table 6 summarizes the composition of the syngas in the inlet and outlet streams.

Table 6 Summary of Composition Information in Syngas(Lee, 2019)

Component	Inlet Percentage (%)	Outlet Percentage (%)
Carbon Monoxide	9	11.5
Carbon Dioxide	5	6.4
Methane	38	48.6
Hydrogen gas	25	32
Tar	23	1.5

5.6 Cyclone

When designing a wet scrubber, a mist eliminator or entrainment separator is required following the venturi scrubber to remove contaminant droplets. Some commonly used mist eliminators are chevrons, mesh pads, and cyclones. Chevrons are baffles that allows for the gas stream to wind in different directions as it passes through the mist eliminator (Unyaphan et al., 2017). The liquid droplets are collected on the blade of the chevron and are recycled back to the scrubber. The collection area of the scrubber is known as mesh pads that are made of interlaced fibers. For small droplets in a venturi scrubber, a cyclone is the best option. The advantages and disadvantages of a cyclone is shown in Table 7.

Table 7 Summary of Advantages and Disadvantages of Cyclone (Cooper,2011)

Advantages	Disadvantages
Low capital cost	High operating costs due to pressure drop
Low maintenance required	Low efficiencies for small particles
Ability to operate at high temperatures	Limited to non-sticky materials
Can handle liquid mists or dry materials	
Requires small space for installation	

5.7 Stripping Towers

Stripping towers are used to help remove lighter hydrocarbons in the product lines, primarily for product purification. Steam is usually used as a stripping component, where the steam will pass in a counter-current direction pulling out lighter hydrocarbon vapors with the steam and reintroduces it to the distillation column (Perry et al., 1997). The stripping towers are usually known to compose of four to ten trays, the more volatile the hydrocarbon is the higher the temperature of the steam that needs to be injected into the column (Perry et al., 1997). In some cases, a second distillation tower is put in place instead of a stripping tower, but the distillation tower would not help induce the same temperature gradient that stripping towers would provide. The lighter hydrocarbons are vaporized and absorbed into the steam that are then refluxed back, while the heavier hydrocarbon product will remain in the liquid state. All the streams going back into the distillation tower from the stripping towers are in the rectifying section of the distillation tower as it is above the feed stage, thus more volatile components are removed. A summary regarding the benefits of the stripping columns used is provided in Table 8.

Table 8 Summary of Advantages and Disadvantages of Stripping Towers (Perry et al., 1997)

Stripping Tower	
Advantages	**Disadvantages**
Has a high latent heat making it better to remove in comparison to a heat exchanger	Can be cost extensive due to energy of steam required
Better control the amount of steam needed based on product and separation	Might need a pump to feed back into distillation tower
Efficient way to remove lighter hydrocarbons	
Helps purify final product	

5.8 Heat Exchangers

The heat exchangers used in this process are required for cooling down viscous liquid streams at high temperatures. Table 9 provides a summary of the benefits and limitations of common heat exchangers.

Table 9 Summary of Heat Exchanger Comparisons

Exchanger	Benefits	Limitations
Shell and Tube	- Capable of operating at high pressures and temperatures - Less costly compared to plate type coolers - Pressure drop over a tube is less - Used for variety of different applications from water treatment to oil refining	- Heat exchange effectiveness is less compared to plate type cooler - Requires more space than plate cooler - Capacity cannot be expanded
Double Pipe	- Simplest and most common form of heat exchanger used - Capable of operating at high pressures and temperatures - Extremely easy to repair and maintain	- Only counterflow operation, no cross flow - Cannot be used for dirty fluids due to choking
Plate Heat Exchanger	- High efficiency at low operating costs - Suitable for highly viscous media	- High initial cost - Limits of working temperature of cooler due to bonding material between plates - Parts of cooling system exposed to corrosion due to titanium plates

Shell and tube heat exchangers will be used in this process due to its versatile applications, low operating costs, and high efficiency (Dekker, 2013). They also have tolerance to thermal stress, high flow, high pressure, and viscous media that would normally block channels in plate heat exchanger. Shell and tube heat exchangers are commonly used in oil refining plants as they have different tube designs and flow patterns for every requirement (Schroder et al. 2014).

5.9 Compressors

Selecting the best equipment for pumping gases in pipelines depends on the flowrate, the operating pressure, and the differential pressure required. Reciprocating, centrifugal, and axial flow compressors are the main types of equipment used in the chemical process industries. The compressor operating ranges are illustrated in the Figure 8. Typically, fans are used where there is a small pressure drop, while reciprocating

compressors can be used over a wide range of pressures and capacities. This process uses only reciprocating compressors as they work best for our operating flowrates that flow through the piping systems. Table 10 provides a more numerical representation of the operating ranges for the different types of compressors. It is evident that the reciprocating compressor has the lowest capacity which works for this system and selecting this compressor will save some capital cost since it is not efficient to use a type of compressor with a much larger capacity than needed.

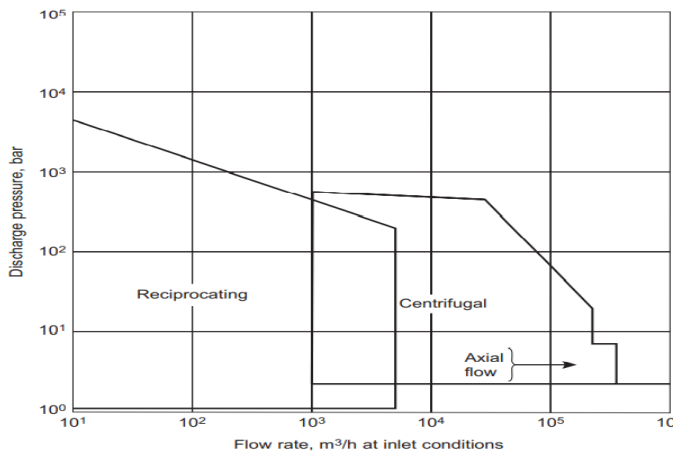

Figure 8 General parameters of Compressor Operating ranges (Towler et al.,2013)

Table 10 Comparison Summary of Different Compressors (Towler et al., 2013)

Types of Compressor	Normal Maximum Speed (rpm)	Normal Maximum Capacity (m3/h)	Normal Maximum Pressure (bar)
Displacement- Reciprocating	300	85000	3.5
Dynamic- Centrifugal Fan	1000	170000	0.2
Dynamic- Axial Flow Fan	1000	170000	0.35

5.10 Pumps

Pumps are almost always used to pump liquids and dilute slurries through piping systems. There are two main types of pumps: dynamic pumps such as centrifugal pumps, and positive displacement pumps such as reciprocating pumps. Centrifugal pumps are the most common type in chemical process industries. Positive displacement metering pumps are often used when small flowrates are fed to a process. Pump

selection is dependent on flow rate and head requirement. Figure 9 provides a graphical representation on the selection of the pump type based on the flowrate and the total head.

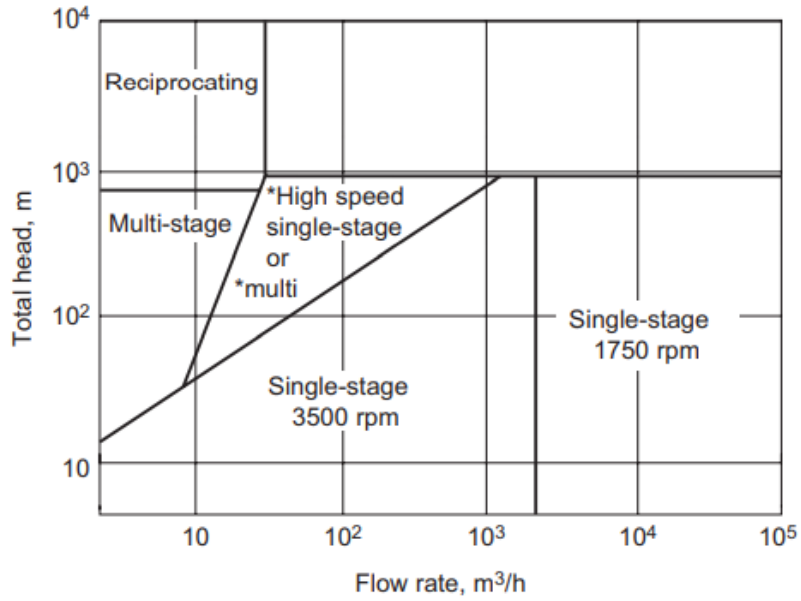

Figure 9 Representation of Pump Type based on Flow Rate (Towler et al., 2013)

6. Mass & Energy Balances Summaries

6.1 Approach

6.1.1 Mass Balance

The law of conservation of mass and energy that is the basis for material and energy balance calculations can be expressed as:

$$Accumulation = Input - Output + Net\ Generation \quad (1)$$

For steady-state operation, the operating parameters are time independent which means there is no accumulation in the system. Moreover, there is no generation since there is no reaction taking place in the units. Equation 1 becomes:

$$Input = Output \quad (2)$$

A summary of all the streams entering and leaving the different units are shown below (Table 12).

6.1.2 Energy Balance

To conduct the energy balance for each unit, the 1st Law of Thermodynamics for a closed system was applied. The general form of the energy equation is as shown:

$$\Delta U + \Delta E_k + \Delta E_p = Q - W \tag{3}$$

Some possible simplifications include:

- If $T_{system} = T_{surroundings}$, then Q=0 since no heat is being transferred due to temperature difference
- If the system is perfectly insulated, then Q=0 (adiabatic system) since no heat is being transferred between the system and the surroundings
- If the system is not accelerating, then ΔE_k=0
- If the system is not rising or falling, then ΔE_p=0
- If energy is not transferred across the system boundary by a moving part (e.g., piston, rotor, impeller), then W=0
- If system is at constant temperature (system is isothermal), no phase changes or chemical reactions are taking place, and only minimal pressure changes, then ΔU=0

The relation between enthalpy and internal energy is as follows:

$$\Delta H = \Delta U + P\Delta V \tag{4}$$

If we assume the pressure is constant, then heat (Q) is equal to enthalpy (ΔH).

6.2 Mass and Energy Balance Assumptions

6.2.1 Disc Filters

The mass balances are based on the reports and filtration efficiency of the rotary disc filter and total of 20.64 kg/day of microplastic is collected through the filtration. It processes total of 1.5 million kg/day of final effluent from the Ashbridge bay wastewater. The mass is separated where filtered flow is let out in the lake and the separated microplastic is sent to the pyrolysis process. The energy balance for the Rotary

disc filter would be zero due to no change in temperature during the process. The energy required would be taken from the energy consumption by the manufacture equipment guide. The total energy consumption was calculated to be $2.925*10^7$ KJ/day (In-ENKO, 2018).

6.2.2 Bubbling Fluidized Bed reactor

The mass balance was calculated, and assumptions were made based on pervious report use of bubbling fluidized bed reactor (BFBR). Some textbooks were also used for the thermal decomposition chemical reaction calculation inside the reactor. As the reaction is complex to understand, a simple model was created to show the thermal decomposition reaction equations and rate constants shown in Table 11 below.

Cell → CELLA (Reaction 1)

CellA→ 0.95 HAA + 0.25 Glyoxal + 0.20 CH3CHO + 0.20 C3H6O + 0.25 HMFU + 0.20 CO2 + 0.15 CO + 0.1 CH4 + 0.9 H2O + 0.65 Char (Reaction 2)

CELLA→ LVG (Reaction 3)

Cell→ $5H_2O$ + 6 Char (Reaction 4)

Table 11 Kinematic Reaction (Ranzi, 2008)

Reaction number	Rate Constant
1	k= $8*10^{13}$exp(-46000/RT)
2	k= $1*10^9$ exp(-30000/RT)
3	k= 4*T exp(-10000/RT)
4	k= 8*107exp(-32000/RT)

The rate constant is compared at 790 K and only reaction 2 and 4 are considered for the BFBR. The mass balance thermal decomposition is based off of reports and the stoichiometric mass balance was calculated based off packed bed reactor equations in Foglers 'Elements of Chemical Reaction Engineering' textbook. The composition of the mass entering is steam, nitrogen, and biomass. The mass leaving the reactor is the thermal decomposed product, but it is analyzed in crude oil, syngas, and char for distillation purposes. The product percentage coming out of reactor is based off of previous studies of bubbling fluidized bed reaction for biomass and plastic pyrolysis. It is recommended for a fast pyrolysis type reactor, the operating temperature should be between 450-550 °C (Jahirul.M, 2012). The energy balance is based

on the input of the biomass feed and its physical and chemical properties of cellulose, with the assumption that sanitary textile products are mostly made up of cellulose. The optimum temperature is based on the report for high bio-oil yield in the BFBR (Jahirul.M, 2012).

6.2.3 Distillation Column

The mass and energy balances that were derived for the distillation column were primarily made through the assumptions that were taken from Nelson's Petroleum Refinery Engineering Textbook. The assumed API of the biocrude oil that was 43, as the specific gravity and API of most crude that is composed of cellulose and similar raw components used for this process is around 0.87-0.8 and 35-45 respectively (Nelson, 1968). The density for the assumed API of 43 is calculated to be around 820 kg/m^3 (Nelson, 1968). In addition, based on the calculated API the suggested product compositions were from Petroleum Refinery Textbook for different temperatures cuts was 26.8%, 5.63%, 20%, 10.6% and 36.97% for gasoline, naphtha, kerosene, gasoil, and reduced crude respectively (Nelson, 1968). The products leaving the distillation column are assumed to have percentages of lighter hydrocarbon fuel in lines were also assumed through Figure 10 (Nelson, 1968), where the only pure component leaving the distillation column would be gasoline at 141℃, or 285°F.

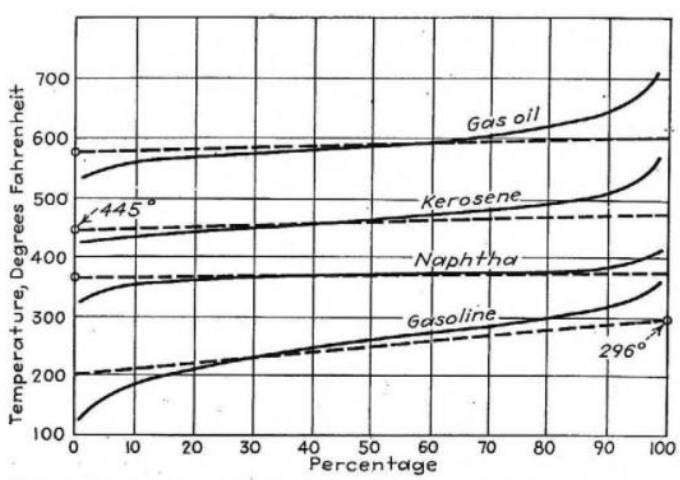

Figure 10 Quantity of Fuel Product Distilled based on Temperature (Nelson, 1968)

The steam that is used in the tower is primarily for temperature control, which would be collected in the receivers or reservoirs of the distillation column located at the bottom (Nelson, 1968). When completing the energy balance the specific heat values were found through Fig 57 in the Appendix section 15.8, where correction values for the specific heat values were need because of the variance in C_p values

that are associated with the components in the mixture for that specific API (Nelson, 1968). Moreover, the enthalpy of the unit and the streams were calculated through considering the sensible heat, specific heat, and latent heat of the components.

6.2.4 Stripping Towers

The stripping towers use stream to strip lighter hydrocarbon fuels from the heavier hydrocarbon product and use reflux streams to bring that back into the distillation column for further separation. The amount of steam required for stripping was found through using enthalpy calculations and the temperature of the steam was found through charts and steam tables indicating the temperature needed for stripping based on the hydrocarbon mixture (Nelson, 1968). Moreover, the amount of unwanted fuel product was assumed through using Figure 10 and through referring to petrochemical charts that indicate product distillate. The assumed percentage of kerosene in the gasoil stripping tower is found to be 2%, percentage of naphtha in kerosene stripper is 4% and the amount of gasoline in the naphtha stripper is 6%. The energy of the stripping towers was calculated through considering the energy required to strip the products which was found through calculating the change in enthalpy in the unit.

6.2.5 Venturi Scrubber

To calculate the mass and energy balance of the scrubber and cyclone units, it is assumed that the gas is incompressible which means that the volume and density of the fluid remain constant. Moreover, the flow of the gas and liquid is assumed to be one dimensional where the flow over the cross-section is negligible. The liquid fed to the scrubber also does not evaporate or flow along the scrubber walls. This means that the amount of liquid and gas entering the scrubber is assumed to be the same as what gets transferred to the cyclone. To find the latent heat of condensation of the condensed tar in the system, the value for toluene at 60°C was obtained as it is assumed to have similar characteristics to tar (Marzouk., 2017). Since the tar composition may vary and it can be difficult to characterize the composition of tar, toluene was used to model tar throughout the report for simplicity.

6.2.6 Heat Exchangers

The heat exchangers that are used in the system are primarily used for cooling the biofuels that are being produced, through using water. The assumptions made for the heat exchanger include that the energy

of the heat exchangers is comprised of the enthalpy and latent heat needed for condensing biofuel vapors. Moreover, the oils that will be entering HXN1, HXN2, HXN3 and HXN4 are considered not to have a correction value associated with the C_p value because the assumed hydrocarbon product is pure (Nelson, 1968). The latent heat and molecular weight of the different fuels from the API of the crude oil was retrieved from Nelson's Petroleum Refining textbook.

6.2.7 Condenser

The calculations pertaining to the condenser used the assumptions that are made from the distillation tower, where the product coming into the condenser is assumed to be 100% gasoline. The assumed temperature of the water coming into the condenser will be a 15℃ and the amount of condensed gasoline refluxing back to the distillation column would be around 20% (Nelson, 1968). In order to optimize the purity of the product, it is suggested that the reflux percentage of the range from 45-60% (Nelson, 1968). However, because the assumption is that the product is all gasoline, the assumed purity of the product will not be affected.

6.2.8 Summary Chart of Mass and Energy Balances

Through performing the mass and energy balance of each unit, an overall scope regarding the quantity of products obtained and the amount of energy needed was calculated. Table 12 shows a summary of all final calculations associated with the equipment and streams. The energy of each stream that was also calculated which was based on the components in the stream was calculated using a reference temperature of around 21℃ for all units. In addition, the sample calculations for the mass and energy content based on the assumptions described for each unit is found in Appendix sections 15.1 through 15.7.

Table 12 Summary of Mass and Balance For Process

Equipment	Equipment label	Stream	Mass Balance Information		Energy Balance Information	
			In (kg/day)	Out (kg/day)	Stream Energy Content (kJ/day)	Total Energy Needed in Equipment (kJ/day)
Disc Filters	CF-1-18	1	1.5×10^6	-	1.256×10^7	2.925×10^7
		2	-	1.5×10^6	1.256×10^7	
		3	-	23.66	3.625×10^1	
Screw Conveyer	SC-1	4	-	2468	1.992×10^3	4.96×10^3
Fluidized Bed Reactor	R-1	5	2468	-	1.992×10^3	1.406×10^9
		6	3871	-	9.724×10^4	
		10+11	839.76	-	3.902×10^4	
		13	339.16	-	-	
		9	-	-	-	
		8	-	-	-	
		7	-	2197.92	3.725×10^6	
		12	-	3871	5.332×10^6	
		41		-	4.28×10^2	
Cyclone	CL-1	7	2197.92	-	3.725×10^6	3.221×10^5
		16	-	2123.76	2.146×10^6	
		14	2000	-	4.376×10^2	
		41	-	-	-	
Distillation Column	DC-1	16	2123.76		2.145×10^6	3.414×10^6
		17	116524		5.294×10^7	
		18	-	624.71	4.015×10^5	
		21	-	452.56	1.351×10^5	
		25	-	95.13	3.424×10^4	
		29	-	337.96	1.661×10^5	

		34	-	179.11	1.146×10^5	
		42	-	116524	5.294×10^7	
		38	-	433.99	9.255×10^4	
Stripping Tower	S-1	25	95.13	-	3.424×10^4	2.071×10^4
		23	11.37	-	2.642×10^3	
		24	-	17.08	1.146×10^4	
		26	-	89.42	1.023×10^4	
	S-2	29	337.96	-	1.661×10^5	9.302×10^3
		30	26.92	-	3.419×10^4	
		28	-	27.10	2.979×10^4	
		31	-	324.44	6.041×10^4	
	S-3	34	179.11	-	1.146×10^5	5.792×10^3
		35	6.97	-	3.399×10^3	
		33	-	10.56	5.249×10^3	
		36	-	175.53	1.062×10^7	
Condenser	C-1	21	452.86	-	1.351×10^5	1.210×10^5
		20	-	90.53	1.275×10^3	
		22	-	362.33	5.105×10^3	
Venturi Scrubber	V-1	38	433.99	-	9.255×10^4	4.781×10^5
		39	304.92	-	1.273×10^4	
		40	-	398.92	6.910×10^2	
		13	-	339.16	4.849×10^4	
Heat Exchangers	HX-1	14	2197.92	-	3.431×10^6	5.787×10^4
		16	-	2197.92	2.145×10^6	
	HX-2	26	89.42		9.677×10^3	7.902×10^3
		27	-	89.42	1.853×10^3	
	HX-3	31	324.44	-	5.698×10^4	4.477×10^4
		32	-	324.44	1.471×10^4	
	HX-4	36	175.33	-	1.001×10^5	8.790×10^4
		37	-	175.33	1.257×10^4	

7. Equipment Design and Sizing

7.1 Rotary Disc Filter

A rotary disc filter is used to filter microplastics from the wastewater treatment plant. It is made up of a shaft of the disc filter with filter cassettes. The filter disc is placed on the shaft of the disc filter. Each disc filter is made up of 12 filter cassettes of annular shape. The filter uses ultrafiltration technique with mesh size between 0.002-0.1 µm. It also has a backwash system to ensure that trapped solids are delivered to a sludge channel and the flow through the filter cloth is restored. Table 13 lists the assumptions made for the rotary disc filter.

Table 13 Assumptions Made for Disc Filters(IN-EnkO,2018)

Parameter	Value	Unit
Disc Diameter	2.2	m
Each Rotary Disc Capacity	36111	m^3/day
Filtration Area	52.9	m^2
Number of Discs	28	-
Number of Cassettes	336	-
Capacity	0.417951	m^3/s

Using the values from the table above, the speed of the filter was calculated to be 7.9 $*10^{-3}$ m/s. Due to the design of the rotary disc filter, changing filter cassettes would be quick and easy. Stainless steel is used in the design as a passive coating as it prevents corrosion and protects from physical damage. The water environment is estimated to have a pH range between 6.5-7.6. The backwash cycle is 4 min idle with a run time of 20 seconds according to the specification set by the In-eko (IN-EnkO,2018).

7.2 Screw Conveyor

Transporting solids is usually more expensive than transporting liquids and gases, which can be easily pumped down a pipeline. Some factors that depend on the best equipment to move solids are the throughput, the length of travel, the change in elevation, and the nature of the solids. Screw conveyors are often used to transport solids over short distances and when some elevation is required. The modern conveyor consists of a helical screw rotating in a U-shaped trough or enclosed pipe. They can be used horizontally or at an incline to lift materials.

The power consumption of a screw conveyor can be correlated using the following equation (Towler et al., 2013):

$$p = 0.038 + 0.0072mL_c^{0.8} \quad (5)$$

Where p= power consumption, hp
m= mass flow, tons/hr
L_c= conveying distance, ft

The coarse screenings (biomass) inlet feed and the microplastic collection from the disc filtration process sums up to a total of 4693.17 kg/day. The distance the feed is travelling from Ashbridge's Bay to the reactor in the plant is assumed to be 20 m. Once these values were converted to the acceptable units, the total power consumption of the screw conveyor in our system is 0.077 hp as shown in the Appendix section 15.10. The type of feed material is granular, free flowing, and contains explosive dust. This type of material has a 45% recommended trough loading (Perry et al., 1997). For the calculated power consumption, the optimal size of conveyer is 0.254 m with a pipe size of 0.0508 m. Table 14 summarizes the sizing of the screw conveyor.

Table 14 Summary Table for Belt Conveyer

Parameter	Value	Unit
Mass Flowrate	4693.117	kg/day
Conveying distance	20	m
Power Consumption	0.077	hp
Recommended trough loading	45	%
Optimal size of conveyor	0.254	m
Pipe Size	0.0508	m

7.3 Design of Bubbling Fluidized Bed Reactor

After the feed is pretreated by drying, it is fed into the reactor (BFBR) using a screw conveyor. The residence time for the solid particles is lot longer than the vapor product. The reactor does have control function to remove the solid particle inside the reactor if necessary. To design the vessel to handle the pressure inside the reactor, ASME BPV Code Sec.VIII Division 1 was used. The safety factor of 3.5 against

tensile failure and 1.25 for 100,000-hour creep rupture was used according to the code. This code design gives us the flexibility of a maximum allowable pressure of 204 atm. The vessel will have a vertical orientation making it take up less space. The ASME BPV follow four categories of welds to ensure that the finished weld joint approximates the quality of the seamless parent material of stainless steel. The four categories of welds are as follows and used for choosing in the pressure vessel design (Towler et al., 2013):

- Category A: Longitudinal or spiral welds in the main shell, necks or nozzles, or circumferential welds connecting hemispherical heads to the main shell, necks or nozzles.
- Category B: Circumferential welds in the main shell, necks or nozzles or connecting a formed head other than hemispherical.
- Category C: Welds connecting flanges, tube sheets or flat heads to the main shell, a formed head, neck or nozzle.
- Category D: Welds connecting communicating chambers or nozzles to the main shell, to heads or to necks.

Table 15 Summary of Parameter details for the Fluidized Bed Reactor (Towler et al., 2013).

Parameter		Value	Justification
Maximum Allowable	Pressure in Vessel, P (Assumed)	10 atm	Arbitrary chosen assuming as the initial design value
	Design Temperature, T (Assumed)	1500 K	Arbitrary since the process is controlled with PID and won't exceed 1000 K temperature
Other Parameter	Factor of Safety, f_s	3.5	The Following code was used ASME BPV Code Sec VIII D.1
	Diameter of Reactor, D (Assumed)	0.5 m	Arbitrary chosen assuming as the initial design value
	Joint Efficiency, E	0.85	Double-welded butt joint or equivalent with join category of A, B,C,D.

7.3.1 Design of Reactor Vessel wall Thickness

In a bubbling fluidized bed reactor, the main stress load is experienced in longitudinal and hoop stress. The value of the thickness of the reactor was calculated using the stress and picked according to the total thickness from the longitudinal and hoop stress. The total thickness for the reactor vessel was calculated to be 7.4 mm (Towler et al., 2013).

Thickness for the Hoop Stress,

$$t = \frac{P_i * D_i}{2SE - 1.2P_i} \tag{6}$$

Where, P_i is the maximum internal pressure allowed (N/m^2)

D_i is the diameter of the reactor vessel (m)

S is the allowable stress (N/m^2)

E is the join efficiency

t is the wall thickness(m)

Thickness for the Longitudinal Stress,

$$t = \frac{P_i * D_i}{4SE + 0.8P_i} \tag{7}$$

Minimum Wall thickness = Hoop wall thickness + Longitudinal wall thickness

= (4.96 + 2.44) mm = 7.4 mm

7.3.2 Design of Distributor Plate

To find the dimensions and the specification of the distributor plate first the porosity of the bed at minimum fluidization velocity and the gas velocity at minimum fluidization velocity should be calculated using equation 8 and equation 9

$$\mathrm{n} = \mathrm{g}(\rho c - \rho g) \tag{8}$$

Where, g is the acceleration due to gravity(m/s^2)

ρc is the density of the particle (Kg/m^3)

ρg is the density of the fluidizing gas(Kg/m^3)

n is the gravitational term (Kg/s^{2}cm^2)

$$\varepsilon mf = 0.586\,\psi^{-0.72}\left(\frac{\mu^2}{\rho g * n * dp^3}\right)^{0.029}\left(\frac{\rho g}{\rho c}\right)^{0.021} \quad (9)$$

$$u_{mf} = \frac{(\psi * d_p)^2}{150u} g(\rho c - \rho g)\left(\frac{\varepsilon mf^3}{1-\varepsilon mf}\right) \quad (10)$$

Where, εmf is the voidage at minimum fluidization velocity(m/s)

ψ is the voidage

μ is the viscosity of fluidizing gas (kg/m.s^2)

dp is the diameter of the particle (m)

umf is the minimum fluidization velocity(m/s)

7.3.4 Superficial velocity (u_s)

The superficial gas velocity will be chosen between the minimum fluidization velocity, the terminal velocity, and the minimum slugging velocities. The velocity must be higher than the minimum fluidization velocity but less than the terminal and slugging velocity to function as a fluidized bed reactor. Assuming a velocity of 0.1 m/s which is higher than the minimum fluidizing velocity, the terminal velocity can be calculated using the following equation 11

$$u_t = \frac{g(\rho c - \rho g)\ \ d_p^2}{18u} \quad (11)$$

Where, u_t is the terminal velocity(m/s)

Since the assumed velocity is lower than the terminal velocity, it is safe to select this velocity for the fluidization of the bed. From that we find the height of the bed during minimum fluidization, which is important to determine the height of the feed. The height was calculated to be around 0.58 m. One of the main factors to consider while designing the reactor is the pressure drop. The pressure drop is determined using the voidage and the height of the particle inside the reactor. Since the minimum fluidization height is set at 1.8m, the height of the reactor could be determined using the bubble size in the reactor. The bubble size is calculated using equation 12, 13 and 14

$$\text{Initial bubble size } (d_o) = 0.00376(u_o - u_{mf})^2 \quad (12)$$

$$\text{Assumed bubble size } (d_b) = 0.0016\text{m} \quad (13)$$

$$\text{bubble size at the bottom } (d_{bm}) = 0.652[A_o(u_o - u_{mt})]^{0.4} \quad (14)$$

Where, d_o is the initial bubble size(m)

u_o is the fluidizing gas velocity(m/s) (Assumed more than the minimum and lower than terminal velocity)

A_o is the Distributor plate area (m^2)

By the combining the equation above, the average bubble diameter was calculated with a size of 0.03139 m using the equation 11:

$$d_{bavg} = d_{bm} - (d_{bm} - d_{b0})e^{-0.3h/D_t} \quad (15)$$

The average bubble diameter will help us determine the height of the reactor itself with Darton et al. (Perry et al., 1997).

$$d_b = \frac{0.54(u - u_{mf})^{0.4}(h + 4\sqrt{A})^{0.8}}{g^{0.2}} \quad (16)$$

Where, h is the height of the freeboard space(m)

D_t is the diameter of the reactor(m)

Using the equation 12, the freeboard height was determined with a height of 0.565m and adding the height of the minimum fluidized bed height of 1.846 m, a total height of the reactor was calculated to be 2.411 m.

7.4.5 Bed Pressure Drop

$$\Delta p = hp(1 - \varepsilon)\, g(\rho c - \rho g) \quad (17)$$

Where, Δp is the pressure drop in the bed particle (N/m^2)

ε is the voidage

hp is the height of the particle (m)

In relation with the bed pressure drop, the distributor pressure drop is set about the 30 % of the pressure drop of 5654.87 N/m^2. With the value of the pressure drop for the distributor plate the gas velocity through each orifice is calculated with a value of 42.1 m/s. This is considered to have be safe for the design.

$$u_0 = C_D * \frac{[2 * \Delta p \quad]^2}{\rho g^2} \tag{18}$$

Where, Δp is the pressure drop in the bed particle (N/m^2)

C_D is the Orifice coefficient

hp is the height of the particle (m)

The number of orifices per unit area was also calculated to know the amount of the orifices in the distributor plate. By assuming the orifice diameter of 0.003 m, the number of orifices per m^2 was amounted to 336/m^2. The orifices were placed in a triangular pitch setting. The triangular pitch was calculated to be 58 mm using the following equation.

$$P = \sqrt{(\frac{2}{N\sqrt{3}})} \tag{19}$$

The number of orifices per nozzle is about 13 in the distributor plate area of 0.19634 m^2. Now the diameter of the nozzle is calculated using equation 16:

$$d_n > \sqrt{n * d_0} \tag{20}$$

Where, d_n is the diameter of the nozzle (m)

n is the number of nozzle

The nozzle diameter was calculated to be higher than 5.19 mm, so a safe 10 mm diameter nozzle was selected to distribute the fluidizing gas for the bed. The thickness of the distributor plate was decided with the corrosion allowance of 63% of the total thickness used in the reactor. The distributor plate nozzle thickness is about 0.2mm to withstand the hoop and longitudinal stress from the velocity of the fluidizing gas.

7.4.6 Diffusion and Mass Transfer Analysis

The mass transfer and reaction parameters somewhat show the process in the fluidized bed reactor using the following equation 21 and equation 22. The equation gives us the mass transfer coefficient between he bubble-cloud and cloud-emulsion to determine the overall mass transfer coefficient in the

BFBR. The bubble model (Kunii and Levenspiel) assumes constant-sized bubbles (effective bubble size d_b) rising through the suspension phase. Gas is transferred from the bubble void to the mantle and wake at mass transfer coefficient K_{bc} and from the mantle and wake to the emulsion phase at mass-transfer coefficient K_{ce}. While the bubble size changes in real life but the reactor performance evaluation can be obtained from these analyses (Perry et al., 1997).

$$K_{bc} = 4.5\left(\frac{u_{mf}}{d_b}\right) + \left(\frac{5.85\left(D_{AB}^{\frac{1}{2}} g^{\frac{1}{4}}\right)}{d_b^{\frac{5}{4}}}\right) \tag{21}$$

$$K_{ce} = 6.78\left(\frac{E_{mf} D_{AB} u_b}{d_b^3}\right)^{\frac{1}{2}} \tag{22}$$

Where, K_{bc} is the mass transfer coefficient bubble-cloud

K_{ce} is the mass transfer coefficient cloud-emulsion

D_{AB} is the mass diffusion coefficient of the fluid

To find the overall mass transfer coefficient in the bubbling fluidized reactor, the mass transfer coefficient between the bubble-cloud and cloud-emulsion was calculated. These values help determine the limitation for scale up as, it is possible for reaction to dominate in a lab unit with small bubbles and for diffusion to dominate in a plant size unit. The Overall mass transfer coefficient was 1.18 meaning that the dominating factor is the rate of reaction, which is very high in the chemical reaction. There will not be a problem while scaling up with the limiting factor of rate of reaction (Perry et al., 1997). Summary of assumed properties and calculated values are shown in Table 16 and 17 below.

Table 16 Assumed Values and Properties Assumed for Reactor (Towler et al., 2013)

Parameter	Value
Diameter of the reactor, D (Assumed)	0.5m
Initial Height of the sand	0.1 m
Initial Height of the sand	0.67m
Initial Height of the particle	0.77m
Density of the gas	1.225kg/m^3
Density of the Sand	1500 kg/m^3
Density of the particles (Sand + biomass)	1530 kg/m^3
Diameter of particle coarse sand	0.00025 m
Acceleration due to gravity	9.81 kg/m^3
Dynamic viscosity	3.4*10^{-5} kg/ms
Natural porosity of sand	0.5

Table 17 Calculated Values for Reactor Design

Parameter	Value
Diameter of the reactor	0.5m
Height of reactor	2.411 m
Residence time	10 sec
Bed Pressure Drop	5654.87 N/m^2
Superficial velocity	0.1 m/s
Number of orifices	13
Reactor vessel thickness	7.4 mm
Distributor plate thickness	7.48mm
Jet height for the orifice	20.93 mm
Minimum nozzle height	0.072 m
Distributor plate nozzle thickness (Safe resistant)	1.79 mm
Overall transport coefficient	1.18
Conversion	0.99

7.3.7 Chemical Reaction

Chemical analysis of the undergoing reactions in the reactor was completed using the packed bed reactor analysis from the (Fogler,2005). The dominant reaction is the thermal decomposition of activated cellulose inside the reactor with the highest rate of reaction of $1.04x10^7\ s^{-1}$. This value was obtained from a research study on the kinematic reaction for a cellulose or biomass pyrolysis reaction as shown in Table 18 (Ranzi, 2008). As it is difficult to determine the composition of the reaction, the best possible parameter to use was from previous report to find the composition of bio-oil of 76.9%, Syngas 19.75% and Char as 3.66%.(Jahirul.M, 2012).

Table 18 Chemical Composition of BioFeed (Ranzi,2008)

Species	Change	Leaving	Concentration (kmol/m^3)	Mol fraction
Cellulose ($C_6H_{10}O_5$)	- $F_{Ao}X$	$F_A= F_{Ao}(1-X)$	1.56E-05	1(feed)
HAA($C_2H_4O_2$)	$0.475F_{Ao}X$	$F_B= 0.475F_{Ao}X$	7.33E-04	0.063973
Glyoxal ($C_2H_2O_2$)	$0.125F_{Ao}X$	$F_C= 0.125F_{Ao}X$	1.93E-04	0.016835
C_2H_4O	$0.1F_{Ao}X$	$F_D= 0.1F_{Ao}X$	1.54E-04	0.013468
C_3H_6O	$0.1F_{Ao}X$	$F_E= 0.1F_{Ao}X$	1.54E-04	0.013468
$C_6H_6O_3$	$0.125F_{Ao}X$	$F_F= 0.125F_{Ao}X$	1.93E-04	0.016835
CO_2	$0.1F_{Ao}X$	$F_G= 0.1F_{Ao}X$	1.54E-04	0.013468
CO	$0.075F_{Ao}X$	$F_H= 0.075F_{Ao}X$	1.16E-04	0.010101
CH_4	$0.05F_{Ao}X$	$F_I= 0.05F_{Ao}X$	7.71E-05	0.006734
H_2O	$2.95F_{Ao}X$	$F_J= 2.95F_{Ao}X$	4.55E-03	0.397306
Char (C)	$3.325F_{Ao}X$	$F_K= 3.325F_{Ao}X$	5.13E-03	0.063973

7.4 Centrifugal Separator Cyclone

A cyclone is used for solid-gas separation for the charcoal and the biogas. Centrifugal force is employed to achieve gas-solid separation in the cyclone. It is designed for high temperatures and a suitable pressure for the operation. The average particle size of the biomass char is considered to be around 250 µm. The reverse flow cyclone is used as the gas enters the top chamber tangentially and spirals down to the apex of the conical section. It then moves upwards in a second, smaller diameter spiral and exits at the top through a central vertical pipe. The solids move radially to the walls, slide down the walls, and are collected at the bottom. Stairmand's method is used to design the cyclone for a high-efficiency cyclone as shown in Equation 23 and Table 19 below (Towler et al., 2013):

$$d_2 = d_1 \left[\left(\frac{D_2}{D_1} \right)^3 * \frac{Q_1}{Q_2} * \frac{\Delta\rho_1}{\Delta\rho_2} * \frac{u_2}{u_1} \right]^{\frac{1}{2}} \quad (23)$$

Where, d_1 is the mean diameter of particle separated at the standard conditions, at the chosen separating efficiency (m)

d_2 is the mean diameter of the particle separated in the proposed design, at the same separating efficiency (m)

Dc_1 it the diameter of the standard cyclone = 8 inches (203 mm)

Dc_2 is the diameter of proposed cyclone, mm

Q_1 is the standard flow rate:

for high-efficiency design = 223 m3/h

for high-throughput design = 669 m3/h

Q_2 is the proposed flow rate, m3/h

$\Delta\rho_1$ is the solid-fluid density difference in standard conditions = 2000 kg/m3

$\Delta\rho_2$ is the density difference, proposed design

μ_1 is the test fluid viscosity (air at 1 atm, 20 °C)

= 0.018 mN s/m2

μ_2 is the viscosity, proposed fluid

Table 19 Stairmand's method to determine the scaling factor (Towler et al., 2013)

Parameter	Value
Diameter of standard cyclone, D_1	203 mm
Diameter of proposed cyclone, D_2 or D_c	336 mm
Standard flow rate (high-efficiency design), Q_1	223 m^3/h
Proposed flow rate, Q_2	367.2 m^3/h
Standard solid-fluid density difference	2000 kg/m^3
Proposed density difference	1000 kg/m^3
Test fluid visocisty (air at 1 atm, 300C)	0.03547 mNs/m^2
Proposed fluid viscosity	0.034 mNs/m^2
Friction factor for gases	0.005

Pressure drop analysis is one of the main features of the cyclone. The pressure drop in a cyclone will be due to the entry and exit losses and friction and kinetic energy losses in the cyclone. The empirical equation given by Stairmand (1949) (equation 24) can be used to estimate the pressure drop. The main things to consider in the Stairmand equation is the cyclone pressure drop factor shown in figure 11, which is obtained by using a void fraction of 0.63 and the radius ratio of 1.8. Moreover, only one highly efficient cyclone was needed due to the capacity. The standard air inlet velocity used was 15 m/s to calculate the cyclone diameter, and other dimensions were scaled accordingly (Towler et al., 2013). This helped us determine the scale up factor of 2.39. The cyclone pressure drop was calculated to be 1.49 mm of H_2O, which is very low to consider for air blower but was put in place in the plant design in case it was needed.

$$\Delta P = \frac{\rho f}{203}\left[u^2\left[1 + 2\Phi^2\left(\frac{2r1}{re}\right) - 1\right] + 2u_2^2\right] \tag{24}$$

Where, ΔP is the cyclone pressure drop (millibars)

ρf is the fluid (gas) density (kg/m3)

u1 is the inlet duct velocity (m/s)

u2 is the exit duct velocity (m/s)

rt is the radius of circle to which the center line of the inlet is tangential (m)

re is the radius of exit pipe (m)

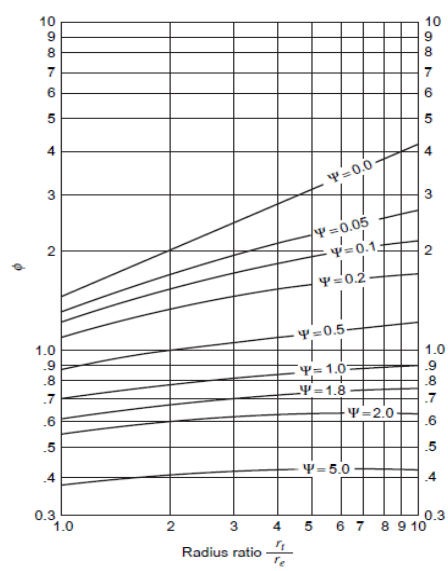

Figure 11 Entrainment of Cyclone

The sizing of the cyclone is done through Towler et al.'s Equipment Design Principle textbook with the following dimensions for a high efficiency cyclone as shown in Figure 12(Towler et al., 2013)

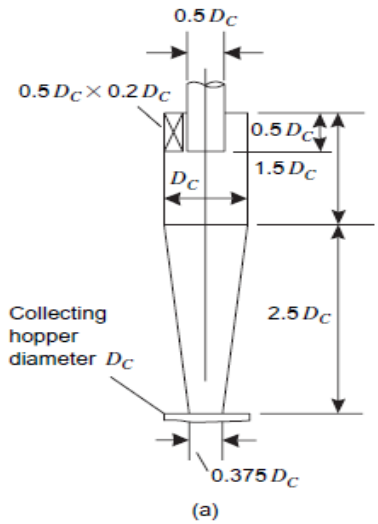

Figure 12 Cyclone Dimensions (Towler et al., 2013)

The following parameters of the cyclone was decided from the assumed and standard values of the cyclone in Table 20.

Table 20 Summary of Cyclone Dimensions

Parameter	Value
Scaling factor	2.39
Area of inlet duct	11289.6 mm^2
Cyclone surface area	1418693 mm^2
Void	0.63
r1/r2 ratio	1.8
Φ	0.89
Inlet speed	9.03 m/s
Area of exit pipe	22167.08 mm^2
Outlet speed	4.6 m/s
Pressure drop	1.49 mm H_2O

Using the cyclone dimension calculated, the following proposed cyclone was designed with the units in mm in Figure 13.

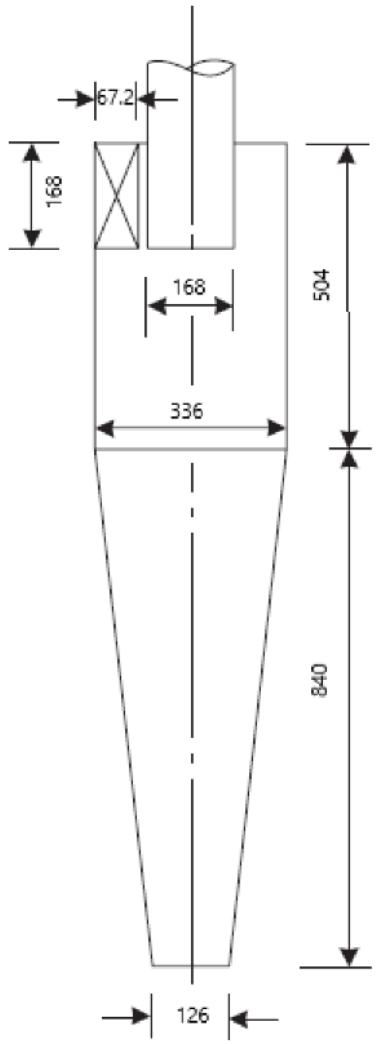

Figure 13 Proposed Plan with Dimensions Calculated Cyclone

7.5 Distillation

The design of the distillation column was separated into two phases to help organize calculations and theories so that the design of a multicomponent distillation column can be achieved. The first phase comprised of gathering information from journals and petrochemical textbooks to find the number of trays needed in the column. The second phase was directed towards finding the dimensions of the tower and understanding the hydraulic behavior that would be present in the column during the distillation process.

7.5.1 Calculation of Column Trays

Distillation processes are used to separate components based on deriving a relation between temperature, partial pressures, and relative volatility to understand the composition of the mixture as it changes with temperature. The biocrude oil that was synthesized in this process is based off a crude oil blend that was given in Nelson's Petroleum Refinery textbook, which was around 43 API (Nelson, 1968). Usually in binary distillation, the McCabe Thiele method is used, and vapor liquid equilibrium data would suffice in understanding the relationship of mixture composition with changes in temperature and pressure (Nelson, 1968). However, for multicomponent distillations the Fenske-Underwood-Gilligand (FUG) equations are usually used. Through the FUG method, this would help to calculate the minimum reflux ratio, the number of theoretical stages, and feed location (Nelson, 1968). The Fenske equation shown below, helps to estimate the minimum number of stages required at total reflux (Towler et al., 2013).

$$(\frac{x_i}{x_r})_d = \alpha_i{}^{Nmin}(\frac{x_i}{x_r})_b \tag{25}$$

$$Nmin = \frac{\log(\frac{x_{LK}}{x_{HK}})_d(\frac{x_{HK}}{x_{LK}})_B}{\log \alpha_{LK}} \tag{26}$$

Where, $\frac{x_i}{x_r}$ is the ratio of concentration of any component and (i) of a reference component

(r) in either the distillate

(d) or the bottoms (b)

$Nmin$ is the minimum number of total stages

α_i is the relative volatility of the component i

α_{LK} is the average relative volatility with respect to heavy key components x_{HK} light key component x_{LK}.

Moreover, to calculate the minimum reflux ratio, Underwood equations should be calculated using the following equation (Towler et al., 2013):

$$\Sigma\frac{\alpha_i x_{i,d}}{\alpha_i - \theta} = R_{min} + 1 \tag{27}$$

Where, R_{min} is the minimum reflux ratio.

$x_{i,d}$ is the relative volatility of component i in the distillate

The underwood equation, more formally undated into the Kirkbride equation, aids in calculating the feed location in the tower using the following equation (Towler et al., 2013)

$$\log\left(\frac{N_r}{N_s}\right) = 0.206\log\left(\left(\frac{B}{D}\right)\left(\frac{x_{b\ LK}}{x_{d\ HK}}\right)\left(\frac{x_{f\ HK}}{x_{f\ LK}}\right)\right)^2 \tag{28}$$

Where, N_r is the number of stages above the feed

N_s is the number of stages below the feed

$x_{f\ HK}$ is the concentration of heavy key components in the feed

$x_{f\ LK}$ is the concentration of light key components in the feed

B and D are the flow rates of the bottoms and distillate respectively

$x_{b\ LK}$ is the concentration of light keys in the bottom

$x_{d\ HK}$ is the concentration of heavy key in the bottoms

Although the FUG method is a common method to find the basis of the distillation column structure, it does not consider side streams because the products are divided into either light key or heavy key components that come from either the bottom in the distillate or from the top (Liu, 2012). To account for calculating the number of trays and feed point location, a journal published by the School of Chemical Engineering and Analytical Science suggested that a decomposition method in multicomponent distillation systems is gives analogous results to the FUG method (Liu, 2012).

The decomposition method proposes that the FUG calculations can be made through linking the distillation column and the side streams that would be going into side strippers as a consecutive process (Liu, 2012). Through breaking down the process and compartmentalizing the distillation column based on the flow of the heavy and light key components, side streams are eliminated, and FUG calculations can be used as shown in Figure 14. The calculations with the decomposition method using the FUG equations and the distillation column with side streams modeled using HYSY were compared, and it is notable that is a ±10% error between the calculated and modelled results as shown in Figure 15 (Liu, 2012).

.

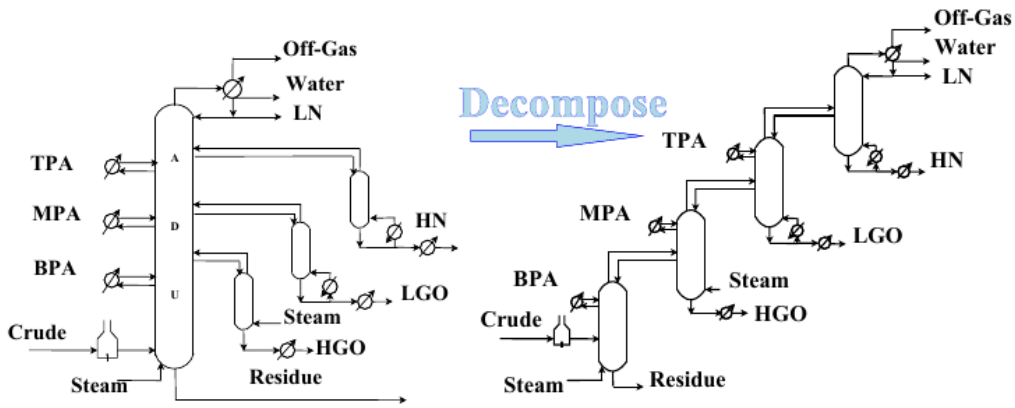

Figure 14 Decomposition Method that enables the use of FUG Equations (Liu, 2002) .

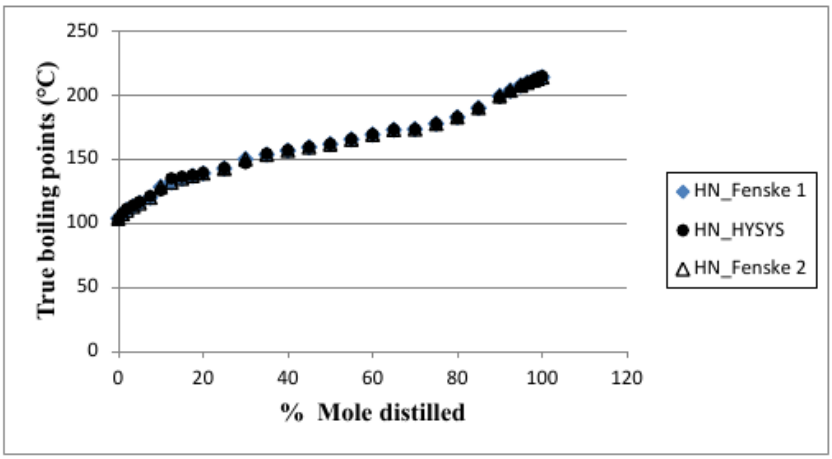

Figure 15 Comparisons made between Decomposition Method Calculations and HYSYS Modelling (Liu, 2002)

Through using the decomposition theory, the data used in the journal was for a crude assay that had an API of around 41.7 which is very close to the API of the biocrude oil used in this process (Liu, 2012). The ASTM and True Boiling Point (TBP) data were gathered for crude oil assays that had an API of 43 and was compared to the assay and charts given in the journal where the results were very similar. Through the TBP data, the amount of product distilled can be found at a given temperature, which would essentially help draw relations to the number of cuts, which is the number of draws or products and the fractions of the components based on the relative volatility calculations (Liu, 2012). The crude assays that were used and compared are found in the Appendix section 15.8, through looking at HYSYS generated TBP charts that displayed for the crude oil and the components that influenced the amount of distillate retrieved shown in Figure 16 and Table 21 respectively, the number of plates was calculated (Liu, 2012).

.

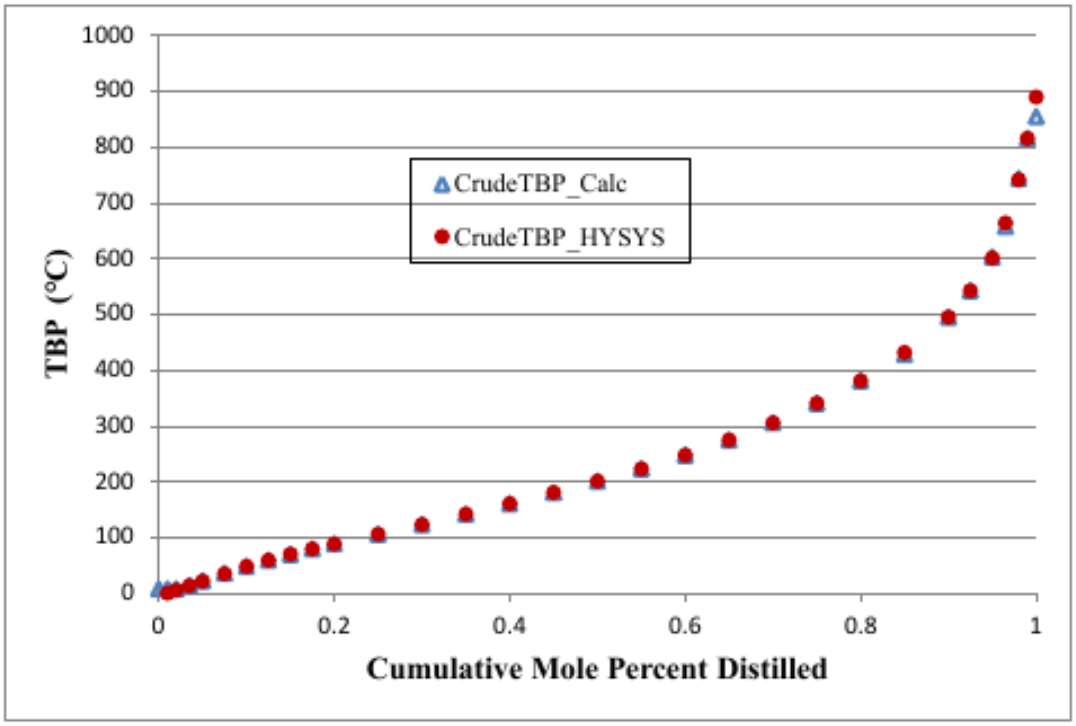

Figure 16 TBP Data that was used to Find Number of Trays (Liu, 2012)

Table 21 Component mole fractions used in comparisons Crude Assay (Liu, 2012).

Component No	NBP (°C)	$x_{i,f}$ (Mole fraction)	f_i (kmol/h)
1	9	0.0502	131.0629
2	36	0.0488	127.4277
3	61	0.0581	151.5974
4	87	0.0709	185.0241
5	111	0.0711	185.6084
6	136	0.0687	179.2449
7	162	0.0661	172.4852
8	187	0.0614	160.2055
9	212	0.0569	148.6483
10	237	0.0517	134.9129
11	263	0.0467	121.8539
12	288	0.0415	108.2346
13	313	0.0373	97.2869
14	339	0.0342	89.2142
15	364	0.0313	81.6637
16	389	0.0286	74.5765
17	414	0.0259	67.6652
18	447	0.0361	94.3710
19	493	0.0267	69.7825
20	538	0.0210	54.9362
21	584	0.0177	46.1598
22	625	0.0126	32.8241
23	684	0.0151	39.2967
24	772	0.0113	29.5907
25	855	0.0103	26.9965

Through comparing the values that were retrieved from HYSYS simulation in the journal that used data from a crude assay that had an API very similar to the process oil, the number of plates that are

estimated for the distillation column in this process is 29. Moreover, this number of trays was referenced through various other petrochemical textbooks as it is stated that the average number of trays in oil refineries was around 20-45 trays, which is primarily based on the API of the crude (Watkin,1979). Referring to Nelson's and Watkin's textbooks also helped give an indication of whether this assumption can be valid and through referring to Figure 17 (Nelson, 1968). Referring to the data calculated in the journal, the number of cuts given in the journal to be around 32 and at a temperature of 10-15°F, thus the number of theoretical plates are around 22 and the number of actual plates range from 25-35, thus 29 is a safe assumption to conclude for this distillation column (Nelson, 1968). The feed location is normally on the fourth trays in oil refineries as suggested in the Kister's textbook, and the reflux ratio often ranges from 1.2-1.5 (Kister, 1992). Therefore, the distillation column feed will be entered on the fourth tray and the reflux ratio will be 1.2 to carry out the rest of the calculations (Kister, 1992).

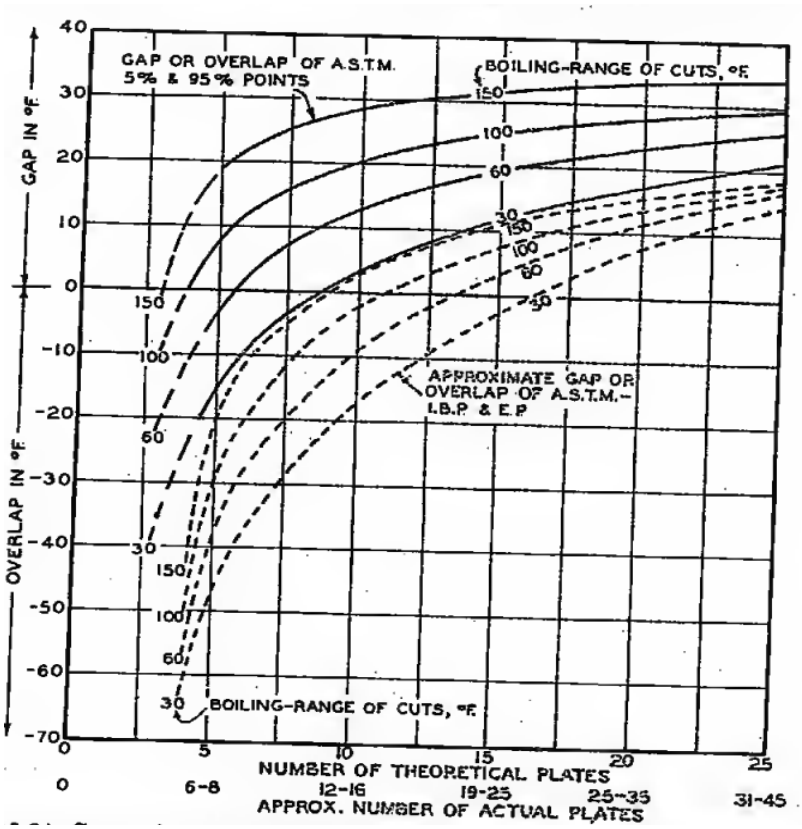

Figure 17 Number of Actual Plates in the Distillation Column (Nelson, 1968)

7.5.2 Calculation of Column Dimensions

In order to calculate the dimensions of the distillation column and understand the hydraulic behavior in the column, Towler et al.'s Chemical Engineering Design textbook was primary used to help choose the correct assumptions. The diameter of the distillation column was first calculated through calculating the minimum vapor and liquid velocities that would lead to flooding and would be circulating throughout the column (Towler et al., 2013). A mass balance was calculated, where the bottoms were considered as any product drawn below the feed and the distillate was considered as any product drawn above the feed (Towler et al., 2013). The calculated flooding vapor velocity and diameter that was calculated for the top and bottom of the column were primarily used using the following equation (Towler et al., 2013):

$$u_f = K_1 \sqrt{\frac{\rho_l - \rho_l}{\rho_v}} \tag{29}$$

Where, u_f is the flooding velocity in (m/s)

K_1 is the constant obtained from Fig 51 in the Appendix section 15.12

ρ_l and ρ_v are the liquid and vapor densities of the products respectively.

The vapor and liquid density for the distillate was assumed to be a combination of the most volatile and most abundant products taken from the distillation which were gasoline and kerosene. The flooding velocity was calculated to be around 0.47 m/s at the bottom and 0.45 m/s at the top. The flooding velocity was assumed to be 85% and the downcomer area as assumed to be 12% (Towler et al., 2013). The column diameter (D_c), was calculated through finding the cross-sectional area (A_c) and volumetric flow rate using equation 31, was calculated to be 0.5m at the bottom and 1.71m at the top. Through the calculations, it is evident that the inner column diameter must be around 1.71m (Towler et al., 2013).

$$A_c = \frac{V_{flowrate}}{u_f} \tag{30}$$

$$D_c = \sqrt{\frac{4 \times A_c}{\pi}} \tag{31}$$

The height of the column was estimated through assuming that the tray spacing was 0.5m and that the column has a hemispherical top, as it is the most resistive to external pressures (Towler et al., 2013). The top and the thickness of the tray will be assumed to be around 5mm thick (Towler et al., 2013). Thus, considering that there are 29 trays in the column, the calculated height for the column is around 16.9m which will be rounded to 17m. This height is also suitable as the critical buckling stress that was calculated was 206 N/mm^2 and the maximum compressive stress which was calculated to be maximum compressive stress was found to be 14.06 N/ mm^2 (Towler et al., 2013). This signifies that the column will not experience any type of buckling (Towler et al., 2013). In addition to this, the hydraulic behavior has examined so that the column does not experience any weeping or flooding were checked through calculating the weep point and weir crest using the following equations (Towler et al., 2013).

$$u_h = \frac{(K_2 - 0.90\ (25.4 - d_h))}{{\rho_v}^{1/2}} \tag{32}$$

$$h_{ow} = 750\ \frac{L_w}{\rho_L I_W}^{2/3} \tag{33}$$

Where u_h is minimum vapor velocity through holes (m/s)

d_h is hole diameter (mm)

K_2 constant based on the depth of clear liquid on the plate

h_{ow} is weir crest (mm liquid)

L_w is the liquid flow rate (kg/s)

I_W is the weir length in (m)

The purpose of the column trays is so that it provides sufficient space for vapor-liquid contact through an active area (Towler et al., 2013). The sieve tray was chosen because it was the simplest type of tray, it offers a low pressure drop and is most cost effective. Although, it is normally used for crossflow, it can also be used for reverse flow conditions which is what this process needs. Bubble cap trays were primarily considered since bubble trays performed better with effective vapor and liquid flow rates (Towler et al., 2013). However, due to the minimal pressure drop, decreased fouling and economic value sieve plates are chosen. The efficiency of the column is usually around 30-80%, thus, the efficiency that was assumed was 60% (Towler et al., 2013). The insulation that was chosen for the distillation tower was

mineral wool instead of foam glass or fiber glass (Towler et al., 2013). Mineral wool was chosen because it is the most common type of insulation that are used in vessels, in addition it has excellent properties to prevent heat transfer (Towler et al., 2013). Mineral wool can stabilize the convection of air through the density, thickness, and the composition of the wool (Kister, 1992). Although the thickness of the insulation will change based on the height of the column and the temperature at which the section of the column is at, the thickness of the insulation will be around 100-200mm (Towler et al., 2013). The following assumptions and calculations for the design of the distillation and the hydraulic specifications are summarized in Table 22.

Table 22 Summary Table of Assumptions and Design Calculations for the Distillation Column (Towler et al., 2013)

Assumptions	
Plates	29
Efficiency (%)	60
Plate Spacing	0.5
Type of Insulation	Mineral Wool
Thickness of Insulation (m)	0.2
Minimum Reflux Ratio	0.2
Plate Thickness (m)	0.05
Hole Depth (m)	0.05
Weir Height (m)	0.5
Calculated	
Column Inner Diameter (m)	1.547
Approximate Height (m)	17
Flow Pattern	Reverse flow
Weir Length (m)	1.176
Total Active Area (m^2)	0.100
Area of 1 Hole (m^2)	1.96×10^{-5}
Minimum Vapor Velocity (m/s)	0.474
Flooding %	52.3
# of Holes	5097.9

7.6 Stripping Towers

The process to calculate the stripping towers were very similar to the calculations pertaining the design of the distillation tower. The number of trays of each stripping tower was estimated to be around 4 trays, as this is the ideal and most common number of trays used for side strippers in oil refineries (Kister, 1992). When calculating the dimensions of the column, it was assumed that the tray thickness is 5 mm and

the column thickness is around 9 mm (Towler et al., 2013). The insulation for the towers will also be mineral wool as this will disable convection, conduction, and radiation from external factors. The thickness of the wool will be around 200 mm and the efficiency of the vessel will also be assumed to be around 60% (Towler et al., 2013). A summary that describes the following information regarding the design parameters for the stripping towers are in Table 23.

Table 23 Summary Table of Assumptions and Calculated for Stripping Tower Design

Assumptions			
Stripping Tower	S-1	S-2	S-3
Plates	4	4	4
Efficiency (%)	60	60	60
Plate Spacing	0.5	0.5	0.5
Type of Insulation	Mineral Wool	Mineral Wool	Mineral Wool
Thickness of Insulation (m)	0.2	0.2	0.2
Reflux Ratio	1.2	1.2	1.2
Plate Thickness (m)	0.05	0.05	0.05
Hole Depth (m)	0.05	0.05	0.05
Weir Height(m)	0.5	0.5	0.5
Calculated			
Column Inner Diameter (m)	0.296	0.493	0.335
Approximate Height (m)	3	3	3
Flow Pattern	Reverse flow	Reverse flow	Reverse flow
Weir Length (m)	0.2551	0.3748	0.2553
Total Active Area (m^2)	0.00366	0.0713	0.0165
Area of 1 Hole (m^2)	1.96×10^{-5}	1.96×10^{-5}	1.96×10^{-5}
Vapor Velocity (m/s)	0.204	0.293	0.304
# of Holes	187	518	240

7.7 Condenser

The condenser that will be near the top of the distillation tower and will be a water-cooled condenser. The sizing of the condenser was very similar to sizing a shell and tube heat exchanger, where the horizontal side will be the shells and the vertical side will have the tubes (Towler et al., 2013). Based off the TEMA design standards, it is also suggested that the tube diameters are 6.4-50 mm as the best standard diameter for cost and operation (Towler et al., 2013). The assumption will be that the tubes have an inner diameter of 16.8 mm, outer diameter of 20 mm and a length of 4.88 m long (Towler et al., 2013).

The material of the tubes will be steel, assuming a square pitch (Towler et al., 2013). For the shell side, carbon steel will be used and the dam baffle spacing will be assumed to be 45% (Towler et al., 2013). In order to find the actual shell inner diameter ($S_{i.d}$), the following equation were used, in which the bundle diameter (D_b) was added to the assumed clearance spacing D_s which was 0.095 m (Towler et al., 2013).

$$D_b = d_0 \left(\frac{N_t}{K_1}\right)^{\frac{1}{n1}} \tag{34}$$

$$S_{i.d} = D_b + D_s \tag{35}$$

Where, N_t is the number of tubes

K_1 and $n1$ are obtained from constants for a square pitch with two passes

d_0 is the tube outside diameter

D_b is the Bundle Diameter

D_s is the Clearance Spacing

$S_{i.d}$ is the inner Shell Diameter

In the condenser gasoline will be entering at 141ºC and leaving at 26.6ºC from the condenser. There were multiple iterations done to find the proper parameters of the condenser. The overall heat transfer coefficient was calculated through using the following equation (Towler et al., 2013).

$$\frac{1}{U_0} = \frac{1}{h_0} + \frac{1}{h_{0d}} + \frac{d_o ln\left(\frac{d_o}{d_i}\right)}{2k_w} + \frac{d_o}{d_i} \times \frac{1}{h_{id}} + \frac{d_o}{d_i} \times \frac{1}{h_i} \tag{36}$$

Where, U_0 is the overall heat transfer coefficient in W/m℃

h_0 and h_i is the outside and inside fluid film coefficient respectively in W/m℃

h_{id} and h_{0d} are the inside and outside dirt coefficient present from fouling in W/m℃

k_w is the thermal conductivity of the wall in W/m℃

d_o and d_i is the tube outside and inside diameter respectively in m

Although there is room for optimization, the calculated overall heat transfer coefficient was around 127.3 in W/m℃ and the assumed value was 110 in W/m℃ for water cooling gasoline (Nelson, 1968). Thus,

the parameters are sufficient for the design of the condenser and the summary of the assumed and calculated values is given in Table 24.

Table 24 Summary Table for Assumptions and Calculations for Design of Condenser

Assumed	
Tube Material	Carbon Steel
Tube Side Fluid	Water
Shell Side Fluid	Condensate
Outer Diameter of Tube (m)	0.02
Inner Diameter of Tube (m)	0.0168
Tube Length (m)	4.88
# of Shell and Tube Passes	1 and 2
Baffle Cut %	45
Assumed Overall Heat Transfer Coefficient (W/m°C)	110
Calculated	
Area Required (m^2)	5.197
Bundle Diameter (m)	0.154
Shell Diameter (m)	0.249
Number of Tubes	16.95
Number of Tubes in Center	6.191
Shell Side Pressure Drop (kPa)	11.85
Tube Side Pressure Drop (kPa)	1.038
Calculated Overall Heat Transfer Coefficient (W/m°C)	127.3

7.8 Venturi Scrubber

To effectively design a venturi scrubber, the collection efficiency, liquid droplet diameter, throat velocity, throat length, throat diameter, and pressure drop must be calculated to size the equipment. The design shape of the venturi scrubber is not as important compared to the liquid distribution within the system. Rectangular units are often simpler to fabricate and can be easily fitted with replaceable wear plates for erosion protection. Rectangular units tend to have steeper converging and diverging angles and often times are the adjustable throat type. Venturi scrubbers are usually operated under conditions of widely fluctuating gas flowrates. Since the efficiency mainly depends on the pressure drop of the unit, it is necessary to adjust the area of the throat to maintain the design pressure drop. Venturi scrubbers of

rectangular cross-section are preferred in these applications where the option to adjust the throat is available to maintain the designed pressure drop.

7.8.1 Aspen Plus Design

The venturi scrubber was designed through Aspen Plus using the Calvert design method. This method is based on maximizing the efficiency with constant pressure drop. This method allows for optimization with the Aspen Plus simulation. To understand the concept behind the results on Aspen Plus, the main equations will be presented to comprehend the background theory and how it effects each parameter. The calculation for the efficiency of the scrubber comes from Calvert's particle penetration equation as follows:

$$Pt_d = exp\left\{\frac{Q_L V_G \rho_L d_d}{55 Q_G \mu_G}\left[-0.7 - K_p f + 1.4 ln\left(\frac{K_p f + 0.7}{0.7}\right) + \frac{0.49}{0.7 + K_p f}\right]\frac{1}{K_p}\right\} \quad (37)$$

Where,

K_p= inertial impaction parameter for the gas velocity at the throat entrance, dimensionless

f= empirical factor (f=0.25 for hydrophobic particles and 0.5 for hydrophilic particles)

d_d= Sauter mean droplet diameter, m

ρ_L= density of the liquid, g/cm^3

V_G= superficial gas velocity, cm/s

Q_L= volumetric liquid flow rate, m^3/s

Q_G= volumetric gas flow rate m^3/s

μ_G= gas viscosity, poise

The calculation of the droplet size which is critical in determining the efficiency which can be approximated using the following equation:

$$d_d = \frac{58600}{V_G}\left(\frac{\sigma}{\rho_L}\right)^{0.5} + 597\left(\frac{\mu_L}{\sigma \rho_L}\right)^{0.45}\left(1000\frac{Q_L}{Q_G}\right)^{1.5} \quad (38)$$

Where, σ = liquid surface tension, dynes/cm

μ_L= liquid viscosity, poise

The pressure drop can be represented with the following empirical equation (Calvert et al.,1972):

$$\Delta p = \beta \rho_l {V_t}^2 \frac{V_{fluid}}{V_{gas}} \tag{39}$$

Where

V_{fluid} and V_{gas} are the inlet volume flowrates of the wash fluid and the gas stream

β is an adjustable parameter (0.85)

Figure 18 which displays the function of pressure drop and particle size, was used to obtain a separation efficiency of 95%. The particle diameter was acquired from Figure 19, where the relation between aerodynamic cut diameter and pressure drop was plotted. Curves 2a and 2b are specific to the venturi scrubber, representing hydrophobic and hydrophilic particles, respectively. Since tar in the syngas composition is considered to be hydrophobic, curve 2a at 50cm Water Column (W.C.) was the point where the average particle size of 1 micrometer was noted. The next parameter that was required to be specified was the entering velocity of the entering throat. This value is often in between the range from 0-30 m/sec. An acceptable value of 20 m/s was chosen. To model the venturi scrubber, the assumption that the flow is one-dimensional is necessary.

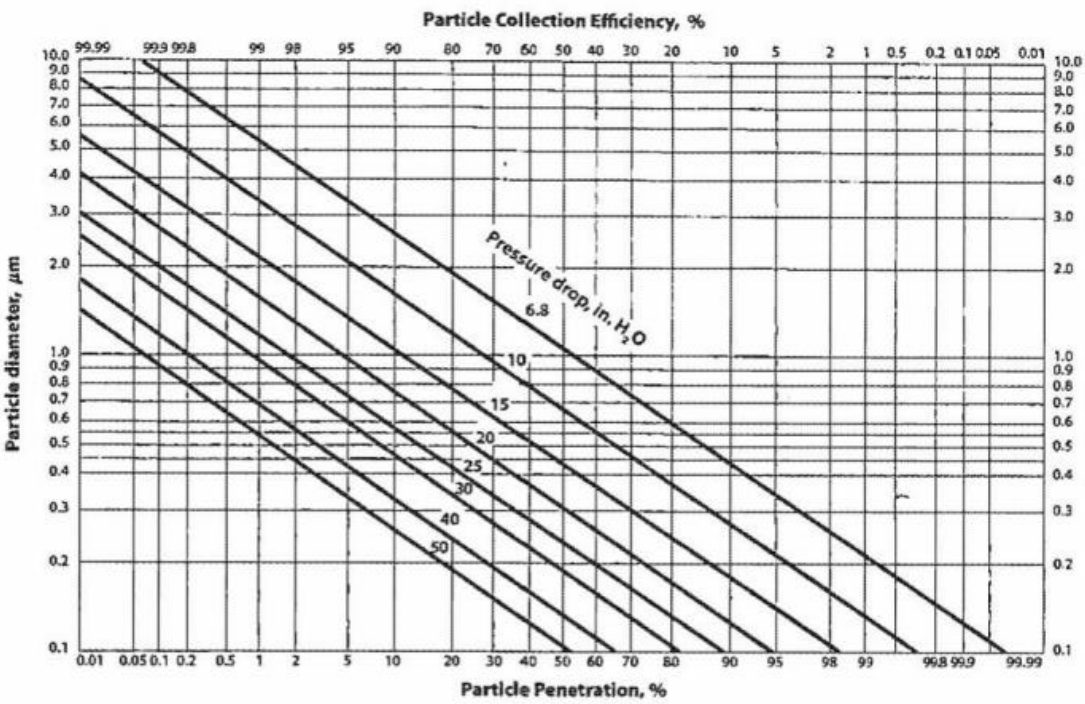

Figure 18 Collection Efficiency as a Function of Particle Size and Pressure Drop in Venturi Scrubber (Cooper et al.. 2011)

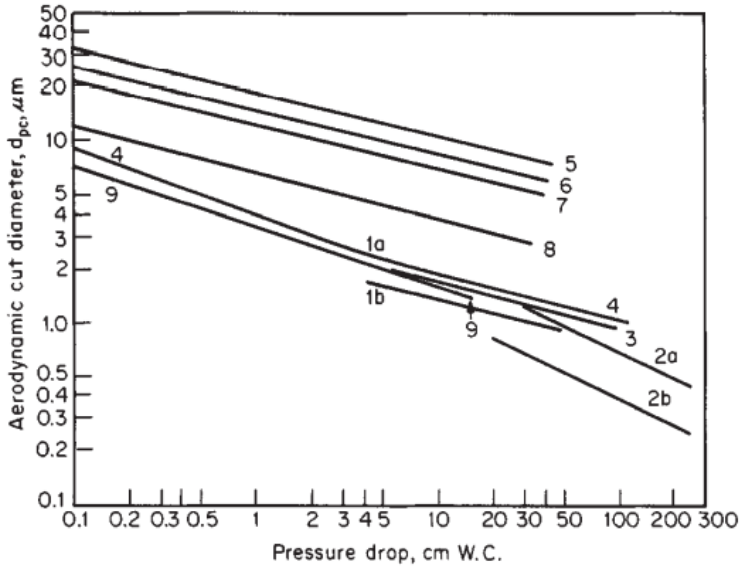

Figure 19 Typical Diameter Cut in Relation to Pressure Drop (Cooper et al.. 2011)

When inputting the required parameters onto Aspen Plus, the mass mean particle size ranged from 5-20 micrometers with a standard deviation of 2.5 was used. Most venturi scrubbers have a diverging angle between 35 to 45° at the throat (Cooper et al., 2011). For high energy systems, it is recommended that the

length of the diverging section of the throat be at least 4 times the width of the throat in order to have sufficient contact time. Venturi scrubbers where the throat is oriented vertically may be likely to experience erosion/abrasion failure at the bottom of the divergent section as the gas stream turns 90° to enter the cyclone. To minimize this problem, a flooded elbow below the venturi throat is added. The width of the venturi is assumed to include the width of the bottom of the venturi scrubber and the width of the flooded elbow. This means that from table 24, the width of the elbow and scrubber are both 0.205 m. The flooded elbow is assumed to be rectangular, so the length is taken as double the width. Moreover, the dimensions of the flooded elbow section are 0.41 x 0.205 m.

Table 25 Summary of Design Results Obtained for Venturi Scrubber (Cooper et al. 2011)

Venturi Scrubber Parameters	Recommended	Results
Total Venturi Width (venturi + elbow width) (m)	0.0508-0.6096 m for a flowrate of 0.708- 1.23 m^3/s	0.41 (0.205+0.205)
Venturi Height (m)	2:1 total venturi width	0.41 x 2=0.82
Length of Scrubber (m)	2:1 width of the venturi	0.205 x 2= 0.41
Pressure drop (kPa)	0.98-14.7 kPa	6.23
Sauter mean drop diameter (m)	---	0.0000137
Gas velocity entering throat (m/s)	5-30	20
Separation efficiency (%)	90-98% (98% for 1-micron particles)	86
Relative gas velocity (m/s)	--	61.5

7.9 Cyclone

Following the venturi scrubber, a cyclone chamber is introduced with a mesh mist eliminator to remove entrainment. Cyclones are very popular in industrial gas-cleaning devices. Their availability is due to its affordability and that it can withstand harsh operating conditions. Cyclone inlet velocities that range from 25-40 m/s effectively remove droplet sizes 75 to 150 microns. Mesh-type mist eliminators are often made from PVC (Cooper et al., 2011). Their open-weave design captures a wide range of water droplet sizes with low pressure drops. Usually, conventional single cyclones have collection efficiencies ranging from 70-90% for particulate matter (PM). Air leakage through the dust outlet pipe can contribute to the

reduction of efficiency due to the contamination of the exiting gas stream with circulated dust. Cyclones are usually designed for an inlet velocity of 15m/s. Additional auxiliary equipment in a cyclone such as cone-and-disk baffles and helical guide vanes are not required as they often have a detrimental effect on the performance of the cyclone. An inlet vane may reduce pressure drop, however, it greatly reduces the collection efficiency, thus it is not recommended in our case. The shape of the cyclone and the tangential entry drives the gas flow into a downward spiral. Centrifugal force and inertia allow for the particles to move outward, collide with the outer wall, and then slide downward to the bottom of the cyclone. At the bottom of the cyclone, the gas moves in an upward, inner spiral where the cleaned gas exits from the top, while the liquid particles exit from the bottom of the cyclone through the valve (Cooper et al., 2011).

7.9.1 Aspen Plus Simulation

Using the numerical method approach which includes designing and sizing the cyclone on Aspen Plus V11, the Shepherd & Lapple calculation method was selected. This method provides the best fit to experimental data and predicted results are more accurate. This model is also widely accepted due to its simplicity and accuracy. To estimate the pressure drop in a cyclone using empirical equations, the Shepherd and Lapple equation is provided as (Cooper et al., 2011):

$$\Delta P = 0.0030 \rho_f {U_t}^2 N_h \tag{40}$$

Where,

ρ_f = Density of the fluid

U_t = Inlet gas velocity

N_h = Inlet velocity speeds

Some things to keep in mind while designing the cyclone are:

- Water droplets are assumed to behave as solid particles in cyclones
- The operating pressure should not exceed atmospheric pressure
- The inlet gas velocity should range from 15-27m/s for the Shepperd and Lapple calculation method

The gas flow rate sensitivity is the main disadvantage of cyclonic mist eliminators. The cost of a stand-alone vessel is another major disadvantage. All of the other types of mist eliminators can be installed

in the outlet portion of the scrubber vessel and therefore do not require their own vessel. The main advantage of the cyclonic mist eliminator is its openness. As long as the cyclonic vessel drain is properly sized and remains open, the mist eliminator is not vulnerable to plugging caused by excessive carryover of solids containing droplets from the scrubber vessel. Due to the spinning action of the gas stream, it is often necessary to install anti-vortex baffles in the stack in order to eliminate cyclonic flow conditions at emission testing locations. It is also common to install liquid flow deflectors to prevent liquid collected on the inner cyclone wall from flowing across the tangential inlet duct and being re-entrained into the gas stream. Table 26 summarizes the results of the cyclone design and sizing obtained from Aspen Plus.

Table 26 Summary of Design Parameters for Cyclone

Parameters	Recommended	Actual Value
Type of cyclone	Conventional	High Efficiency
Number of cyclones	1	1
Efficiency (%)	70-90	73
Pressure Drop (N/m^2)	Less than 2500 N/m2	1244
Diameter of cylinder (m)	0.1-5 m	1
Length of cylinder (m)	2:1 ratio with diameter of cylinder	2
Length of cone section (m)	2:1 ratio with diameter of cylinder	2
Diameter of overflow (m)	0.5:1 ratio with the diameter of cylinder	1
Length of vortex finder (m)	0.625:1 ratio with the diameter of cylinder	0.625
Width of gas inlet (m)	0.25:1 ratio with diameter of cylinder	0.25
Height of gas inlet (m)	0.5:1 ratio with diameter of cylinder	0.5
Diameter of underflow (m)	0.25:1 ratio with diameter of cylinder	0.25
Number of gas turns	7 or 4	7
Axial inlet gas velocity (m/s)	20	19.77

7.9.2 Small Scale Wastewater Treatment system

Typically, the scrubber system includes a tank to temporarily store the wastewater that further undergoes treatment before it can be drained. This is because tar causes several environmental and

industrial problems. Releasing large amounts to the environment can have harmful effects because of the toxic compounds it contains. The wastewater can either be “once-through” or recirculated. Most wet scrubber systems have a recirculating liquor system to reduce the volume of water required and reduce the cost of treating the effluent wastewater. The recirculating liquor circuit is more complicated due to the additional components required such as the recirculating tank, the purge stream controls, and the recirculating pump. The recirculating system is prone to buildup of solids and corrosive agents, while the once-through system is free of these problems. Depending on the frequency of wastewater replacement, the quality of the water and the efficiency of the scrubbing liquid varies. The wastewater treatment system reduces the total solid content of the liquid prior to its return to the scrubber. Common equipment for the treatment includes a clarifier and a rotary vacuum filter. Flocculant is added to the clarifier to improve the settling characteristics of the solids. The reduction of the solid content reduces the potential for pump impeller erosion, nozzle erosion, and pipe blockage.

Firstly, to determine whether the effluent of the scrubber system can be disposed of without treatment, compliance was assessed with the Environmental Compliance Approval (ECA) conditions. The ECA limit for the Total Suspended Solids (TSS) was 25 mg/L. The calculated value is 291.3 g/L which is much greater than the limit. This means that further treatment of the wastewater is required before it can be disposed of. The industrial waste surcharge offers treatment of the total suspended solids at a rate of $0.70/kg. Since the scrubber effluent consists of 88.84 kg of wastewater/day, the total cost of the treatment of water at Ashbridge’s Bay Wastewater Treatment Plant would be $21,600/yr. This benefits our plant because the cost of the treatment is less than installing our own treatment equipment (Ashbridges Bay Report, 2019).

7.10 Heat Exchanger Design

Aspen PLUS v10 was used to simulate the heat exchangers used in the process. There are six heat exchangers required for the entire system, however, three of them are energy outlets such as a radiator or heat sink that provides steam at a required temperature. Therefore, three exchangers are sized for the system; HEX1, HEX2, and HEX3. These are illustrated in the PFD (figure 4). The components chosen on Aspen PLUS were approximated using studies and research to find the optimum settings for the process. The fluid package chosen was Pen-Robinson. The flowrates and operating conditions were set based on specific requirements from mass and energy balance calculations related to the distillation column and fluidized bed reactor. The heat exchanger were used to reduce the temperature of the exiting stream from

the distillation column into the storage tank. HEX1 is used to reduce the temperature of naphtha from 68ºC to 30ºC using cold water as the cooling medium. HEX2 is used to reduce the temperature of kerosene from 94.6ºC to 40ºC using cold water as cooling medium. HEX3 is used to reduce the temperature of gas oil from 252ºC to 50ºC using cold water as cooling medium.

Table 27 Calculated Heat Load Summary for Fuel Heat Exchangers

Heat Exchanger	Heat Load (KJ/Day)
HEX1	-7902.6
HEX2	-44778.75
HEX3	-87586.7

Aspen PLUS v10's Exchanger Design and Rating (EDR) simulation tool was used on the 'Sizing' setting to optimize the dimensions for the shell and tube heat exchanger. With the specific outlet conditions and heat loads known for each of the heat exchangers, the EDR tool can iterate and find an optimal size for the heat exchanger. The 'Sizing' method allows the EDR to fix the outlet temperature and the heat load to a set number and iterate the sizing in order to find an optimal solution based on the specified parameters. The results of the calculations and optimizations are shown in Table 28.

Table 28 Summary of Results Obtained from HYSYS for Heat Exchangers

Heat Exchanger	Heat Duty (Cal/s)	Required Exchanger Area (sqm)	Actual Exchanger Area (sqm)	Avg heat transfer coefficient (cal/sec-sqcm-K)	U_A (cal/sec-K)
HEX1	24.45358	0.66	2.01617	0.00056	3.70073
HEX2	111.03	1.91434	2.01617	0.0007	13.4194
HEX3	497.655	0.54138	2.01617	0.0014311	7.77293

7.11 Pipes and Pumps

7.11.1 Piping System Design Codes

A piping system is engineered to transport a fluid or gas safely and reliably from one equipment to another to ensure smooth operation of the plant. A piping system typically consists of pipes, fittings, valves, and specialty components. The piping design and engineering involves the following major considerations:

1. Selection of pipe materials on the basis of the characteristics of the fluid and operating conditions
2. including maximum pressures and temperatures
3. Finding economical pipe diameter and wall thickness
4. Selection of fittings, joints, and other components and connections

The main piping codes and standards for process industry in the US are (Towler et al. et al., 2011):

- ASME: American Society of Mechanical Engineers
- ANSI: American National Standardization Institute
- ASTM: American Society of Testing Materials
- API: American Petroleum Institute (Oil and Gas Industry)

The basic rules for piping engineering follow the ASME B31 codes. The ASME B31.3 code applies to piping for petroleum products such as gas, steam, air, and water. The schedule of the pipe refers to the wall thickness of pipe in the American system. The thickness of the pipe increases with the schedule number. The most popular are schedules are 40 and 80 (Towler et al., 2013). Schedule 80 steel pipes are usually heavier and stronger than schedule 40 which provides a greater factor of safety, allowing it to handle much higher design pressures. This schedule number will however use more material and therefore cost more to install. Stainless steel piping schedules generally match with carbon steel piping schedules. Low carbon steel is the most common industrial piping material that work well with non-corrosive fluids such as steam and cooling water. Stainless steel, on the other hand, is ideally used when dealing with corrosive fluid such as fuel gas and oil.

The design factors that influence piping engineering include:

- Fluid Service Categories
- Flowrate
- Operating Pressure and Temperature
- Corrosion rate

The ASME B31.3 recognizes the following fluid service categories in Table 29 that apply to the different fluids in the plant.

Table 29 ASME B31.3 Relevant Standards for Fluids (Bhatia, 2016)

Fluid Service	B31.3 Definition	System Characteristics
Category D	• Fluid handled is non-flammable, non-toxic, and not damaging to human tissues • Design gauge pressure does not exceed 1035 kPa • The design temperature is between -29℃ to 186℃	• Lowest cost • Not fire resistant
Category M	• A fluid service in which the potential for personnel exposure is significant and in which a single exposure to a very small quantity of a toxic fluid, caused by leakage, can produce serious irreversible harm to persons on breathing or bodily contact	• High cost • Usually fire resistant

Usually, the thickness of the pipe increases with respect to corrosion. The typical corrosion allowance for water is 3mm (Bhatia, 2016). The typical corrosion allowance for fuel gas or oil is 1 mm. The type of joint used for dangerous fluids such as the syngas stream are conveyed in fully welded pipes where leaks are not accepted (Bhatia, 2016). For designing the pipe diameter for a given flowrate, the smaller the diameter results in a higher velocity of the conveyed fluid and the opposite can be said for lower velocities. The velocity of the fluid in pipelines usually affect the pressure losses along the pipeline and the vibration of the pipeline. The typical velocities of gas and liquid inside pipelines are 15-40 m/sec and 2-4 m/sec, respectively (Towler et al., 2013).

Usually pumps, compressors, and control valves are designed with the piping system. The amount of pressure drop through the piping system would help determine what additional equipment is required to make up for the pressure drop along the length of the pipe. The pressure drop in a pipe due to friction is dependent on the fluid flowrate, density, viscosity, diameter, pipe roughness, and the length of the pipe. The pressure drop in pipes can be represented using the following equation (Towler et al., 2013):

$$\Delta P_f = 4f\left(\frac{L}{di}\right)\rho u^2 \tag{41}$$

Where,

ΔP_f = pressure drop due to friction, N/m^2

f = friction factor (depends on Reynolds number and pipe roughness)

L = pipe length, m

di =pipe inside diameter, m

ρ = density of fluid, kg/m^3

u = fluid velocity, m/s

The diameter of the pipe was obtained using the following equation:

$$D = \sqrt{\frac{4Q}{\pi \mathrm{u}}} \tag{42}$$

Where,

D= inside diameter of pipe, m

Q= Volumetric flowrate of fluid, m^3/s

A sample calculation for stream number 2 for the water leaving the disc filters is shown in Appendix section 15.9. To calculate the friction factor, the Reynolds number and pipe roughness must be known. The Reynolds number can be calculated using the following equation:

$$Re = \frac{\rho * u * di}{\mu} \tag{43}$$

Where, μ is the fluid viscosity in units of pa*s

When calculating the Reynolds number, the fluid viscosity and density are taken to be constant as it is assumed that the fluid in the system is a Newtonian liquid. Likewise, for a gas flow through pipes, the pressure of a gas is assumed to not change more than 20% and is treated as an incompressible fluid with constant density. The absolute surface roughness of commercial steel pipe was 0.046 mm that was used throughout the piping system. To find the relative roughness of the pipe in stream 2, the absolute roughness was divided by the inside pipe diameter using the equation below.

$$relative\ roughness, e = \frac{absolute\ roughness}{inside\ pipe\ diameter} \tag{44}$$

The friction factor can be found using the friction factor chart as in Figure 20 using the calculated Reynolds number and the relative roughness value. The friction factor was found to be around 0.018 and a length of 20 m was assumed from the 3D model.

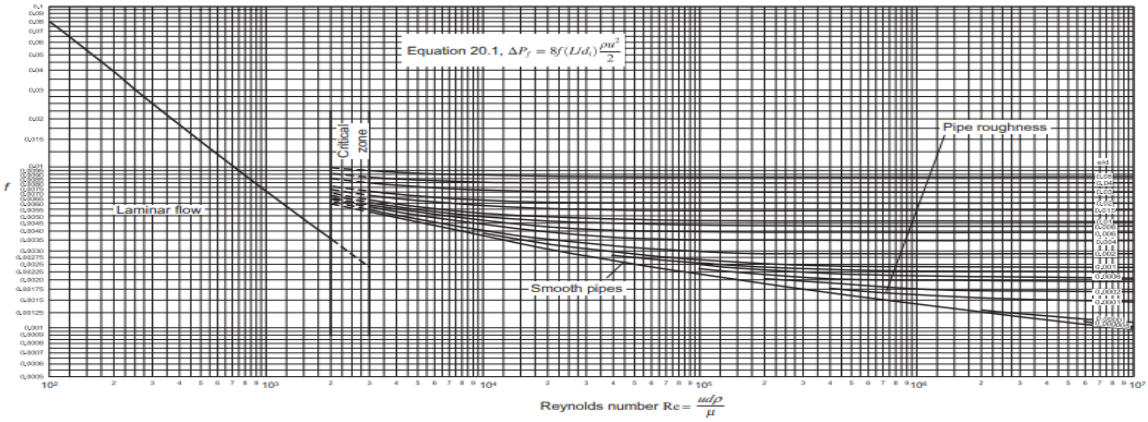

Figure 20 Pipe Friction Versus Reynolds and Relative Roughness

Pipe fittings such as bends, elbows, and valves will increase the pressure drop in a pipeline. The pressure drop due to miscellaneous losses can be estimated using the number of equivalent pipe diameters. The length of the pipe is added with the actual pipe length by multiplying the total number of equivalent pipe diameters by the diameter of the pipe being used. The pressure loss in pipe fittings and valves for turbulent flow can be estimated for the common types of fittings and valves used in our process as shown in Table 30.

Table 30 Equivalent Pipe Diameters for Fitting and Valves

Fitting or Valve	Number of Equivalent Pipe Diameters
45º elbow	15
90º standard radius elbow	30
Globe valve, plug disk, fully open	450
Gate valve, fully open	800
Tee-entry from leg	60
Sudden expansion (tank inlet)	50

From the calculations in the Appendix section 15.9, the total pressure drop due to friction is about 163kPa. The work is then calculated to check whether a pump or compressor is required. To find work, Bernoulli's equation is used where it is assumed that there is no change in pressure at the two points (P1 and P2). The height change is assumed to be 5 m. Thus, to calculate work, the following equation is used.

$$W = g\Delta z + \frac{\Delta P}{\rho} - \frac{\Delta P_{total}}{\rho} \quad (45)$$

Where

g acceleration due to gravity (m/s^2)

Δz Height change between the two points in the piping system (m)

$\frac{\Delta P}{\rho}$ change in pressure at different points (N/m^2)

$\frac{\Delta P_{total}}{\rho}$ the overall change in pressure at the point where the fluid enters the pipe to where it exits (N/m^2)

The negative work indicates that a pump or compressor is required to compensate for the pressure drop within the piping system. Since the stream is water, a pump is used for liquids. The power of the pump required is calculated using the following equation.

$$P = \frac{W\ x\ Q}{\eta} \quad (46)$$

Where, W is the work in J/kg

Q is the flowrate in kg/s

And η is the efficiency of the pump

Similar calculations were conducted for the remaining pipes and pumps. A summary of the pipes and pumps calculations are shown in Table 31 below. The pump number and power results are shown in Table 32.

Table 31 Summary of Calculated Piping Parameters

Line #	Mass Flow rate (kg/day)	Inner diameter (m)	Nominal Pipe Size (m)	Length (m)	Height (m)	Pressure Drop (N/m^2)	Work (J/Kg)
1	1500000	0.11	0.127 (Schedule 40)	40	-5	97688.32	-3638.103175
2	1500000	0.105127158	0.127 (Schedule 40)	20	5	163788.8	-2846.944444
6	2617.92	0.006211212	0.003175 (Schedule 40)	20	-5	56112	-4.549848

7	2197.92	0.081	0.0889 (Shedule 40)	4	5	8598.88	-690.958
10+11	839.76	0.032	0.03175 (Schedule 80)	4	5	12794.7842	-201.814
12	2617.92	0.006211212	0.003175 (Schedule 40)	20	5	53440	-0.192188571
13	339.16	0.0132	0.0127 (Schedule 80)	17.69	4	334080.76	-133593
16	2123.76	0.081	0.0889 (Schedule 80)	10.488	-5	989.0527088	-0.053
17	116524	0.0417	0.0508 (Schedule 40)	32.96	3	8684461.566	-264418.27
18	624.71	0.001934505	0.001905 (Schedule 40)	20.00304998	0	1220777.389	1488.752913
19	2196	0.02545	0.0254 (Schedule 40)	27.075	4	619.584	-39.82016
20	90.53	0.014728445	0.01905 (Schedule 80)	5.176795574	0	501.0712345	1222.124962
21	452.86	0.032941442	0.0381 (Schedule 80)	5.88438798	0	224.0339059	546.4241606
22	362.33	0.065886704	0.0762 (Schedule 80)	43.53796203	17	35.84334734	79.34720161
23	11.37	0.0145	0.0127 (Schedule 40)	14.9586	5	95.04596	-11.04167
24	17.08	0.005288358	0.003175 (Schedule 80)	5.022792887	0	2042.221711	3403.702852
25	95.13	0.012480606	0.0127 (Schedule 80)	5.126948909	0	865.3425793	1442.237632
26	89.42	0.012100248	0.0127 (Schedule 80)	20.11932904	0	3570.174804	5950.29134
27	89.42	0.013255157	0.0127 (Schedule 80)	20.14319485	12	2.715923992	117.7163788

28	40.45	0.013050388	0.0127 (Schedule 80)	5.138804794	0	107.2765027	153.2521467
29	337.96	0.021778912	0.0254 (Schedule 80)	0.386571638	0	578.541285	826.48755
30	26.92	0.0125	0.009525 (Schedule 40)	20.901	10	499.63	1.001195
31	324.44	0.021338836	0.0254 (Schedule 80)	20.37110694	0	2361.890729	79.34720161
32	324.44	0.01508884	0.01905 (Schedule 80)	20.00185553	8	35.84334734	0.002006219
33	10.56	0.03514349	0.0381 (Schedule 80)	5.000024701	0	32267.71258	38413.94355
34	179.11	0.014473476	0.01904 (Schedule 80)	5.167585196	0	1044.669604	1243.654291
35	6.97	0.010134	0.00953 (Schedule 40)	26.675	15	38.21	145.089
36	175.53	0.0143281	0.01905 (Schedule 80)	20.16423555	0	4221.076184	5025.090695
37	175.53	0.01038169	0.00953 (Schedule 80)	20.00086224	4	2219290.894	-2734.873617
38	433.99	0.013	0.0127 (Schedule 80)	22.75	5	1017545	-0.583
39	304.92	0.0095	0.00953 (Schedule 40)	25.31	3	1014.13	1.03E-04
40	398.92	0.032	0.0317 (Schedule 40)	38.16	5	8284078	-3.68
41	26671.68	0.146254656	0.1524 (Schedule 80)	4	5	6808.66515	-2472.728454

Table 32 Properties Calculated of Pumps

Pump #	Mass Flowrate (kg/day)	Power of Pump
PM-1	1500000	-4.879
PM-2	1500000	-3.818
PM-4	2196	-0.00194
PM-5	398.92	-0.09125
PM-3	26671.68	-3.315

7.12 Compressors

The equipment used to compensate for pressure drop in a pipeline containing gas is often times a compressor. At low pressure drops, a simple fan may be used. At higher pressure drops, compressors are commonly used. To calculate the work done in a compressor, a relationship between pressure and volume during the expansion is required. We assume that the compression follows a polytropic path where it is assumed that the specific heat remains constant with any change in the thermodynamic properties of a gas. Equation 47 shows the work equation of a gas undergoing compression or expansion.

$$-W = Z\frac{RT_1}{M_W}\left(\frac{n}{n-1}\right)\left[\left(\frac{P2}{P1}\right)^{\frac{(n-1)}{n}} - 1\right] \tag{47}$$

Where;

W= work done (J/kg)

Z= compressibility factor (1 for ideal gas)

R= universal gas constant (8.314 JK^{-1} mol^{-1})

T_1= inlet temperature (K)

M_W= molecular weight of gas

$P2$= final temperature

$P1$= initial temperature

n= polytropic expansion coefficient

The polytropic expansion coefficient is equal to the ratio of specific heats for reciprocating compressors. The polytropic coefficient can be calculating using the following equation:

$$n = \frac{1}{1 - m} \tag{48}$$

Where,

$m = \frac{\gamma - 1}{\gamma E_p}$ for compression

$m = \frac{(\gamma - 1)E_p}{\gamma}$ for expansion

E_p= polytropic efficiency which can be obtained from the figure below.

Appendix section 15.10 provides the continuation of the sample calculations for the compressors. Table 33 provides a summary for all compressor results.

Table 33 Summary for Compressor Design Parameters

Compressor	Mass Flowrate (kg/day)	Actual Work (kJ/kg)	Power of Compressor (kW)
CMP-1	2197.92	-690.958	16.89
CMP-2	839.76	-201.814	4.25
CMP-3	339.16	-183.9	0.72
CMP-4	2123.76	-292.01	9.129
CMP-5	116524	-142.02	191.32
CMP-6	433.99	-295.54	0.618

7.13 Storage Tanks

There is a total of four storage tanks that are needed to hold products, and three crude and char tanks that will be used in the process. The storage tanks that will be used to hold the products include; gasoline, naphtha, kerosene, and gasoil will be held in floating roof storage tanks (Treese et al., 2015). Floating roof storage tanks are meant to usually operate at atmospheric temperature where the roof floats on the surface of the liquid contents (Treese et al., 2015). Through having a floating roof tank, it will minimize the amount of liquid vaporization that may occur within the tank, which will also minimize the probability of explosion occurrence (Treese et al., 2015). A drain line will also be put into the roof of the tank to minimize the amount of flooding in the occurrence of heavy rain. In addition to this, there will be rim vents, floating gauges, anti-rotation devices and manholes to increase the efficiency and safety of the

storage tanks (Treese et al., 2015). The floating roof tank is preferred over cone roof depending on the flash point of the materials. Usually if the flashpoint is 120°F, a floating roof tank is recommended (Treese et al., 2015). Although, the flashpoint temperatures of these fuels will not ignite or be hazardous in Canadian weather, floating tanks are used in case of weather fluctuations that would affect the storage temperature of the products.

For the char and reduced rude collection tanks, they will be normal cone roof tanks as these products are less likely to ignite and have higher flash points, resulting in less vapor released at the storage temperature (Ludwig, 1997). The storage tanks will be equipped with fire protection such as foam around the base of the tanks for safety control (Ludwig, 1997). These tanks will also operate at atmospheric pressure and will have a vent that is open to the atmosphere, as crude and char have low volatility. The assumptions for the storage tanks are that they are made of carbon steel material, it will have the same length to diameter ratio, and the calculations will assume that there is 20% overcapacity (Ludwig, 1997). In addition, the residence time of the storage tanks will be bi-monthly, and it will be located 20-40 m away from processing units depending on the storage tank (Ludwig, 1997). The following table 34 displays calculations of the dimensions of each storage tank are summarized in the following chart.

Table 34 Summary Table for Storage Design Parameters

Assumptions							
Storage Tank	T-1	T-2	T-3	T-4	CC-1	CC-2	CC-3
Orientation	Horizontal	Horizontal	Horizontal	Horizontal	Horizontal	Horizontal	Horizontal
Type	Floating Roof	Floating Roof	Floating Roof	Floating Roof	Floating Roof	Floating Roof	Floating Roof
Material	Carbon Steel	Carbon Steel	Carbon Steel	Carbon Steel	Carbon Steel	Carbon Steel	Carbon Steel
Calculated							
Mass Flow Rate (kg/day)	362.33	89.42	94.6	252	73.61	37.2	73.61
Density (kg/m^3)	700	721	780	800	220	220	820
Volume (m^3)	31.06	7.45	7.297	18.9	24.09	12.17	6.46
Height (m)	13.1	3.16	3.09	8.01	8.52	4.31	2.29
Length (m)	13.1	3.16	3.09	8.01	8.52	4.31	2.29

8. Process Control

This section of the report will be dedicated to investigating the automatic control of each unit, to ensure that the unit is working safely, and that control is consistently maintained. The process control parameters for each unit will be explained and justified accordingly. Figure 21 is a complete P&ID of this process, which will be discussed in detailed within this section.

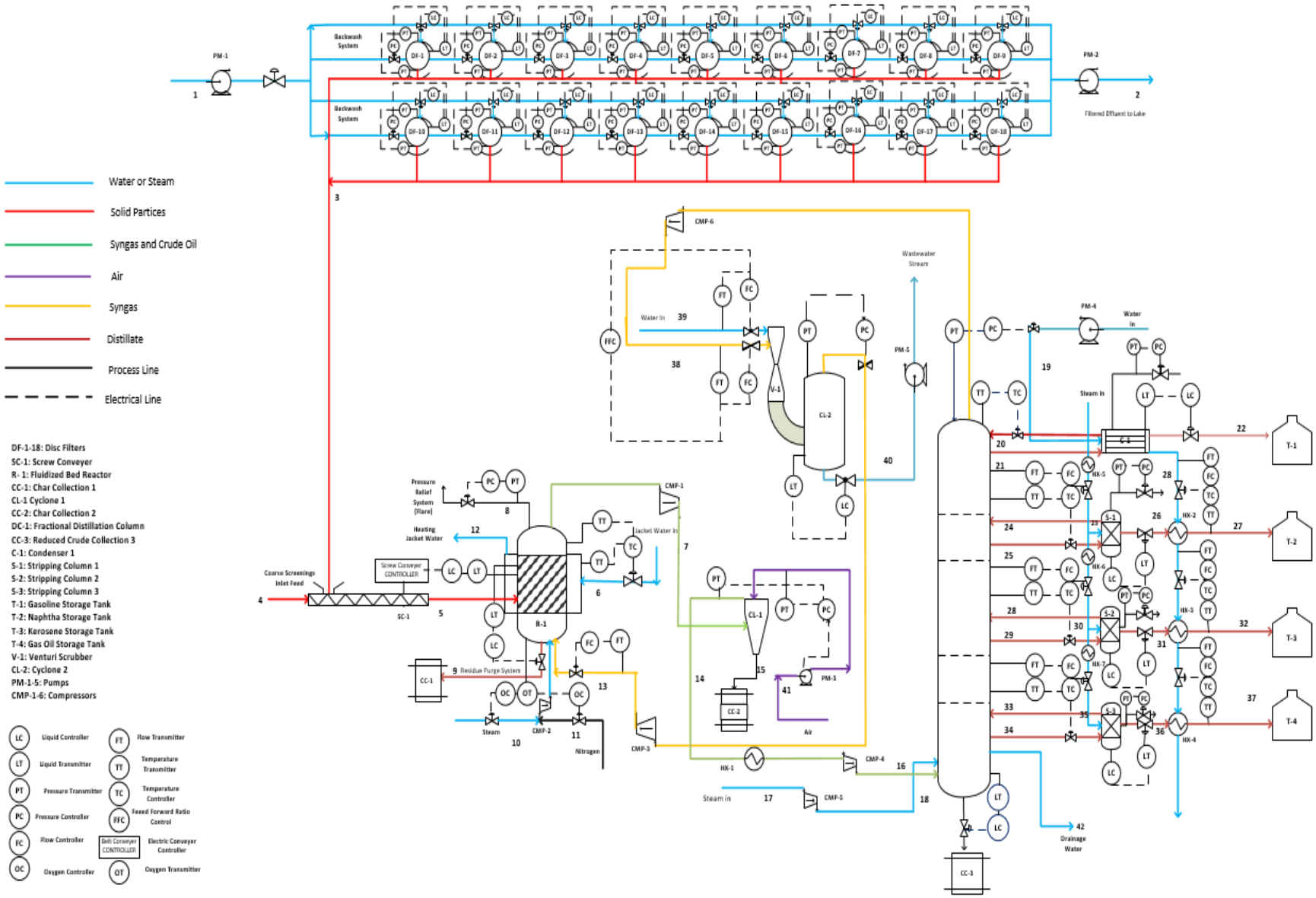

Figure 21 P&ID of Process

8.1 Disc filter

In the disc filter process, there are capacitive level sensors, also known for the electrical method of collecting the liquid level. The application of electrical conductivity is the fixed-point level detection of a conductive liquid such as high and low water levels. A voltage is applied between two electrodes inserted into the vessel at different levels. When both electrodes are immersed in the liquid, a current flows. The capacitance type level measurements are based on the fact that the electrical capacitance between two electrodes varies with the dielectric constant of the material between them (Perry et al., 1997).

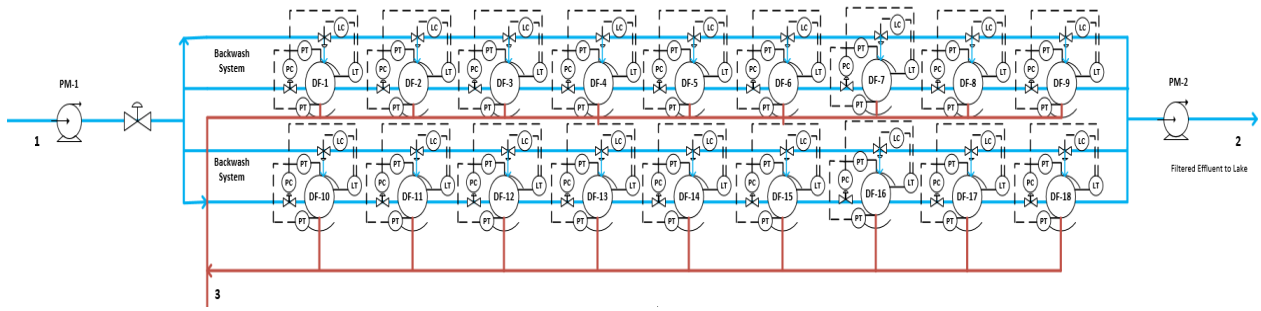

Figure 22 P&ID of Disc Filters

A typical continuous level-measurement system consists of a rod electrode positioned vertically in a vessel and the other electrode is the vessel itself. The electrical capacitance between the electrodes is a measure of the height of the interface along the rod electrodes. This process also uses strain gauge pressure transducers for measuring pressure. The strain gauge probe is placed in the inlet and another probe is in the sludge tank. Usually in this type of rotary disc filter, gravity discharge is chosen. In the rotary disc filter, if more filters are chosen, one pressure probe is used to control the PID as one unit. This allows the PID of individual filter to evenly distribute flowrate to avoid overloading one or more filter units. Despite the level controller, PID is used for all of the controllers in the disc filter due to the versatility of the controller to switch to a PI or PID controller instead of just P controller for the liquid level controller. Table 35 provides a summary of the transmitter, controller, and valve type as well as the fail-safe positions.

Table 35 Summary of Process Control Details for Disc Filters (Perry et al., 1997).

Process Parameter	Pressure	Level
Transmitter Type	Strain gauge pressure transducer	Chain Gauge
Controller Type	PID	P
Valve Type	Globe	-(Screw conveyer feeder)
Fail-Safe Position	Fail-open	Fail-Close

8.2 Bubbling fluidized bed reactor

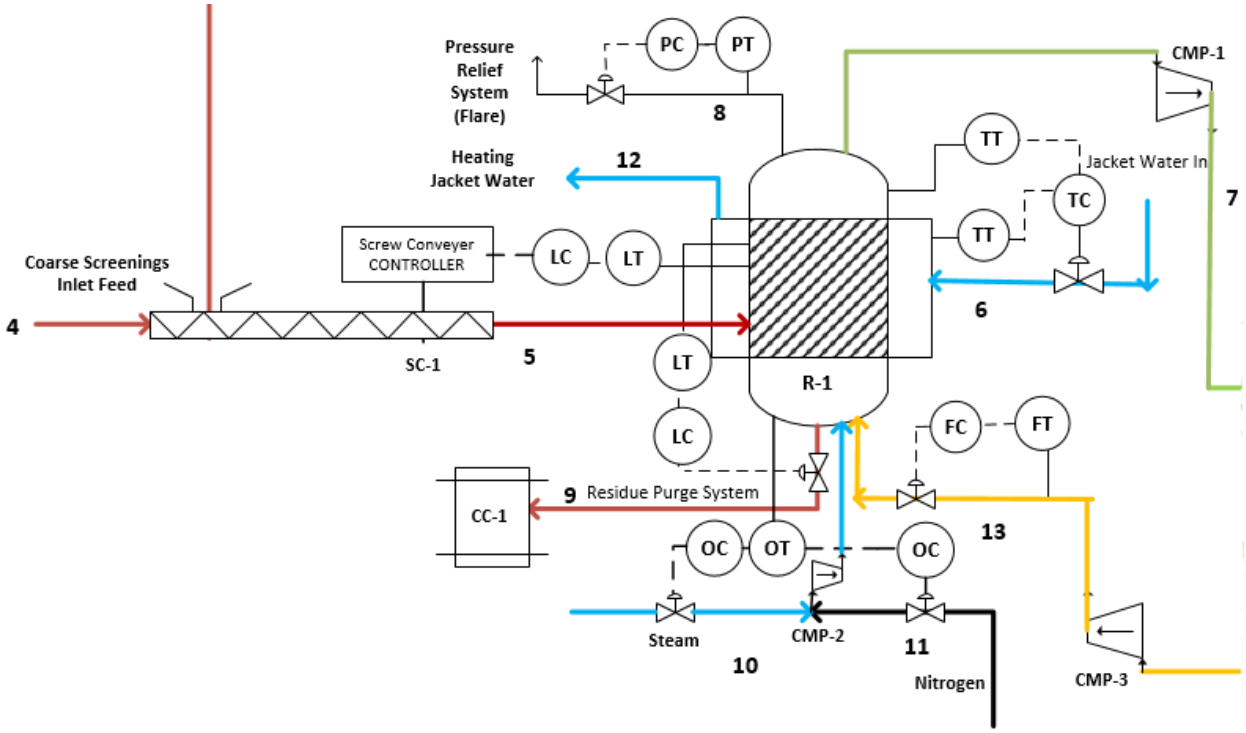

Figure 23 P&ID of Fluidized Bed Reactor

There are a variety of different control schemes available for a bubbling fluidized bed reactor. The operating process dictates the safety of the equipment and the continuous process for the reaction to occur. The controller set points are adjusted to maintain the product within specifications, based on periodic laboratory analyses. The fluidized bed reactor temperature is controlled by regulating the flow of heating or cooling medium in the heating jacket via a feedback controller system. The temperature is transmitted from the reactor and the cooling jacket, whose impulses are combined in a temperature controller for a change in flow in the valve. The control variable is the valve, and the process variable are the fluctuating temperatures. The valve dictates the heat transfer and makes the process variable achieve the target set point of 517 °C. Normally, pressure in not an issue in a pyrolysis reaction for fluidized bed reactor, however, a pressure transmitter is placed to redirect the excess pressure as precaution for safety hazard into a flare. The relief valve is opened after the pressure is transmitted via a feedback control loop. Through this process, the pressure is held constant in the reactor as the target setpoint is 5 atm. In the gas-phase reactor, pressure is often controlled by maintaining a vapor space above the feed reagents. The material balance control will be maintained using the liquid level controller for the system. The correct flow of biomass to the reactor and the flow of products and unreacted materials from the reactor will be monitored

using this method. The bubbling nitrogen and steam gas flow rate controlled by the flow transmitter and valve at the bottom of the reactor controller (Perry et al., 1997).

The temperature sensor used in the reactor is a thermocouple sensor with a code type of K, which means that the sensing temperature ranges from -180°C to 130°C and made is from Nickel Chromium/Nickel Aluminum. The temperature sensor is placed just on top of the fluidized bed inside the reactor where the rate of change of temperature with change in composition of the key component is maximum. As the temperature increases the electrical signal is transmitted to the temperature controller to increase the flow of cooling fluid in the heating jacket to decrease the temperature of the reactor. When there is lower level of temperature cooling fluid flow is lowered. The pressure sensor used in the reactor is sealed gauge pressure and a rupture disc relief system is put in place in case of accident due to pressure built up. The location of the pressure sensor as well as liquid sensor will be at the top of the reactor. Since we are dealing with vapor products, the vapor pressure is essential for process safety measures. While rupture valve will enable to have a failsafe system. We need to control the process by lowering the pressure if required to mitigate the influence of pressure drop in the fluidized bed. The liquid level sensor used is at multiple point due to the fluctuation nature of bubbling fluidized bed. Multiple location needs to be monitored for a stable process. The liquid level sends signal to the controller to either lower the speed of the conveyer belt or decrease the flow of the fluidizing gas below the reactor. The fluidized gas cannot go lower than 30% of the minimum fluidization velocity (Perry et al., 1997).

The fluidized reactor has various controllers for liquid level, pressure, temperature, and flow rate. Proportional controller is most often used for liquid level where variations in the controlled variable carry no economic penalty. Proportional controller is used with averaging level control techniques, whereby setting the proportional band just below 100%, the level can vary over the range in capacity needed for stripping columns and fluidized bed. This helps minimize the rate of change of manipulated outflow into a more stable flow. Fluidized bed reactor control system mainly consists of feedback control system with a cascade control system for the cooling jacket. The temperature and pressure controllers are PID controllers for its versatility. This means the function of the PID could be changed to PI if necessary, for faster but littler unstable response instead of more stable and slower response as a PID controller. The liquid level controller valve is set at fail-close for feed and fluidizing flue going into the reactor. The temperature controller valve and the pressure relief valve are set at fail-open for the temperature and pressure to go down if the process control is not working properly (Perry et al., 1997). A summary of the process control parameters for the fluidized bed are displayed in Table 36.

Table 36 Summary of Process Control Details for Fluidized Bed Reactor (Perry et al., 1997).

Process Parameter	Tempreature	Pressure	Level
Transmitter Type	Thermocouple	Sealed gauge pressure	Ultrasonic
Controller Type	PID	PID	P
Valve Type	Globe	Butterfly	Butterfly/Screw conveyer feeder
Fail-Safe Position	Fail-open	Fail-open	Fail-Close

8.3 Cyclone

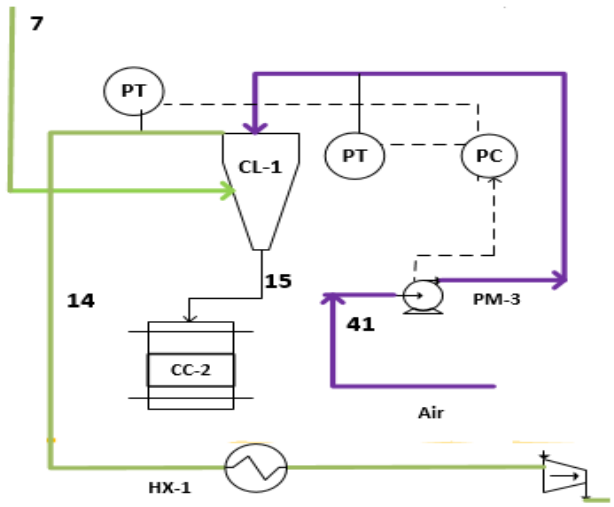

Figure 24 P&ID of Cyclone

For the cyclone it is crucial to ensure minimum amount of pressure drop for the cyclone to have effective solid gas separation of material. The pressure transmitter measures pressure to make sure that pressure drop is not too high and if the pressure drops deviates from the desired setpoint, the control variable of flowrate is changed. This in turn changes the process variable closer to the set point. The set point for the pressure drop is 1.49 mm of H_2O.

The pressure sensor used is Strain Gauges sensor, which has extremely fast response time and suitable for a high frequency dynamic pressure measurement such as the cyclone. Strain gauge sensor utilizes resistance-wire grids for measuring small distortions in elastically stressed material to measure pressure. The bonded strain gauges are bonded directly to the surface of the elastic element whose strain is to be measured (Perry et al., 1997).

For the tuning purposes PID controller is used for the versatility of PID controller. The system has a fail-close controller for the air pump as the only consequences would be a decrease in quality of the product than a hazard in the plant. A summary of the process control parameters for the cyclone are displayed in Table 37.

Table 37 Summary of P&ID Details of Cyclone

Process Parameter	Pressure
Transmitter Type	Strain gauge absolute pressure transducer
Controller Type	PID
Valve Type	Air pump
Fail-Safe Position	Fail-close

8.4 Distillation Column

The process control of the distillation column will help with various elements such as, achieving a stable and safe operation, maintaining product quality, and minimizing disturbances entering the automation system. In order to know which controls to put in place, it is important to the process parameters that are most important, such as the pressure of the column, the temperature, and flow leaving the column. The control system will consist of having a pressure control on the top of the distillation column, temperature, and flow controllers where side streams are drawn, and a level controller at the bottom of the column (Love, 2007). The first parameter of interest is the pressure, most vessels that deal with gases need some sort of venting system. The pressure transmitter and controller stabilize the pressure in the column by ensuring that the column is always operating at 10 bar (Love, 2007). If the pressure increases the transmitter detects the increase, sends the signal to the control, which controls the water going into the condenser (Love, 2007). Through manipulating the flow of water through the condenser, the pressure of the column will change due to changing the amount of liquid and vapor refluxing back into the column (Love, 2007).

In addition to the pressure transmitter, the temperature transmitter at the top of the column will also help control the flow going back into the column as this would affect the top pressure (Love, 2007). Moreover, temperature transmitters and controllers are put throughout the distillation column, as temperature is an indirect measurement of product composition (Love, 2007). If the temperature of the product drawn is accurate, it also indicates that the product purity is up to standard. The temperature

transmitter that is connected to Line 20 is also put there to measure the composition of gasoline coming back to the column, which would be assumed as the same composition as the gasoline leaving the condenser (Love, 2007). The rest of the temperature controllers will be used throughout the column to measure the composition of the products leaving on Line 25, 29 and 34 from the distillation column travelling to the stripping towers (Love, 2007). Although the distillation column has a wide range of temperature changes throughout the column, it is recommended to place temperature transmitters closest to the point where the stream is drawn instead of a few trays below or above, as this would give the most accurate reading (Love, 2007).

The flow of the product being drawn in that stage will also be sensed through a flow transmitter, then relayed onto the flow controller which will also be connected to the temperature controller (Love, 2007). Therefore, based on the flow that is sensed from the liquid and vapor flow at that point in the column, the composition of vapor and liquid in Line 25. 29, and 34 can be retrieved. Depending on the composition and flowrates read by the flow and temperature transmitters, the flow controller will control the amount of steam being sent to the stripping tower based on the amount of unwanted product needing stripping (Love, 2007). The temperature controller will control the valves that are connected to product Lines, 25, 29 and 34, therefore if the temperature is higher or lower than what it desired for that specific product than the valve will close the line until that temperature is corrected (Love, 2007). Lastly, level controllers are also put in place in the bottom as the level controller helps to indicates and control the liquid level in the column in case it experiences any flooding or weeping (Love, 2007). The fail-safe position of the valves will be fail-open as this will prevent the accumulation of vapor pressure that can result into equipment damage or an explosion. The fail-safe positions that control the steam on Lines 23, 30 and 35 will be fail-closed to stop steam flow through the stripping towers (Love, 2007).

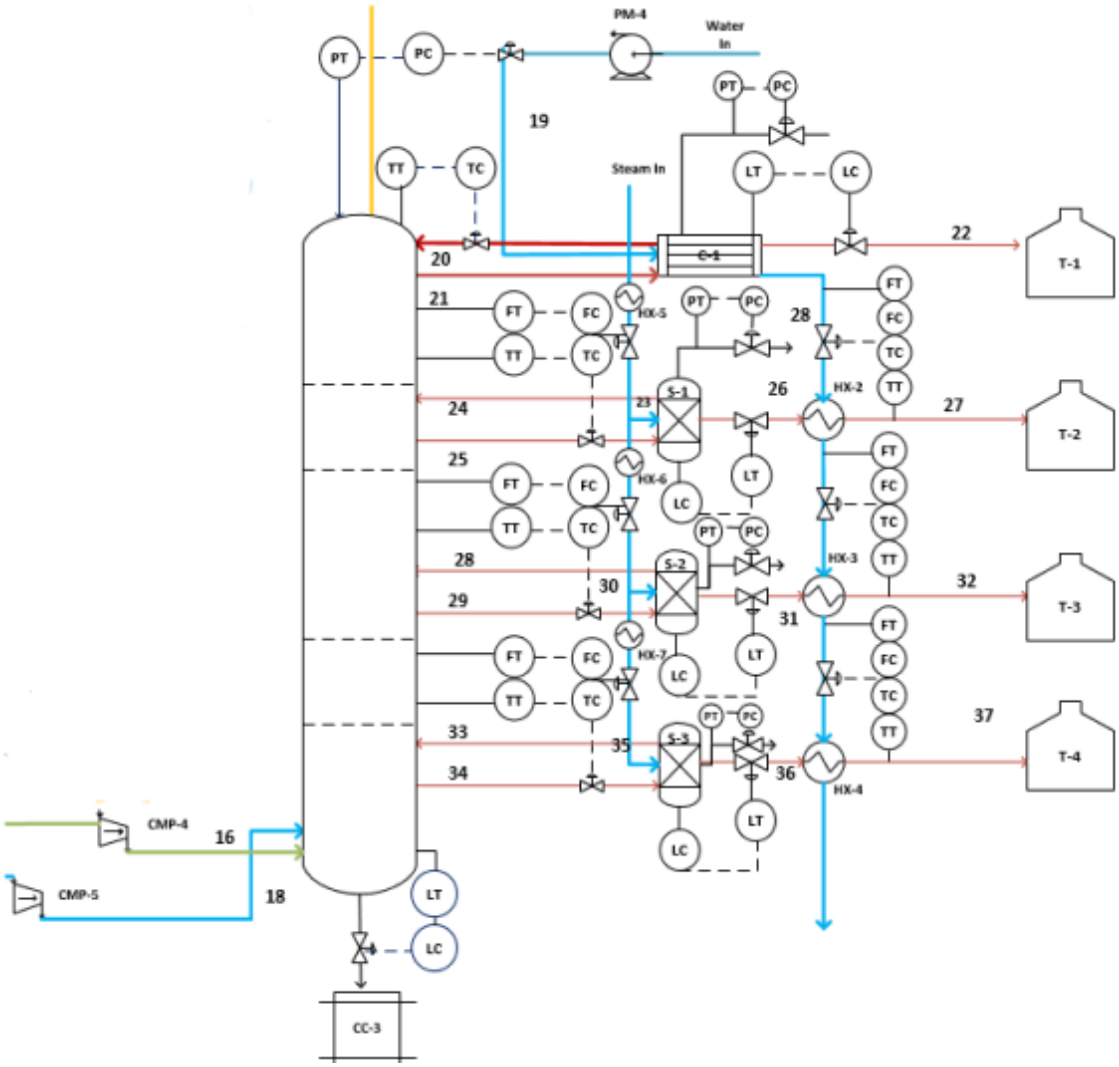

Figure 25 P&ID of Distillation Column

The transmitters that are used in the column are all dependent on the parameter being controlled, and the mechanism needed to read the signal. Most commonly, thermocouples are used for temperature transmitters as these sensors can calculate the change in electromotive forces created by temperature changes (Love, 2007). Moreover, a differential pressure transmitter will be used to help indicate the multiple pressures from various vapors that will be circulating in the column and will help reinforce the correct value the partial pressures the components need to be at to achieve the right operating pressure (Love, 2007). The level controller will be of an ultrasonic level transmitter as these transmitters are effective in reading the component being measured without any contact. For the controllers, the level and pressure controllers will be a P controller because if there are disturbances that affect those parameters, the controllers must act fast to minimize the damage that may be done to the distillation column itself (Smith

et al., 2015). Moreover, disturbances affecting the pressure and level of the distillation column could damage other units further down the line or result in an explosion. On the other hand, the temperature and flow transmitters will be PID controllers because the according to what the temperature and flowrate was measured the controllers need to be more accurate in controlling the steam and flow coming out of the distillation column (Smith et al., 2015). These controllers are chosen to be a PID, for the accuracy which in this process is important to help determine product purity (Smith et al., 2015). In addition, the transmitter, controller, and valves are placed in a reasonable distance to one another, thus delivering the control actions should not take long to deliver despite the lag time that can come with these types of controllers (Smith et al., 2015). Lastly, there will be different valves used depending on the control variable, for example a ball valve will be used for the level controller because although it does not have as much accuracy as the other types of valves it has the best "shut off" capabilities and is suitable for controlling flow (Smith et al., 2015). The valve connected to the pressure controller will be a diaphragm valve used to control the water in the condenser. Diaphragm valves are very quick pressure responsive in comparison to any other type of valve, it has a maximum pressure range of 300 psi which is well above the operating pressure and can be repaired without interrupting the pipeline it is connected to (Love, 2007). For the valves that are connected to temperature and flow controllers, will be globe valves as these valves are accurate and has a very fast mechanical advantage as it can be constantly recalibrated if needed (Smith et al., 2015). A summary of the automation and control elements, along with the fail-safe position is described in Table 38.

Table 38 Summary of P&ID Parameters of Distillation Column

Process Parameter	Tempreature	Pressure	Flow	Level
Transmitter Type	Thermocouple	Differntial pressure Transmitter	Ultrasonic	Ultrasonic
Controller Type	PID	P	PID	P
Valve Type	Globe	Diaphram	Globe	Ball
Fail-Safe Position	Fail-open	Fail-open	Fail-closed	Fail-Open

8.5 Stripping Tower

The process control for the stripping tower is connected to and similar to the control system of the distillation tower. The process control mechanism for the stripping towers (S-1, S-2, S-3) involve having a

pressure controls attached to the top of the columns and a level controls attached to the bottom of the column (Love, 2007). The pressure controller will act as a purging system that will be sensed by the transmitters if there is a buildup of vapor pressure (Love, 2007). The flow of the contents coming into the stripping column are controlled by the control system in the distillation column. However, if there is a surge in flow that can be damaging to the equipment, the level transmitter will sense the liquid level that must be maintained to avoid flooding (Love, 2007).

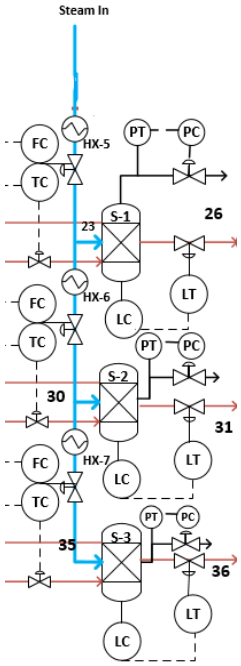

Figure 26 P&ID of Stripping Towers

The pressure transmitter that will be used for the stripping towers will be an absolute pressure transmitter that will compare the process pressure to what the desired pressure is (Love, 2007). The level transmitter will be ultrasonic as this is one of the best types of transmitters that are good at reading process measurements without too much process interference (Love, 2007). The controllers for pressure and level will be a P Controllers as the detection of undesired parameters needs to be fast, rather than precise. Lastly, the valves that will be used that are attached to the pressure and level controllers in this unit will be a pressure relief valve and a butterfly valve, respectively (Love, 2007). Butterfly valves help to regulate the flow of the liquid and is similar to the ball valve as it has quick shut off capabilities for a different flow range (Love, 2007). Whereas the pressure relief valve is suitable for pressure controllers as the detection of off pressure will manipulate the valve to minimize the disturbance (Love, 2007). The fail-safe position

for both these valves will be fail-open as this will help flush any contents out of the stripping tower if shut down was activated. The following is Table 39 and displays the process control specifications of the stripping towers.

Table 39 Summary of P&ID Parameters for Stripping Towers

Process Parameter	Pressure	Level
Transmitter Type	Absolute pressure Transmitter	Ultrasonic
Controller Type	P	P
Valve Type	Pressure Relief Valve	Butterfly
Fail-Safe Position	Fail-open	Fail-Open

8.6 Condenser

The control system for the condenser is also connected to the distillation tower, as the pressure and flow associated with the gasoline coming from the distillation column are the process variables that need to be regulated. For the condenser, there will be a pressure control system placed at the top, similar to the stripping tower, to act as a purging and venting mechanism in case there is a pressure build up (Love, 2007). Due to the pressure controller on the distillation column that controls the water into the condenser, the pressure controls on the actual condenser would be a secondary control system that is more used for safety (Love, 2007). This is because it would act according to the flow of the condenser water. Moreover, there will also be a level controller, to ensure that there is no flooding that is happening in the condenser, as it will control the gasoline leaving the condenser (Love, 2007).

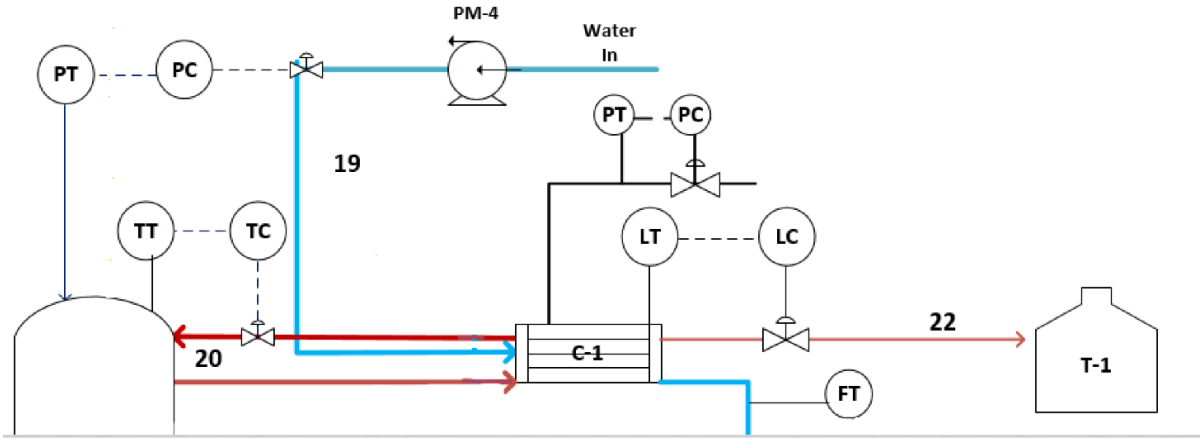

Figure 27 P&ID of Condenser

The transmitters to read pressure and level will be an absolute pressure transmitter and an ultrasonic transmitter, respectively. Both controllers will be P Controllers to ensure that it is fast acting as these controls are primarily put in place for safety. Lastly, the type of valves that will be used will be a pressure relief valve connected to the pressure controller and a butterfly valve connected to the level controller because of the quick shutoff capabilities associated with these valves (Love, 2007). The condenser process control details are specified in Table 40, along with fail-safe positions.

Table 40 Summary of P&ID Parameters of Condenser

Process Parameter	Pressure	Level
Transmitter Type	Absolute pressure Transmitter	Ultrasonic
Controller Type	P	P
Valve Type	Pressure Relief Valve	Butterfly
Fail-Safe Position	Fail-open	Fail-Open

8.7 Heat exchangers

The heat exchanger will be controlled through a cascade, feedback control system that are set to try to control the temperature and flow process variables. The purpose of the heat exchangers is the need to cool the products so that it can be kept at a safe storage temperature. If the heat exchangers were not controlled properly, this could lead to the products being highly prone to ignition and a possible explosion occurring if the fuel products are not cooled prior to storage. For each heat exchanger connected to Line 27, 32 and 37 the temperature will be read by a temperature transmitter leaving the products and the flow of the water coming into the condenser (Smith et al., 2015). Based on the two transmitter readings the flow of the cooling water, Line 28, will be controlled in the heat exchanger. If the temperature reading, the controller will open the valve more, so that it can cool the fuel to the desired temperature (Smith et al., 2015).

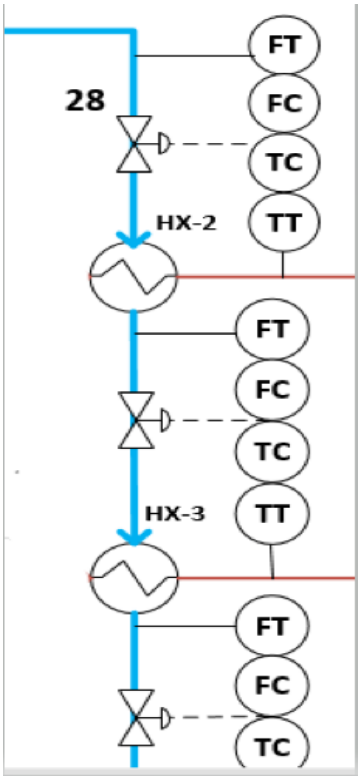

Figure 28 P&ID of Heat Exchanger

The temperature transmitter that will be used for this control system will be an RTD transmitter, although these transmitters are a bit more expensive than thermocouples, they are far more accurate (Smith et al., 2015). The accuracy for the product storage temperatures must be very accurate to prevent any hazards that may occur with these flammable products (Smith et al., 2015). The thermocouple can also be used because it has a wide temperature range, however the RTD is more stable, thus that is the transmitter type that will be chosen (Smith et al., 2015). For the flow transmitter that reads the water flowrate, that will be an ultrasonic transmitter as those are best for measuring fluid without any type of process interference. Moreover, the control type for the temperature and flow controls will be a PID controller. This is due to the accuracy that the PID controller provides as well as the to minimize the about of overshoot in the readings that can be experienced by the process (Smith et al., 2015). The final control elements, the valves, will be globe valves as they have multi-turn capabilities, meaning it is suitable for regulating flow, throttling applications and for precise control flow (Smith et al., 2015). Moreover, the fail-safe position of the valve will be fail-open, this is to let the cooling water into the heat exchanger to wash out the system and to prevent any damage to the equipment if fuel was trapped and the plant is not able to operate (Smith et al., 2015). The following Table 41 that summarizes the control specifications for the heat exchangers.

Table 41 Summary of P&ID Parameters for Heat Exchangers

Process Parameter	Tempreature	Flow
Transmitter Type	RTD	Ultrasonic
Controller Type	PID	PID
Valve Type	Globe	
Fail-Safe Position	Fail-open	

8.8 Venturi Scrubber

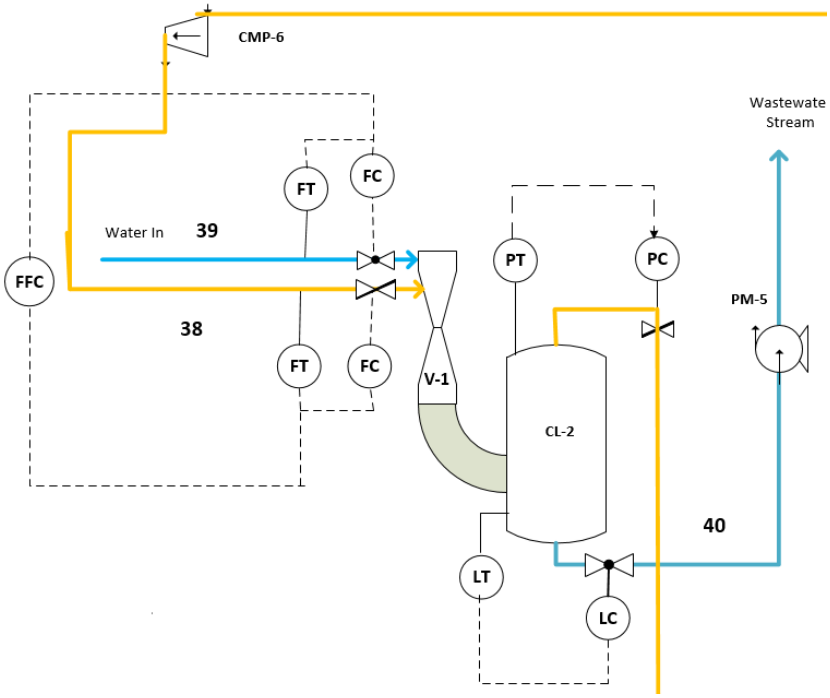

Figure 29 P&ID of Venturi Scrubber

The control scheme for the scrubbing system that includes the venturi scrubber followed by the cyclone is shown in Figure 29. The inlet gas and water streams are controlled by a ratio control to maintain the two flows at a constant ratio. This type of feed forward controller measures the disturbances, and the ratio is held at a desired set point by controlling one of the streams. In addition with the ratio relationships between the gas and liquid streams (L/G ratio specified in calculations), this controller makes it easy for those flowrates to be maintained. The flow of the liquid water stream is controlled based on the amount of gas flow entering. The flow transmitter measures the gas entering where the electrical signal reaches the ratio controller where it adjusts the valve of the water flow. This ensures the ratio of liquid to gas is maintained to improve collection efficiency and optimum performance. The level controller at the bottom

of the cyclone ensures that there is no overflow at the flooded elbow. Once the transmitter senses there is more liquid in the system than the operating conditions, it sends a signal to the controller to open the valve to allow the flow of the wastewater stream to pass. The pressure controller at the top of the cyclone ensures that there is no pressure build up in the system where the exiting syngas does not cause further problems down the pipes. Furthermore, this safety measure reduces the risk of overpressure in the pipes that may result in leakage or worse. A summary of the process control parameters for the venturi scrubber is given in Table 42.

Table 42 Summary of P&ID Parameters for Venturi Scrubber

Process Parameter	Pressure	Level	Flow
Transmitter Type	Absolute Pressure Transmitter	Ultrasonic	Ultrasonic
Controller Type	P	P	PID
Valve Type	Butterfly	Globe	Globe
Fail-Safe Position	Fail-Close	Fail-Open	Fail-Close

9. Safety, Loss Prevention & Environmental Impacts

9.1 General Considerations

Before managing and running a plant, safety evaluations must be made based on regulations that are already existing in the given jurisdiction to ensure that the safety of worker, public and the environment are protected. This section of the report will be dedicated to emphasizing on certain regulations and standards that must be followed, chemical awareness, environmental impacts and emissions, relief systems for units, flammable product and fire analysis, toxic dispersion investigations and possible precautions that can be taken to avoid detrimental outcomes. The two primary governmental regulations that must be followed in regards to the Occupational Safety and Health Act (OHSA) and the laws governed by the Environmental Protection Agency (EPA) (Crowl et al., 2002).

The OSHA holds employers responsible for creating a safe working environment and enforcing safety standards. According to the OHSA it states that employers must allow OHSA compliance officers into the site to do safety inspections, that can be warranted without any prior warning or notice (Crowl et al., 2002). Moreover, if the OSHA officers feel that plant is not operating in safe conditions, they can shut down the plant. In 1992, the OSHA finalized a management rule that all facilities must abide by which was called the “Process Safety Management of Highly Hazardous Chemicals” (Crowl et al., 2002). The rule is

comprised of several components such as, Process Safety Management (PSM) which is further broken into the responsibilities of the employers and employees (Crowl et al., 2002). The OSHA states that the process safety information must be identified and investigated by a team of employee, most facilities have a health & safety committee (Crowl et al., 2002). This information on chemical hazards that are in regards to plant operation must also be available to all workers and clients, contractors or guests coming into the plant. Moreover, the hazard analysis will be regularly checked and a method plan, that will be discussed in the next section will be put in place to avoid possible situations (Crowl et al., 2002). Consequently, the operating procedures, emergency shut off operations, normal shutoff operations must also be available to all workers in the plant (Crowl et al., 2002). The OSHA is put in place to ensure and highlight the importance of safety, through having an effective training system and awareness to the various hazards around the plant, a safe working environment can be established (Crowl et al., 2002). The EPA also correlates to the OSHA through creating a Risk Management Plan (RMP) which is more hazard focused but aims to emphasis the same goal which is safety control and implementation (Crowl et al., 2002). Other standards and guidelines that the plant will follow besides those outlined by the OSHA and EPA are found in the following figure 30.

Number	Description
29 USC 651	Occupational Safety and Health Act (1970)
42 USC 7401	Clean Air Act (1970)
33 USC 1251	Clean Water Act (1977)
42 USC 7401	Clean Air Act Amendments (1990)
15 USC 2601	Toxic Substances Control Act II (1992)
42 USC 300f	Safe Drinking Water Act Amendment (1996)
40 CFR 280.20	Underground Storage Tank Leak Tests (1988)
40 CFR 370.30	Annual Toxic Release Report, SARA 313 (1989)
29 CFR 1910.120	Training, Hazardous Materials Technician, HAZMAT (1989)
29 CFR 1910.1450	Exposure to Hazardous Chemicals in Laboratories (1990)
40 CFR 370.20	Annual Inventory of Hazardous Chemicals, SARA 311 (1991)
29 CFR 1910.119	Process Safety Management (1992)
40 CFR 68.65	Risk Management Program (1996)
29 CFR 1910.134	Respirator Program (1998)

Figure 30 Common Acts and Regulations Plants must abide by (Crowl et al., 2002)

9.2 Reactor Safety

In the Reactor and cyclone design for PID alarms are used to alert operators to serious and potentially hazardous, deviation in process condition. In the process design, reactor and conveyer belt are fitted with switches and software that make audible or visual alarms to the control panels and shared display screens. If there are lack of response from the operators, the reactor or the conveyer belt will be automatically shut down to avert the hazardous situation. The automatic trip system used in the reactor and conveyer belt are a fail-close process control (Towler et al., 2013). Each Component have their own failure rate and have to be replaced according to the required guideline from the following Figure 31.

Instrument	Faults/year
Controller	0.29
Control valve	0.60
Flow measurement (fluids)	1.14
Flow measurement (solids)	3.75
Flow switch	1.12
Gas-liquid chromatograph	30.6
Hand valve	0.13
Indicator lamp	0.044
Level measurement (liquids)	1.70
Level measurement (solids)	6.86
Oxygen analyzer	5.65
pH meter	5.88
Pressure measurement	1.41
Pressure relief valve	0.022
Pressure switch	0.14
Solenoid valve	0.42
Stepper motor	0.044
Strip chart recorder	0.22
Thermocouple temperature measurement	0.52
Thermometer temperature measurement	0.027
Valve positioner	0.44

Figure 31 Failure Rate for Various Process Control Components (Towler et al., 2013)

9.3 Environmental Impact

To operate a biooil fuel plant, it is required to follow the regulations set by the municipal, provincial, and federal government for environment regulation. The administration of the Canadian Environmental Protection Act, 1999 (CEPA) enforces various rules and regulations for environmental matters such as air and water pollution, waste management and toxic substances. The pollution of emission of the plant is monitored, reported and researched according to the Part 3, Section 44 of the Act, the minister of the environment. The following rules are set for the Canadian Environmental Protection Act:

- Environmental monitoring station should be established.
- Collect and publish data on environmental quality in Canada.
- Conduct research and studies on pollution control and environmental contamination.
- Formulate pollution prevention plans.
- Publish information on pollution prevention plans and on the quality and stat of the environment in Canada.

As the fuel produced by the biofuel plant would be considered under clean and renewable fuel standard, it will have significant benefit towards the environment. The only sources of carbon emission would be from the operation of the plant and from the energy required to run the plant. Most of the emission is recycled in a venturi scrubber to mitigate the environmental pollution. In this regulation a performance-based approach that would incent the use of a broad range of low carbon fuels, energy sources and technologies, such as electricity, hydrogen, and renewable fuels, including renewable natural gas. It would establish lifecycle carbon intensity requirements separately for liquid, gaseous and solid fuels, and would go beyond transportation fuels to include those used in industry and buildings. The approach would not differentiate between crude oil types produced in Canada or imported. The clean fuel standard would complement the pan-Canadian approach to pricing carbon pollution (Towler et al., 2013). Minimum expulsion of air pollution to the environment, would be the ideal goal of the project. The National Emission Standard for Hazardous Air Pollutants (NESHAP) regulates leaks, flares, and excess emissions from chemical plants that contain hazardous air pollutants. The Clean Water Act's National Pollutant Discharge Elimination System (NPDES) program, the EPA regulates pollutant discharges from industrial facilities, and these guidelines must be followed to reduce water pollution.

9.4 Chemical Hazards

9.4.1 Methane

Methane is considered hazardous by the OSHA hazard communication standard (29 CFR 1910.1200). It is a category 1 flammable gas, may explode if heated under pressure. Keep away from heat, open flames, or ignition sources. Store in well-ventilated place away from sunlight as seen in Figure 32.

9.4.2 Benzene

Benzene is considered hazardous by the OSHA hazard communication standard (29 CFR 1910.1200). It is a category 2 flammable liquid, category 2 skin irritation, category 2A eye irritation, category 1 germ cell mutagenicity, category 1 carcinogenicity, and category 1 specific target organ toxicity. It may be toxic if inhaled, it may damage fertility to unborn child, it may cause damage to organs with prolonged or repeated exposure. It must be given special instructions before use. Must wear protective gloves, protected clothing, eye, or face protection. Keep away from heat, or other ignition sources and do not smoke around it. Use only outdoors in ventilated areas. Do not breathe gas. Do not eat, drink, or smoke near product as seen in Figure 33.

Section 2. Hazards identification

OSHA/HCS status	:	This material is considered hazardous by the OSHA Hazard Communication Standard (29 CFR 1910.1200).
Classification of the substance or mixture	:	FLAMMABLE GASES - Category 1 GASES UNDER PRESSURE - Compressed gas
GHS label elements		
Hazard pictograms	:	
Signal word	:	Danger
Hazard statements	:	Extremely flammable gas. May form explosive mixtures with air. Contains gas under pressure; may explode if heated. May displace oxygen and cause rapid suffocation.
Precautionary statements		
General	:	Read and follow all Safety Data Sheets (SDS'S) before use. Read label before use. Keep out of reach of children. If medical advice is needed, have product container or label at hand. Close valve after each use and when empty. Use equipment rated for cylinder pressure. Do not open valve until connected to equipment prepared for use. Use a back flow preventative device in the piping. Use only equipment of compatible materials of construction. Approach suspected leak area with caution.
Prevention	:	Keep away from heat, hot surfaces, sparks, open flames and other ignition sources. No smoking.
Response	:	Leaking gas fire: Do not extinguish, unless leak can be stopped safely. Eliminate all ignition sources if safe to do so.
Storage	:	Protect from sunlight. Store in a well-ventilated place.
Disposal	:	Not applicable.
Hazards not otherwise classified	:	In addition to any other important health or physical hazards, this product may displace oxygen and cause rapid suffocation.

Date of issue/Date of revision : 11/15/2020 Date of previous issue : 3/14/2019 Version : 1.08 1/11

Figure 32 Hazard Identification and Safety Information for Methane (ESPA,2020)

Section 2. Hazards identification

OSHA/HCS status	:	This material is considered hazardous by the OSHA Hazard Communication Standard (29 CFR 1910.1200).
Classification of the substance or mixture	:	FLAMMABLE GASES - Category 1 GASES UNDER PRESSURE - Compressed gas ACUTE TOXICITY (inhalation) - Category 3 TOXIC TO REPRODUCTION - Category 1 SPECIFIC TARGET ORGAN TOXICITY (REPEATED EXPOSURE) - Category 1
GHS label elements		
Hazard pictograms	:	
Signal word	:	Danger
Hazard statements	:	Extremely flammable gas. Contains gas under pressure; may explode if heated. Toxic if inhaled. May damage fertility or the unborn child. Causes damage to organs through prolonged or repeated exposure. Asphyxiating even with adequate oxygen. May form explosive mixtures with air.
Precautionary statements		
General	:	Read and follow all Safety Data Sheets (SDS'S) before use. Read label before use. Keep out of reach of children. If medical advice is needed, have product container or label at hand. Close valve after each use and when empty. Use equipment rated for cylinder pressure. Do not open valve until connected to equipment prepared for use. Use a back flow preventative device in the piping. Use only equipment of compatible materials of construction. Approach suspected leak area with caution.
Prevention	:	Obtain special instructions before use. Wear protective gloves. Wear protective clothing. Wear eye or face protection. Keep away from heat, hot surfaces, sparks, open flames and other ignition sources. No smoking. Use only outdoors or in a well-ventilated area. Do not breathe gas. Do not eat, drink or smoke when using this product.

Figure 33 Hazard Identification and Safety Information for Benzene (ESPA,2020)

9.4.3 Carbon Monoxide

Most of the materials used in the manufacture of biooil are poisonous, to some extent and almost every chemical is toxic. One of the components is carbon monoxide formation during pyrolysis process. It is very toxic and can harm the blood (decreases ability to carry oxygen). Moreover, Figure 34 was used to determine the toxicity of the fluidized bed reactor products and the ways to prevent hazard from the materials

Table 10.1 Toxicity Data

Compound	PEL (ppm)	LD50 (mg/kg)
Carbon monoxide	50	1807
Carbon disulfide	20	3188
Chlorine	1	239
Chlorine dioxide	0.1	292
Chloroform	50	1188
Cyclohexane	300	
Dioxane	100	4200
Ethylbenzene	100	3500
Formic acid	5	1100
Furfural	5	260
Hydrogen chloride	5	4701
Hydrogen cyanide	10	3.7
Isopropyl alcohol	400	5045
Toluene	100	5000
Xylene	100	4300

Source: OSHA.

Figure 34 Toxicity Data (Towler et al., 2013)

One of the main products produced in the reactor is carbon monoxide, which has LD_{50} value of 1807. A simple standard for oral absorption is that anything between 200 to 2000 is harmful in nature to human beings. The World Health Organization (WHO) has a TLV-TWA of 10 ppm for 8-hour exposure to carbon monoxide. The reactor is placed in a closed system, where the product is non refined biooil, vapor, and char. The operators might get exposed to the flue gas from the plant and the following symptoms in Table 43 would be crucial to determine the extent of exposure.

Table 43 Effects of Exposure Routes of Carbon Monoxide (Towler et al., 2013)

Contact	Effects
Eye Contact	• Contact with rapidly expanding gas may cause burns or frostbite
Inhalation	• Toxic if inhaled
Skin contact	• Contact with rapidly expanding gas may cause burns or frostbite
Ingestion	• As this product is a gas the same happens as inhalation
Repeated exposure	• Reduced fetal weight, increase in fetal death and skeletal malformation • Causes damage to organs • Asphyxiating even with adequate oxygen

The control methods to limit the workers exposure to carbon monoxide is to make sure that workplace has lower than 50 concentration of carbon monoxide in the working area. This could be achieved by implementing various tactics such as:

1. Ventilation in work area
2. Personal protective equipment
3. Process remain a closed system

The major concern would be the disposal of various greenhouse gases in the environment. The Canadian Environmental Protection Act (CEPA, C-15.31, 1999) enforces Environment Canada to controlling toxic substances, reducing pollution, and eliminating persistent bioaccumulating toxic substances. This act focuses on Greenhouse gas emission of carbon dioxide, water vapor and methane produced by this pyrolysis plant. We also have a venturi scrubber, which produces water waste and falls under pollution prevention act to minimize the waste from the plant. The gaseous effluents that contains toxic or noxious substance are treated in venturi scrubber before releasing it to the environment. The aqueous waste is in such small quantities that it could be incinerated with minimum environmental damage. The solid waste as char would be used as fertilizer for plant or could be incinerated for fuel use.

9.5 Emissions

For the environmental impacts to consider for a biofuel plant, would be the carbon emission from the reactor and the steam utilization. The reactor itself through the process of pyrolysis of biomass generates 700 kg/day of carbon emission in total of carbon, carbon monoxide and carbon dioxide, which is later purged in a venturi scrubber to lower the environmental impacts. The rest of the carbon emission is produced through steam boilers used to provide energy for the units. The total carbon emission for the operation of the bubbling fluidized bed reactor is 1361 kg/day. The Canadian Government Carbon and Greenhouse Gas legislation has placed a limit of 420 tonnes of CO_2 for each gigawatt-hour of electricity produced from coal per year (Laws-Lois, 2015). The regulations regarding to the reduction in the release of methane and certain volatile organic compound was enforced on January1-2020, except for section 26, 27, 37 to 41, which state:

- Impose certain requirements on the oil and gas sector in order to reduce emissions of methane and certain volatile organic compounds.
- Designate the contravention of certain of its provisions as serious offences by adding them to the schedule to the regulations designating regulatory provisions for purposes of enforcement.

9.10 Fire & Flammability Assessment

Due to the lack of oxygen present in this system, it lowers the likelihood of a combustible runaway reaction. There have been previous studied cases of pyrolysis reactors exploding due to excess oxygen feed in India, Finland, Germany, and Russia. There have also been some cases where there has been leaks of pyrolysis gas into the air causing various forms of harm to the surrounding neighborhood. However, there is usually a safety protocol put in place in these situations as displayed in Figure 35.

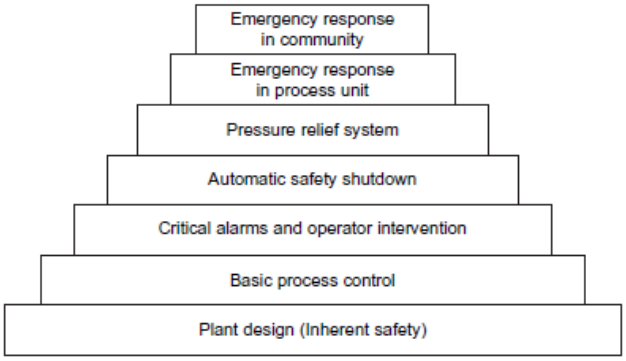

Figure 35 General System of Priority for Plant Safety (Towler et al., 2013)

Using the chart for a layer of plant safety was designed. The reactor has various volatile chemical compounds but one of the concerning toxic products is carbon monoxide. The toxic compound LD50 is in 1807 mg/kg. According to the Classification of European union guideline, LD50 oral absorption over 50 ppm is considered harmful for the humans. The carbon monoxide is purged and used in venturi scrubber to mitigate the expulsion of carbon monoxide from the plant. Above all, the flammability of the reactor needs to be taken into consideration, thus a flammability chart was constructed to show safe operating percentages in Figure 36.

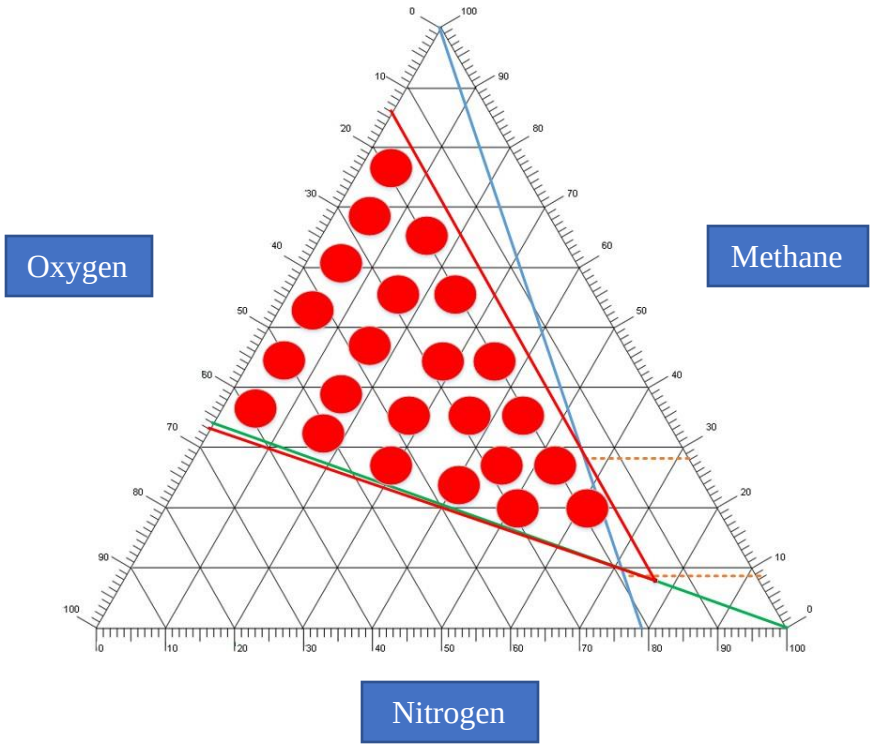

Figure 36 Flammability for Methane in Process

A general way to show the flammability of a gas or vapor is by the triangle diagram. As the most dominant and flammable gas in the reactor is methane, it is chosen as a fuel in the diagram to have the safest possible operating region. The blue line represents the Air line, green line represents the stoichiometric line, and the red line represents the flammability line encapsulates the flammability zone of the process. The following elements in Table 44 are taken in consideration for the conclusion of the flammability diagram:

Table 44 LFL and UFL for Various Elements (Crowl et al, 2002)

Element	Lower Flammability Limit	Upper Flammability Limit
Glyxcolaldehyde ($C_2H_4O_2$)	-	-
Acetylenediol($C_2H_2O_2$)	2.5	100
Vinyl alcohol C_2H_4O	-	-
Allyl alcohol C_3H_6O	2.5	18
Hydroxyquinol $C_6H_6O_3$	-	-
Carbon Dioxide CO_2	-	-

Carbon monoxide CO	12.5	74.2
Methane (CH_4)	5	15
Water (H_2O)	-	-
Total (mix value)	7.76	28.86

The mixed upper flammability is 28.86 and the mixed lower flammability is 7.76. The minimum oxygen concentration is 15.51. This means that for the reactor to be in safe operating conditions, without the possibility of explosion, the percentages of the components should be around 65% oxygen, 15% methane and 20% nitrogen. This is achieved through process control and various mechanism for quality as well as safe products.

9.11 Toxic Dispersion Models

Toxic dispersion incidences must be taken into consideration when trying to design a plant, as potential chemical releases may be hazardous to workers and the public around the plant. There are multiple examples of toxic dispersion that can happen within this process such as an explosive rupture of any process equipment, runaway reactions, or even if the storage temperature and pressures are above what is needed for safe storage. To access the behavior of toxic dispersion cases it is important to first identify the release incident, develop some sort of source model estimating the size and release rate and lastly to evaluate downwind concentrations that can be inflected onto people. Although there can be may incidences where toxic hazards can be released, which is more explored in the Risk Assessment Section, two cases that have high probabilities of occurring will be investigated.

The first case is a scenario involving a possible leak in one of the units such as the condenser. Pipe cracks, failure of equipment or failure of process control mechanisms are all possibilities that need awareness. The toxic chemical being released is benzene from the synthesized gasoline, usually when gasoline is stored at room temperature after processing the benzene concentrations are not hazardous (Crowl et al., 2002). However, before gasoline is completely processed, most gasoline mixtures are known to have very high percentages of benzene concentrations in the mixture. The TLV-TWA for benzene is around 10 ppm for an 8-hour period (Crowl et al., 2002). The toxicity of this release will be assessed from the point of the condenser, which is 17m above ground level. To find the evaporation rate and the concentration the Pasquil-Gifford Model will be used (Crowl et al., 2002).

$$\frac{mg}{m^3} = \frac{Q_m}{pi() * \sigma_y \sigma_z} \tag{49}$$

Where Q_m is the evaporation rate in g/s

H_t is the effective height in m

u is the wind speed velocity

σ_y and σ_z are obtained from the Pasquil-Gifford relations based on the environmental conditions and the downwind distance.

For this case, it will be assumed that the model is in urban conditions as the plant is in Toronto and will be of class D conditions. The estimated plume dimensions will be around 20m by 20m because it is assumed that the dispersion of benzene is high, as the relative volatility of benzene is around 0.6 (Crowl et al., 2002). The concentration was found to be around 0.3214 ppm and an evaporation rate of 446.6 g/s. In addition, through trial and error the downwind distance that is affected by the plume release is around 165m.

For the second case, the leaking of reactor carbon monoxide or fracture near the reactor for leaking carbon monoxide. The leak could happen from the pipe cracks, fracture of the reactor, failure of the process control or fracture in rupture disk. The threshold limit value for carbon monoxide is 25 ppm (Crowl et al., 2002). In the LD_{50} chart it is considered to be seriously toxic for humans. To find the evaporation rate and the concentration the Pasquil-Gifford Model will be used.

In Table 45 a summary of the dispersion model for the condenser releasing a gasoline-benzene vapor is shown.

Table 45 Summary of Toxic Dispersion Values for Cases

Assumed		
Case	**1**	**2**
Class	D	D
Wind Speed (m/s)	4.02	4.02
Area	Urban	Urban
Sky Cover	Day Overcast	Day Overcast
Ambient Pressure (atm)	1	1
Ambient Temperature (℃)	21	21
Length (m)	20	20
Width (m)	20	20
Calculated		
Evaporation Rate (g/s)	446.78	13231
Concentration of Toxin (ppm)	0.3	0.00041
Affected Downwind Area (m)	165	1010

10. Risk Assessments

Through constructing an in-depth analysis on the possible risks that can occur in the plant, safety measures and possible solutions can be created. Table 46 is a synthesized Hazard and Operability Study (HAZOP) Guide that can help grade the level of risk for possible outcomes. Moreover, Table 47 is a summary of the parameters of special interest prone to being in risk, possible causes and solutions graded using the guide for each unit.

10.1 Hazard Assessment Study

Table 46 Developed Hazard Assessment Guide (HAZOP) (Crowl et al., 2002).

HAZOP Guide					
Likelihood	1	2	3	4	5
	Unlikely	Remote	Possible	Probable	Frequent
	Occurrence probability of event is low in the industry	Likelihood is low, however, probability is more than a few times in the industry	Has occurred numerous times in the industry	Has the potential to occur several times and is more likely	Occurrence is very likely and may occur more than once a year
Severity of consequences	1	2	3	4	5
	Minor	Serious	Major	Critical	Catastrophic
	None to low impact on environment, people, and plant	Awareness of event likelihood and event must reported. May cause harm to workers	May cause damage to people, plant, and environment. Media must be informed	High risk to people, plant, and environment. Regional media attention and legal action may be required	Loss of life, damage to plant, long term impact. Shutdown must occur and international media attention
Relative Risk (Likelihood x Severity	L		M		H
	Low risk to plant operations		Medium risk to plant operations		High risk to plant operations
Range	1-6		7-15		16-25

Table 47 HAZOP Study of Processing Units in System

Hazard and Operability Study (HAZOP)									
Unit	**Process Parameter**	**Deviation**	**Possible Causes**	**Possible Consequences**	**Action Required**	**Likelihood of Occurrence (L)**	**Severity of consequence (S)**	**Risk**	**Relative Risk**
Disc Filter	Flowrate	>1500 m^3/hour	1. extreme weather conditions 2. debris accumulation in influent stream	1. filter damage 2. ineffective filtration 3. increase in pressure drop	1. manual cleaning of debris 2. maintenance of filters 3. flow by-pass in case of wet weather	3	1	3	L
Fluidized Bed Reactor	Temperature	>517 C	1. Heating jacket malfunction 2. increase in measured combustion in chamber 3. failure of process control system	1. possible explosion 2. decrease in product quality 3. increased rate of reaction	1. Increase flowrate in cooling jacket 2. Shutdown of plant 3. decrease fuel use for combustion 4. maintenance to ensure control system is functional. 5. Increase the nitrogen feed.	3	5	15	M
	Pressure	> 6.5 atm	1. increase in feed flow 2. Pressure transmitter malfunctions 3. increased rate of reaction 4. not enough flow to cyclone due to increased pressure drop	1. Possible explosion 2. Cracking of reaction vessel 3. increased temperature	1. activate pressure release system 2. Increase suction from reactor	1	5	5	L
	CH_4 Leak	-	1. Fracture in the reactor 2. Loose pipes from the reactor to cyclone	1. Decline of product quality 2. Suffocation and headache if inhaled 3. possible explosion	1. gas detection sensor 2. Increase the ventilation in the leaked area 3. Seal the fractures pipe area or reactor	4	5	20	H

					4. tighten the connection				
	CO Leak	-	1. Fracture in the reactor 2. Loose pipes from the reactor to cyclone	1. Decline of product quality 2. Toxic if inhaled and possible death	1. Carbon Monoxide detection sensor 2. Increase the ventilation in the leaked area 3. Seal the fractures pipe area or reactor 4. tighten the connection	4	5	20	H
Cyclone	Pressure	000>pressure drop	1. Not enough flow rate from air pump 2. Not enough flow rate from reactor 3. Fracture in the cyclone	1. Impure Product 2. Inaccurate effluent flow 3. leak of biogas and syngas at high temperature	1. Seal the fractured area 2. Ensure pressure system is functioning 3. Regular maintenance of cyclone	3	3	9	M
Distillation Column	Flowrate	>2123 kg/day	1. Incoming feed not controlled/sensed. 2. The composition of vapor in feed is greater than operating conditions	1. Impure product 2. Column experiences weeping and flooding. 3. Decrease in efficiency	1.Maintence of flow and level sensors checked regularly. 2. Install drainage system 3. Use an emergency shutdown for column	3	5	15	M
	pressure	>10 Bar	1. Steam required is greater than operating conditions. 2.Vapor flowrate is higher based on feed composition. 3. Uncontrolled incoming feed rate	1. possible explosion of column 2. Impure product	1. Ensure that pressure control system is working. 2. Regular maintenance of flow sensors for feed and steam streams 3. Inspection of pipes to ensure no blocking	2	5	10	M
	Temperature	Undesired	1.Incoming feed into at a greater temperature than operating conditions 2.Tempreature sensors throughout	1. possible explosion of column 2. Impure product	1. Ensure that temperature control system is working. 3. Have a drainage system before shutdown.	3	5	15	M

			column become inactive. 3. Steam feed is insufficient. 4. Insulation tear		3. Put better insulation on the column. 4. Areas where product draw is measured to ensure that it is taken at right temperature				
Venturi Scrubber	Temperature	Undesired	1. Failure of heat exchanger 2. Feed temperature of water is higher than operating conditions.	1. Lower efficiency of tar removal 2. Increase in clogging between scrubber and cyclone 3. Release of toxic emissions	1. Send syngas to flare. 2. Regulate temperature with control system. 3. Adding more water and cooling with quench system to regulate temperature	2	3	6	L
	Flowrate	Undesired	1. Failure of ratio controller 2. Failure of pumps	1. Lower efficiency of tar removal 2. Increase clogging and overflow of system 3. Release of toxic emissions	1. Maintenance of control system to regulate flow. 2. Bypass to flare	1	3	3	L
	Syngas Pipeline Leakage	Leak	1. Erosion of control valves and relief valves 2. Material defect such as poor welded connection and lack of protection against corrosion cracking 3. Lack of pipeline cleanliness	1. Clogging in piping system 2. Release of syngas to the environment that may cause detrimental health effects if inhaled 3. May lead to explosion	1. Regular maintenance of control system 2.. Maintaining cleanliness of pipes by removing any potential condensed tar in pipelines 3. Replace corroded and eroded materials and increase pipe thickness	3	3	9	M

10.2 Risk Assessment Analysis

Creating a safe work environment begins with a detailed risk assessment. Risk assessments determine if there are any hazards associated with the plant and equipment to establish preventative measures to protect the life of individuals, property, and the environment. Risk assessment includes incident identification and consequence analysis. Incident identification describes how an incident occurs using an analysis of the probabilities. Consequence analysis describes the expected damage which can include loss of life, damage to the environment or capital equipment, and days outage. The two probabilistic methods conducted in this report are the event trees and fault trees.

10.3 Event Trees

This approach begins with an initiating event and works towards a possible solutions and results. The event tree provides information on how a failure can occur and the probability of the occurrence. In addition, the event tree is useful for providing scenarios of possible failure modes to modify the design to improve the safety. The typical steps in an event tree analysis are:

1. Identify an initiating event of concern.
2. Identify the safety functions designed to deal with the initiating event.
3. Construct the event tree.
4. Describe the resulting accident event sequences.

10.3.1 Syngas Leakage

For Event Tree 1 in Figure 37, the initiating event in this study is the syngas leakage that occurs through the pipelines. This event was chosen as it can lead to many consequences if safety measures are not considered and put into place. A gas or syngas leakage is likely to occur 0.00005 times a year (Crowl, 2011). To mitigate the risk of leaks in syngas piping systems, the installation of a Leak Detection System (LDS) is implemented. The system can detect a leak in real time and estimates the size and location of the leak which allows operations staff to assess the severity of the leak and the type of response that is required. The system safety function in this case is the LDS is assumed to have a failure rate of 0.05 failure/demand (B) (Quest Consultants, 2010). In case of a syngas leakage, the detector generates an alarm that starts a forced ventilation system to dilute and disperse the gas to the atmosphere. Welding and painted piping is highly recommended to protect against atmospheric corrosion to minimize the chances of pipeline leaks (Quest Consultants, 2010). Often, corrosion can be easily controlled through visual inspections if piping

is above ground. We assume that the operator will notice the leak during examination or inspection 3 out of 4 times (0.25 failure/demand) (C). It is also assumed that the operator quickly repairs the leak from the pipelines 9 out of 10 times (0.10 failure/demand) (D). The probability of the severity of the syngas pipeline leak to lead to the shutdown and evacuation of the plant is 0.01 failure/demand. The release of carbon monoxide and syngas can lead to the formation of a toxic and flammable cloud in the surrounding plant which may ignite. It is important to take this event into consideration as any chance of occurrence to this event will lead to great risks. From the sample calculations in the Appendix (section 15.15), it can be concluded that the probability of a syngas leakage to the atmosphere is approximately 9.9×10^{-9} occurrences/year as shown in Table 48.

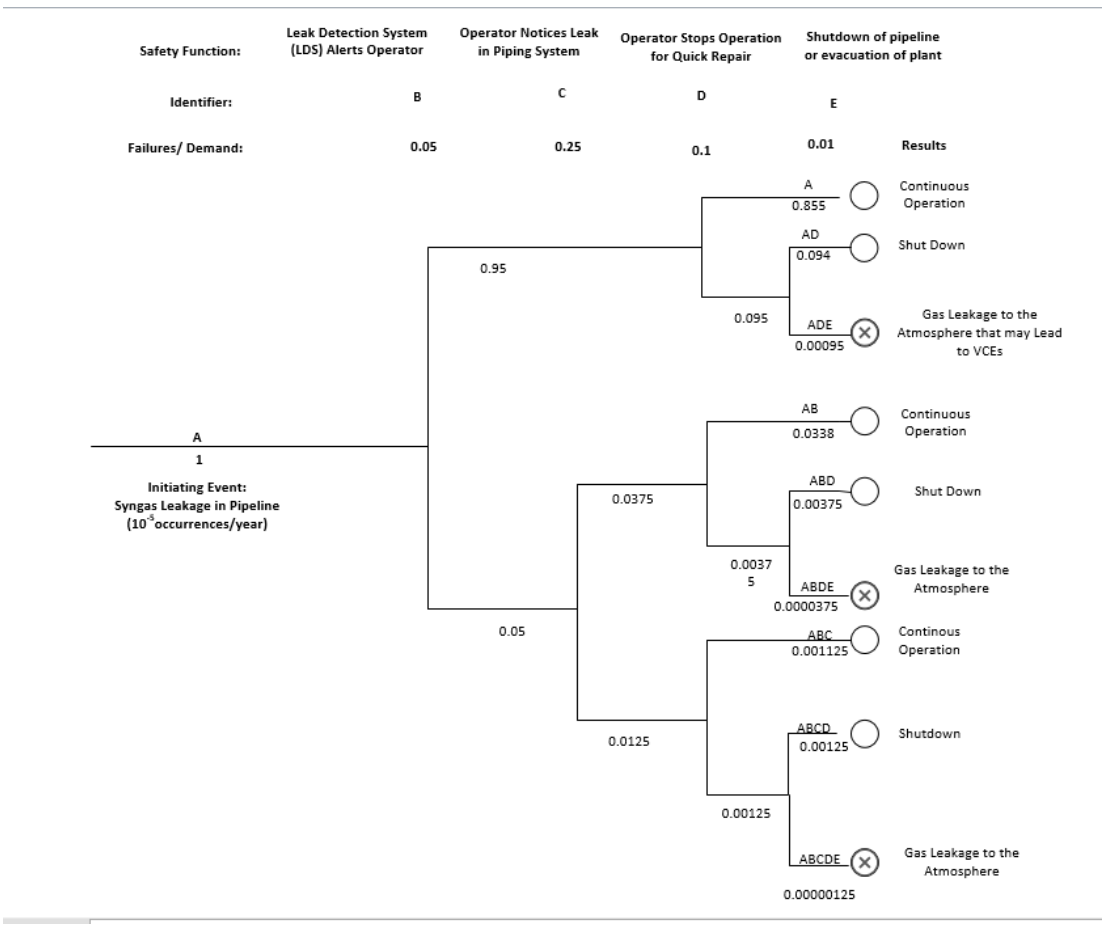

Figure 37 Event Tree 1 Syngas Leakage

Table 48 Calculated Probability Results for Event Tree 2

Results	Probability
Continuous Operation	8.89×10^{-6} occurrences/year
Shutdown	9.9×10^{-7} occurrences/year
Gas Leakage	9.9×10^{-9} occurrences/year

10.3.2 Over Pressure in Distillation Column

It can be noted that the main risks of distillation columns are weeping, flooding and overpressure (Crowl et al., 2002). The overpressure of a distillation column was the primary focus of Event Tree 2 as shown in Figure 38. This scenario was chosen as a build of pressure in the system without taking any safety measures may lead to damaging and high-risk outcomes. The probability of the overpressure of a distillation column is approximately 0.07 occurrences/year (Maget et al., 2019). If the pressure transmitter or controller and the pressure relief system all fail, it may lead to the damage or rupture of the distillation column which may release some of the toxic chemicals within the system that can result in a similar scenario to Figure 38 if syngas is leaked. Any damage to the distillation column or leakage of toxic syngas or fuel can lead to an explosion or fire. From the event tree, the probability of the damage to the distillation column is about 1.05×10^{-6} occurrences/year as shown in Table 49.

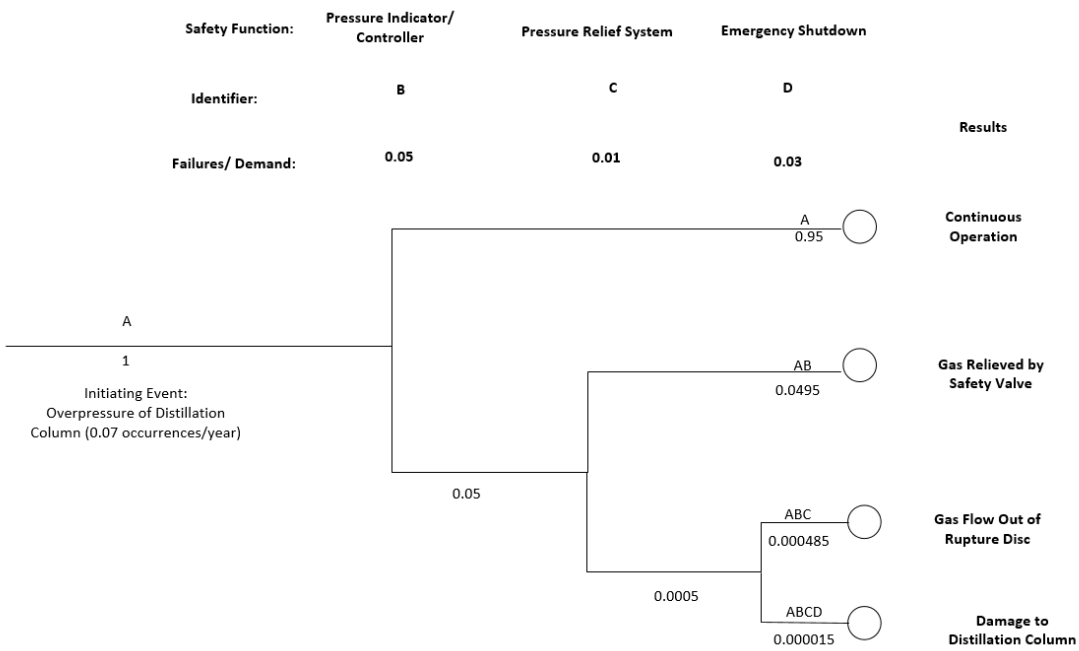

Figure 38 Event Tree 2 for Overpressure in Distillation Column

Table 49 Calculated Probability Results for Event Tree 2

Results	Probability
Continuous Operation	0.0665 occurrences/year
Gas Relieved by Safety Valve	3.47×10^{-3} occurrences/year
Gas Flow out of Rupture Disc	3.395×10^{-5} occurrences/year
Damage to Distillation Column	1.05×10^{-6} occurrences/year

10.3.3 Safety System Failure

Event Tree 3 in Figure 39, demonstrates the probability of different safety relief system failures. Since, this process is similar to a petroleum refinery, it is important to take all safety measures as the risks for the people and the plant. The probability of a process control failure is approximately 0.01 (Crowl et al., 2002). This situation again leads to mandatory closure to the plant if the alarm and high safety instruments fail. The failure of the process control equipment is generalized to any unit. This means that this situation may occur within the reactor, the distillation column, or even the venturi scrubber. From the results below in Figure 39, the probability of exposure to toxins and possible explosion due to process control system failure is about 9.98×10^{-6} occurrences/year as shown in Table 48.

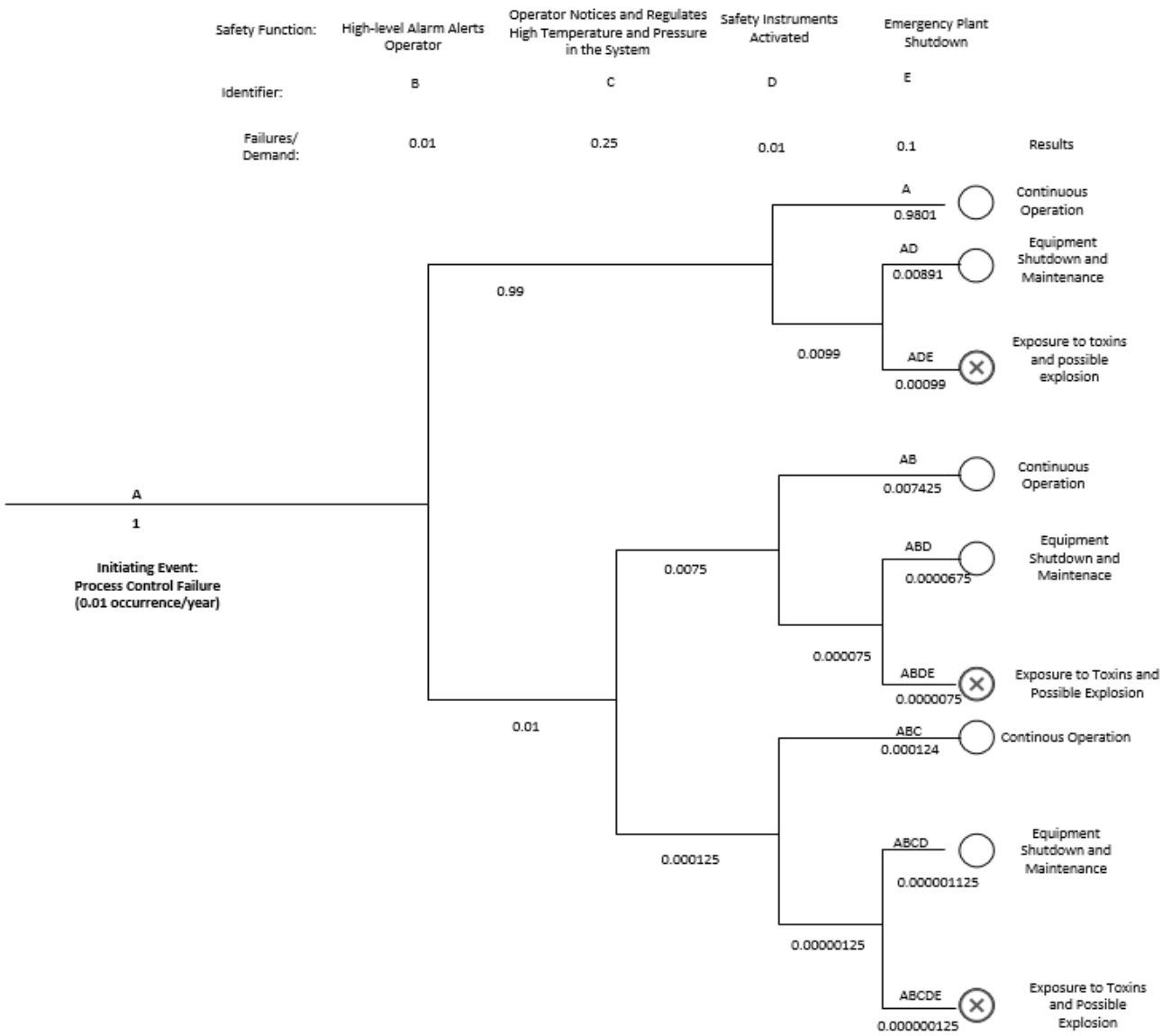

Figure 39 Event Tree 3 for Process Control Failures

Table 50 Calculated Probability Results of Event Tree 3

Results	Probability
Continuous Operation	9.88×10^{-3} occurrences/year
Equipment Shutdown and Maintenance	9.88×10^{-5} occurrences/year
Exposure to Toxins and Possible Explosion=	9.98×10^{-6} occurrences/year

10.4 Fault Trees

Fault trees are a deductive method for identifying ways in which hazards can lead to accidents. This method starts with the top event or accident and works backwards towards the different scenarios that may have led to the accident. Some of the symbols used in the fault tree are explained in Table 51 as shown below.

Table 51 Fault Trees Legend (Cooper et al. 2011)

Symbol Name	Symbol Diagram	Description
INTERMEDIATE Event	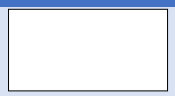	An event that results from the interaction of a number of other events
AND Gate		The resulting output event requires the simultaneous occurrence of all input events
OR Gate	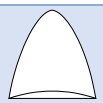	The resulting output event requires the occurrence of any individual input event
BASIC Event	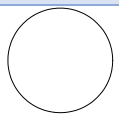	A fault event that needs no further definition
EXTERNAL Event	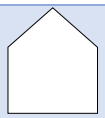	An event that is a boundary condition to the fault tree
UNDEVELOPED Event	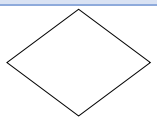	An event that cannot be developed further due to lack of suitable information

The fault tree typically depicts the reliability and failure probability of each event. The reliability (R), can be calculated using the Poisson distribution using the following equation:

$$R(t) = e^{-\mu t} \tag{50}$$

Where.

μ is the average failure rate with units of faults/time

t is average period of time it takes for the instrument to fail

The failure probability, (P) is represented using the following equation:

$$P(t) = 1 - R(t) \tag{51}$$

The summation of the reliability and failure must be equal to one. For the fault trees in Figure 40 and Figure 41 the event of Syngas leakage and the overpressure of a distillation column is considered. The failure probability that would result in damage to the distillation column caused by excessive pressure beyond what the column is designed for overpressure is assumed to be 0.07 occurrences/year. The root cause of this event is split into three sections: failure of pressure indicator, failure of emergency shutdown, and failure of pressure relief devices. The column can be protected by means of pressure relief devices such as pressure relief valves or rupture disks. The failure probabilities of these devices along with the other devices used in this event are displayed in Table 52.

Table 52 Summary of Failure Probabilities for Devices (Crowl et al., 2002)

Component	Failure Rate μ (faults/year)	Reliability $R(t) = e^{-\mu t}$	Failure Probability P=1-R(t)
Alarm Indicator	0.044	0.957	0.043
Pressure Measurement	1.41	0.244	0.756
Pressure Switch	0.14	0.869	0.131
Solenoid Valve	0.42	0.657	0.343
Pressure Relief Valve	0.022	0.978	0.376
Rupture Disk	0.2	0.819	0.441

10.4.1 Fault Tree of Syngas Pipeline Leakage

Fault tree 1 was created to correspond with event tree 1 shown in Figure 40. The syngas pipeline leakage may have occurred due to failure of pressure indicator, failure of pressure relied device, or failure of

emergency shutdown. Instruments such as the alarm indicator, pressure relief valve, and rupture disk are some of the causes of this leakage. The probability values are taken from Table 48.

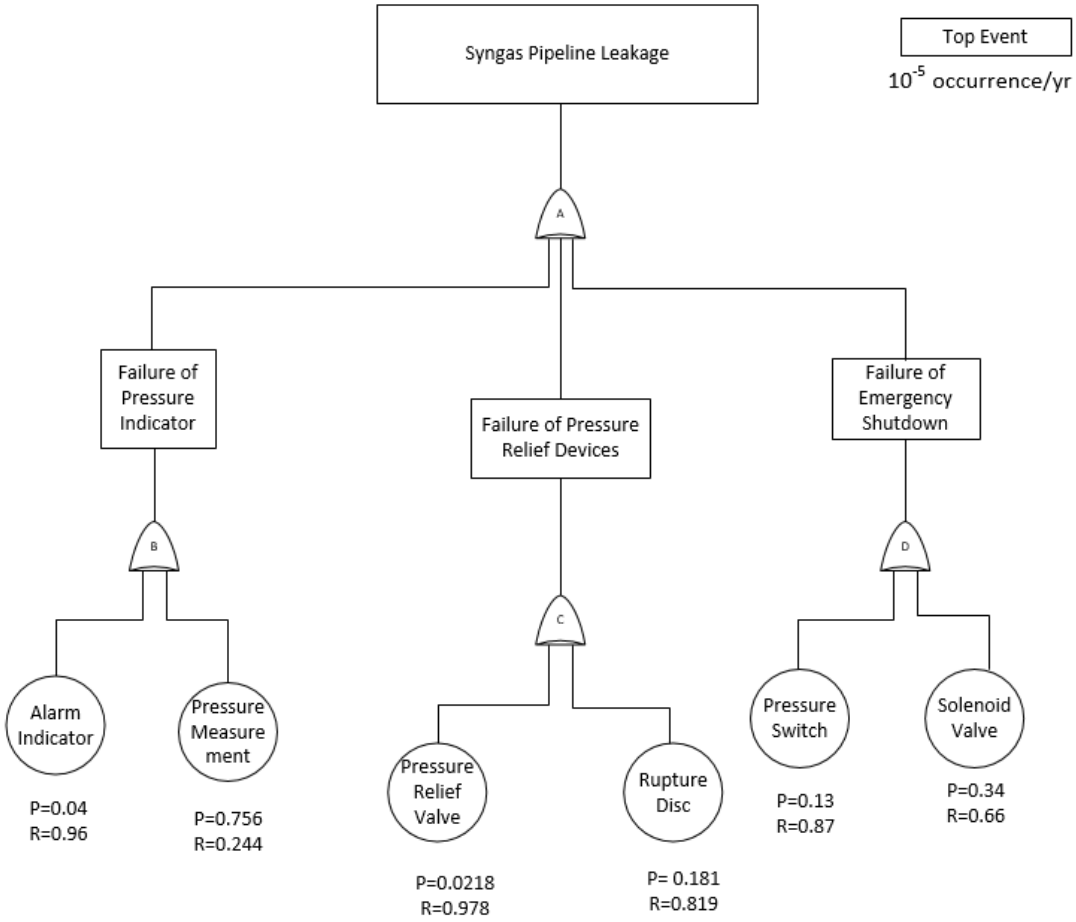

Figure 40 Fault Tree 1- Syngas Pipeline Leakage

10.4.2 Fault Tree of Over Pressure in Distillation Column

The overpressure of the distillation column may have occurred due to the failure of pressure indicator, failure of the pressure relief system, and failure of the emergency shutdown of the column operation. The fault tree in Figure 41 demonstrates the causes of these failures including the pressure switch and pressure measurement as potential reasons of the overpressure in the column.

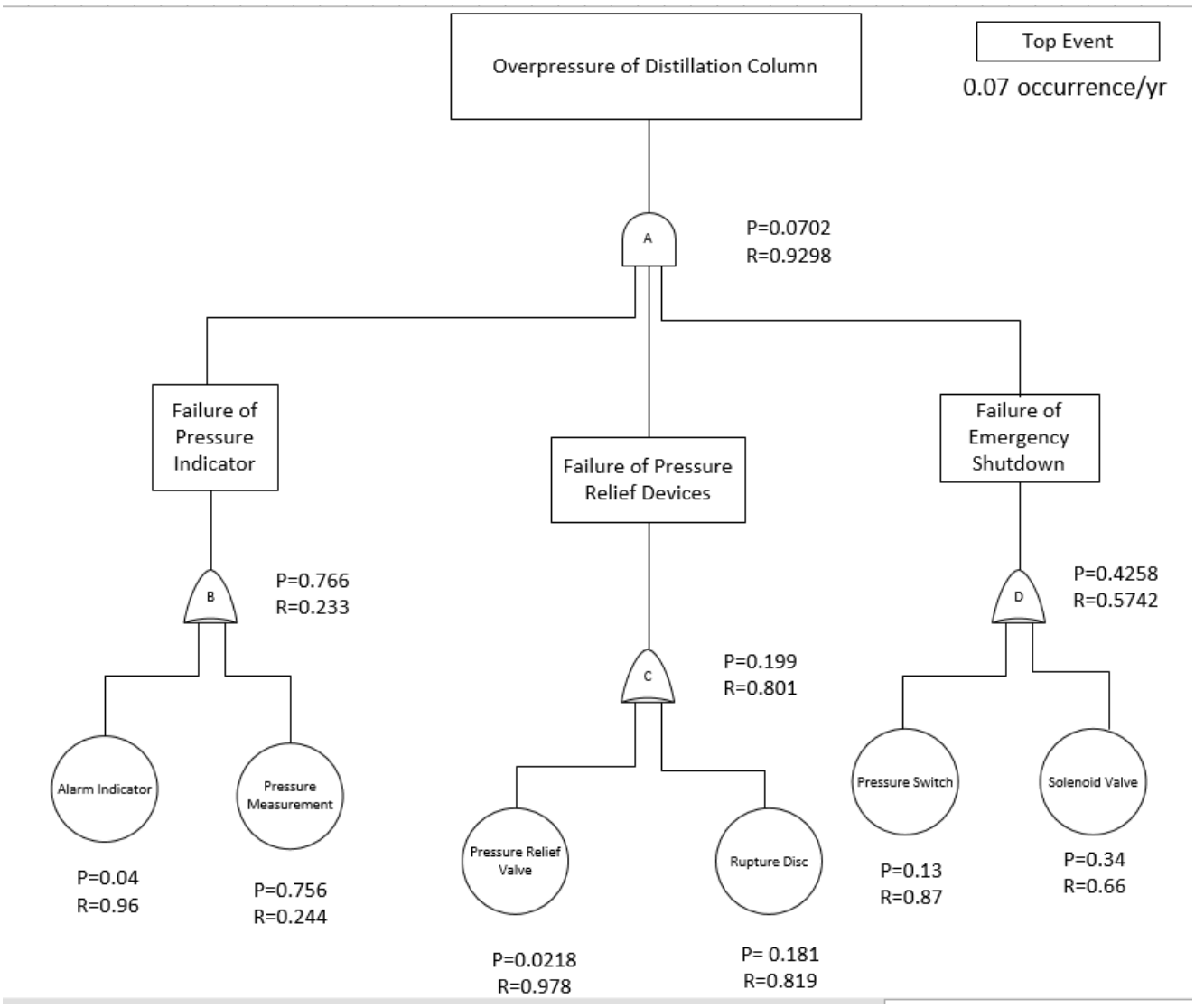

Figure 41 Fault Tree 2- Overpressure in Distillation Column

10.4.3 Fault Tree of Explosion

Fault Tree 3 as shown in Figure 42, demonstrates the causes for the top-level fault which is the event of an explosion. The cause of an explosion is divided into three main categories: overpressure, high temperature, or buildup of flammable fuel and gas at dangerous limits. Any equipment in the plant experiencing these dangerous limits is at a greater risk of an explosion since the majority of the chemicals that are dealt with in this plant is toxic or has the potential of causing an explosion. A failure of the oxygen controller would result in inadequate manipulation of the oxygen levels in the reactor that would cause the oxygen limits in the reactor to be within the flammability limits. As for the failure of the cooling jacket in

the reactor, this may lead to an overheated system that may cause they reactor to rupture or leakage of the fuel and gas that can also lead to an explosion. The failure of the flare and venting system would result in the toxic gas not being removed and accumulation may occur where if there is enough flammable gas it can also lead to an explosion. The probabilities of each scenario are shown in Figure 42.

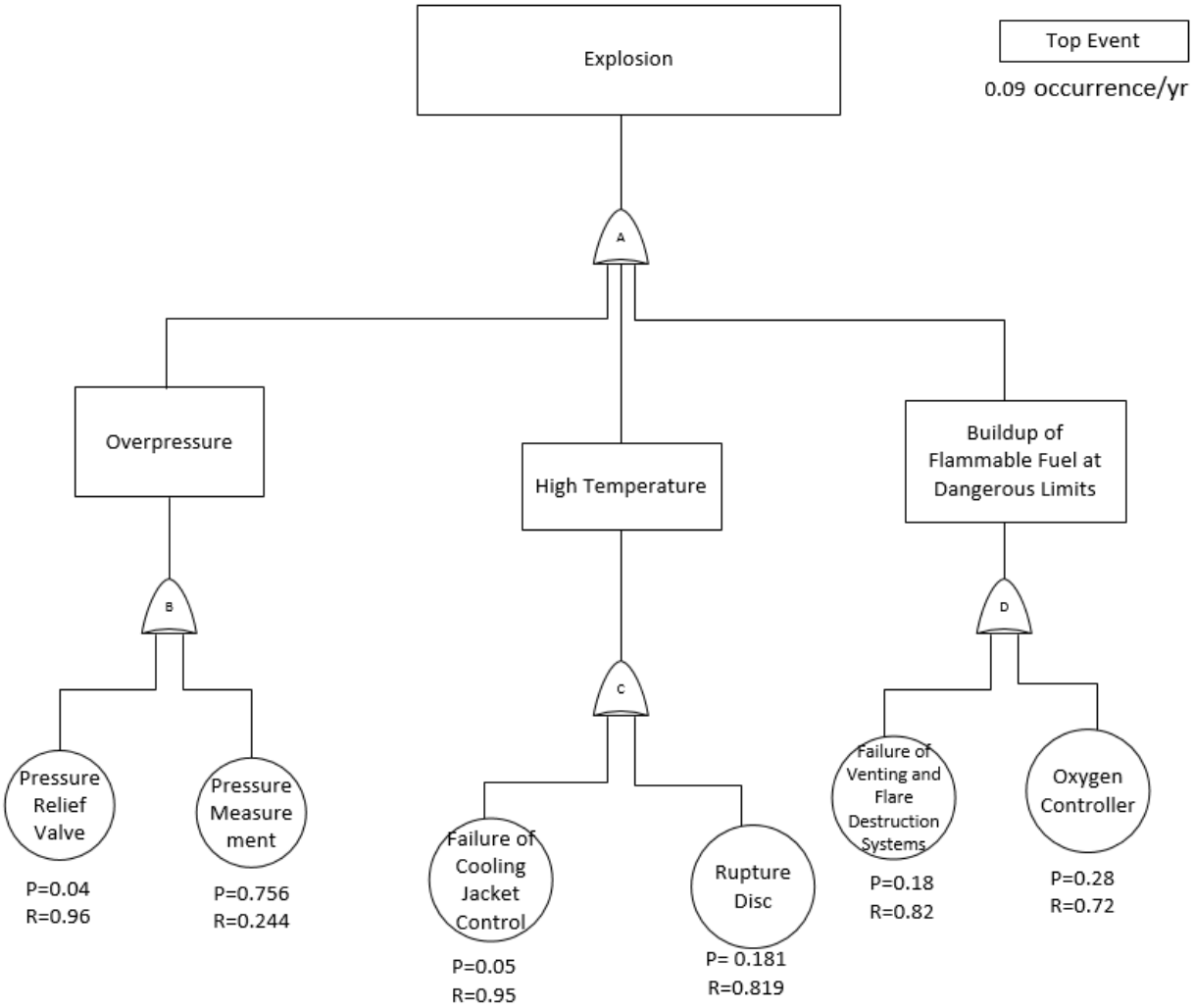

Figure 42 Fault Tree 3 of Critical Case of an Explosion

11. Plant Layout

The plant layout is outlined the Figure 43, displaying that the plant will be placed at the Southwest corner of S Service Rd and W Shore Line Rd, where the Ashbridge's Bay landform project is meant to be located as discussed in Section 4 Plant Location. The Disc filter process will be the closest to Ashbridge's Bay to retrieve the final effluent and filter out microplastic before releasing into Lake Ontario. The plant site will be consisting of an area of approximately 157 m^2, and will include a parking zone, fire station, emergency water station, workshops, laboratory, office building, operations building, canteen, utilities building, and process control building along with all the process units. The reactor and the scrubber processing units will be housed in indoor buildings to control external heat transfer. In addition, the reactor building, and scrubber are placed further away from other administrative and technical facilities due to safety concerns. While the tank farm will be the situation in the far corner to restrict potential gas leaks to one area.

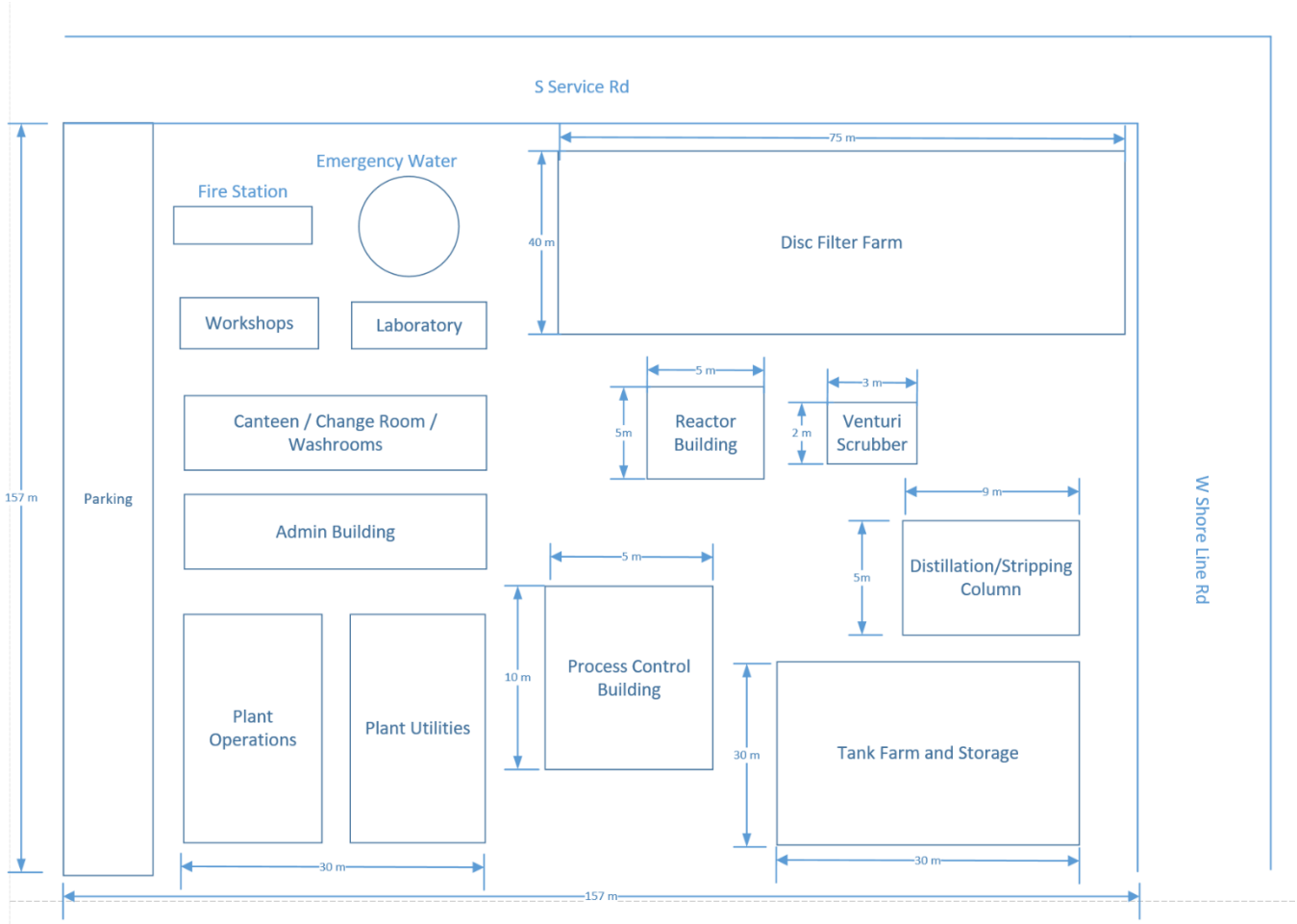

Figure 43 2D Plant Layout

Sketch-up was used to create a 3-D rendering of the process according to scale and color-coded piping. Figure 44 below shows the overall process plant, including the disc filter process at the Northeast corner, and the process units in the front. The different colored pipes represent different process fluids; blue pipe represents the biogas leaving reactor and entering distillation column, the light grey pipe represents the product leaving stripping column and entering storage tanks, the yellow pipe represents dirty syngas from distillation column into venturi scrubber, and the dark grey pipe represents the cleaned syngas from the scrubber entering the reactor for a complete continuous process. The layout was generated and spaced in accordance with the PIP-PNE00003 standards of placing all reactors, vessels, and heat exchangers, containing volatile gases under atmospheric pressure, one full diameter away from all equipment (Process Industry Practices, 2013).

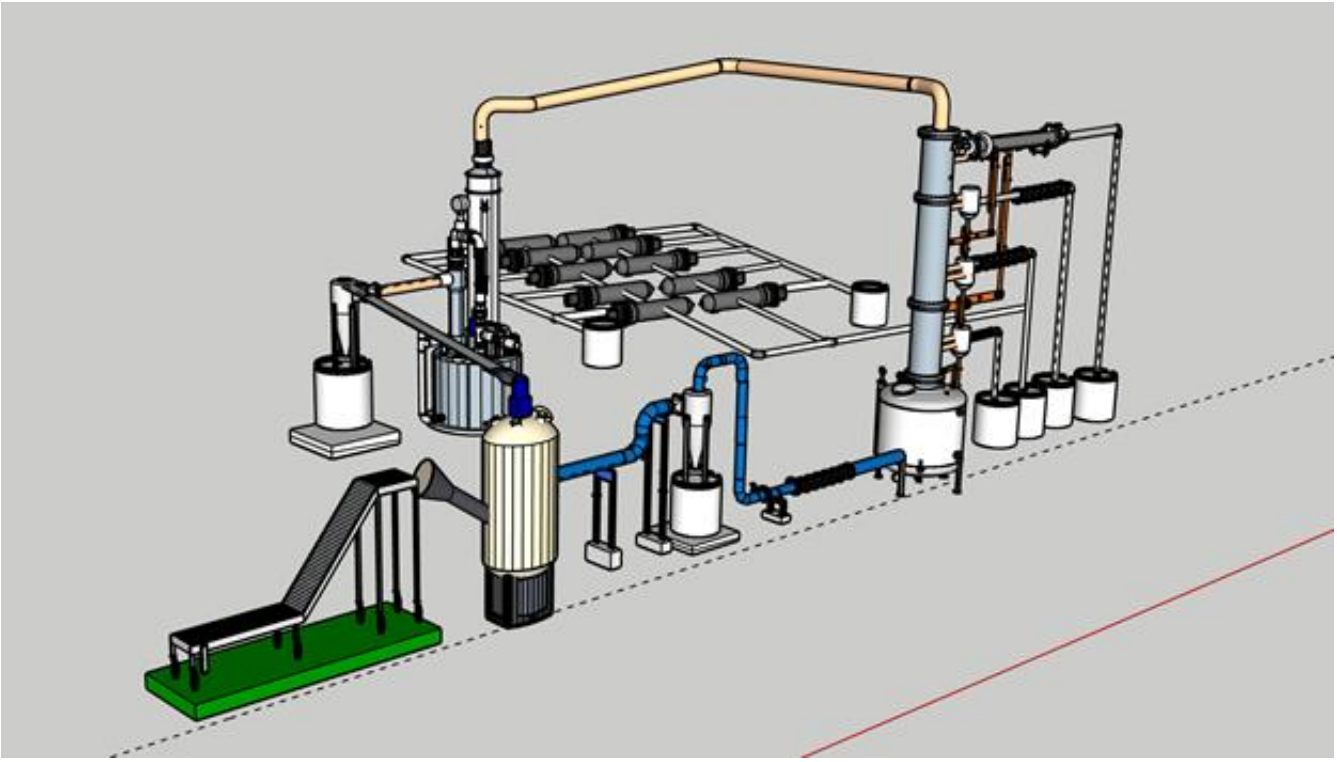

Figure 44 3-D Design of Plant Process

12. Economic Evaluation

12.1 Overview

This section gives a detailed rough outline of the economic analysis of our pyrolysis plant. An estimate the capital costs, installation, costs, and operating expenses of the plant and compare it to the yearly benefit of production. It must be mentioned that the charts and resources used do not give an exact, definite, or a fixed price for any piece of equipment as there are many styles, quality specifications, optional features, and designs to meet specific needs and services. All numbers are shown in CAD.

12.2 Total Fixed Capital Costs

The capital cost of each individual process is summarized in Table 53. The majority of capital costs were estimated using manufacturing cost analysis studies adjusted to scale, and the remaining were found from vendor websites. Due to the small scale of the plant, the cost of sizing was difficult to account for as cost estimation curves denature at extremes of small and large sizes.

Table 53 Summary of Equipment Costs

Equipment	Cost
Rotary disc filter x 16	$40,000/filter
Screw conveyor	$8,400
Fluidized bed reactor	$98,600
Cyclone 1	$1,500
Distillation Column	$1,079,645
Stripping Tower 1	$13,083
Stripping Tower 2	$18,326
Stripping Tower 3	$11,790
Condenser	$52,498
Heat Exchanger (Aspen cost) x 6	$9004/heat exchanger
Venturi Scrubber	$3400
Cyclone 2	$1100
Piping	$7/ft = $13,524
Bubble cap trays	$511
Pump x 5	$800/pump
Compressor x 6	$1000/compressor
Process control equipment	$33,500
Total Capital Cost	$2,085,945
Total installation, shipping and working capital	$104,297.25
Total Taxes	$32,854.63
Total Loan Required	$2,223,096

The cost of the rotary disc filter, belt conveyor, reactor, cyclones, venturi scrubber, piping, pump, and compressor were found using scale charts from chemical engineering appendices. The cost of the distillation tower, stripping towers, and condenser was estimated through calculation followed from Towler et al. & Sinnot 'Chemical Engineering Design Principles Practice and Economics of Plant and Process Design'. The cost of the process control equipment was taken from a chemical engineering database of common prices for flow, pressure, temperature, and level transmitters and controllers.

The six heat exchanger costs were estimated through Aspen Plus's EDR, as they were designed with specific requirements. The actual cost of the heat exchanger may vary due to the customized design; it is expected to be slightly higher than the estimate due to the special heat resistant materials needed to withstand high temperatures in and around the fuel processing units.

12.3 Production Cost and Cost Analysis

Based off a pervious study of economic feasibility of a fast pyrolysis plant of conversion of biomass to biofuel, the shipping, installation, and working capital is assumed to be 5% of total capital costs, and annual maintenance is 2% of total installed equipment cost (Wright et al. 2012). The cost of electricity is assumed to be $0.06/kwh. The cost of steam and nitrogen is assumed to be $0.02/lb. Insurance and taxes will be 1.5% of total installed equipment costs (Towler et al., 2013). Total year expenses are summarized in Table 54. Inflation rate will be assumed constant at 2%. Assume life of plant is 20 years. Based off previous studies of small-scale biodiesel plant, labor costs are around 5% of total capital costs. (Haas et al. 2005)

Table 54 Yearly Expenses in Plant Life Time

Yearly Expense	Amount
Yearly payment on loan	$253,352.37 for 10 years
Yearly annual maintenance	$44,462
Yearly electricity cost	$6,996.42
Yearly Steam and Nitrogen cost	$13,487
Yearly Labor Cost	$111,154.80
Total yearly Expense first 10 years	$429,452.60
Total Yearly Expense after 10 years	$176,100.23

Table 55 Total Cost for Products

Product	Quantity kg/day	Price (Mar 1 2021) $CAD/day
Gasoline	362.33	$552.10
Naphtha	89.42	$62.59
Kerosene	324.44	$368.50
Gas Oil	175.53	$132.12
Total		$1,115.32/day
		$407,091.91/year

The cost-benefit analysis was performed by comparing the estimated capital and operating costs to the sustainable product produced by the process. The plant is 100% equity financed with a 2.45% prime rate at 10-year payback period, payment require once a year. The inflation rate is taken as 2% per year, this applied to yearly operation costs, labor costs, loans, product prices, and savings generated through haulage and disposal fees. The yearly benefit in dollars to produce bio-gasoil, bio-kerosene, bio-gasoline, and bio-naphtha was taken using world average prices of regular fuel on Mar 1, 2021, the generated amount is calculated to be $407,091.91 CAD/year as shown in Table 55. However, due to the quality of the product attained and limited uses compared to regular fuel due to regulations, this amount is expected to be much lower. This is the amount of fuel generated in dollars from waste material that was otherwise meant to be thrown in municipal trash and produce more pollution. The generated savings from utilizing waste from Ashbridge's Bay results in $357,484/year in waste haulage and disposal costs. This amount was given to us from a representative at Ashbridge's Bay based off 2020 values.

After obtaining all the capital costs, financing costs, operating costs, and maintenance costs, assuming the plant is 100% equity financed with no up-front fees, the plant will generate a net profit of $335,122.40 in Year 1, this amount if expected to increase by 2% every year based off of inflation rate, and by Year 11 the net profit will increase to $755,912.43 once the loan for the plant is paid off. Life of plant is assumed to be 20 years, and the generated net profit for the 20-year plant life is estimated at $11,946,526.97 as shown in Table 56 and Figure 45.

12.4 Cash Flow Analysis

Looking through 10-year commodity prices for gasoline, heating oil, crude oil, and natural gas, the price is quite volatile rising and falling to extremes of 40% in a volatile year such as 2008 or 2020. It is difficult to know where oil prices will be in the future due to the current volatility of the commodities market. Applying fundamental analysis on the commodity market, it seems as if it will enter a bull cycle that may last a few years which will increasing profitability of our process; however, markets can always change based on news and OPEC deals. The benefit that our product has over regular natural gas and oil is that our product is made from generated waste and is sustainable. Therefore, if the crude market gets a shock and prices rise or fall to extremes, world governments and private companies will look towards sustainable replacements. According to theory, the product produced from our process can replace some of the commercial uses of gasoline, heating oil, and naphtha.

Due to the renewable nature of the biofuel produced in this process, it can be regarded as a kind of liquid solar energy. The carbon emission from this process is almost negligible compared to traditional fuel producing plants and the use is good for the local economy. This product can also have great benefit to countries with limited access to oil (Pagliuso, 2010). As more countries shift to renewable energy, transportation fuel derived from biomass will be of great demand, as it can be a low-cost commercial process from renewable waste, and it can be more evenly distributed over the planet than fossil fuels.

Biofuel and biogas can also be used in CHP units that can be converted directly to electricity. Biogas can be refined to remove carbon dioxide, water vapor and other trace gases to meet natural gas industry standards and be injected into the existing natural gas grid and used interchangeably with conventional natural gas (Tanigawa, 2017).

Table 56 Summary of Yearly Expenses and Savings in Long Term

	Year 1	Year 2	Year 3	Year 4	Year 5	Year 6	Year 7	Year 8	Year 9	Year 10
Cumulative Yearly Expense	$429,452.60	$438,041.65	$446,802.49	$455,738.53	$464,853.31	$474,150.37	$483,633.38	$493,306.05	$503,172.17	$513,235.61
Yearly Savings	$357,484	$364,633.68	$371,926.35	$379,364.88	$386,952.18	$394,691.22	$402,585.05	$410,636.75	$418,849.48	$427,226.47
Yearly Product sales	$407,091	$415,232.82	$423,537.48	$432,008.23	$440,648.39	$449,461.36	$458,450.59	$467,619.60	$476,971.99	$486,511.43
Net profit	$335,122.40	$341,824.85	$348,661.34	$355,634.57	$362,747.26	$370,002.21	$377,402.25	$384,950.30	$392,649.30	$400,502.29
	Year 11	**Year 12**	**Year 13**	**Year 14**	**Year 15**	**Year 16**	**Year 17**	**Year 18**	**Year 19**	**Year 20**
Cumulative Yearly Expense	$176,100.23	$179,622.23	$183,214.68	$186,878.97	$190,616.55	$194,428.88	$198,317.46	$202,283.81	$206,329.49	$210,456.08
Yearly Savings	$435,771.00	$444,486.42	$453,376.15	$462,443.67	$471,692.55	$481,126.40	$490,748.92	$500,563.90	$510,575.18	$520,786.69
Yearly Product sales	$496,241.66	$506,166.49	$516,289.82	$526,615.62	$537,147.93	$547,890.89	$558,848.71	$570,025.68	$581,426.19	$593,054.72
Net profit	$755,912.43	$771,030.68	$786,451.29	$802,180.32	$818,223.92	$834,588.40	$851,280.17	$868,305.77	$885,671.89	$903,385.33
Total profit for life of plant	$11,946,526.97									

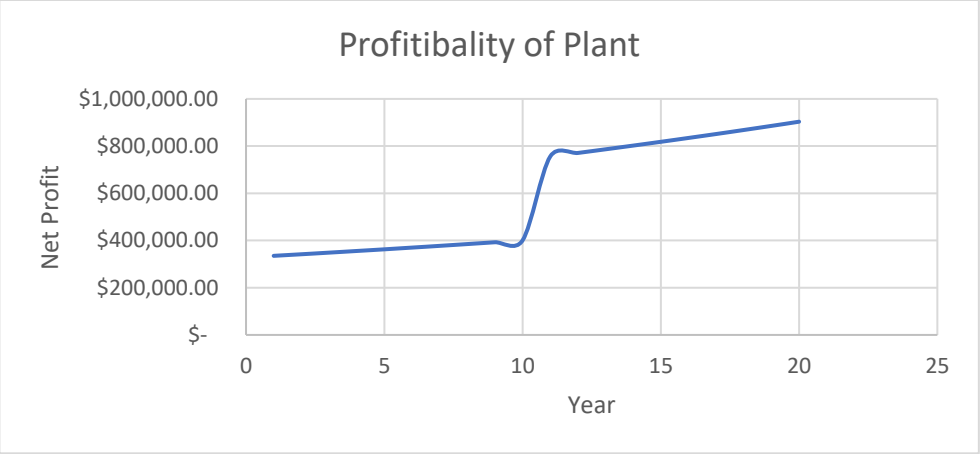

Figure 45 Calculated Profitability of Plant for 20 Year Span

13. Conclusions & Recommendations

Pyrolysis is one of the best technologies available to transform solid biomass waste with rich hydrocarbon elements into a sustainable, usable bio-oil. The proposed process is dealing with the solid waste gathered from waste-water treatment facilities and can help in creating clean sustainable energy. This project can be implemented in the future, when governments and organizations can give incentives to produce clean energy and limit the pollution to the environment. The proposed design can not only tackle the problems of land and water pollution but can also tackle the need for sustainable energy. The proposed design is a sustainable project to minimize the carbon footprint of industrial processes and generate a profit from the products of various qualities of bio-oil.

There is cost to efficiency balance that must be considered when optimizing the operating conditions of the reactor. However, one of the advantages of such type of pyrolysis design is that it is very flexible with the feedstock and can be implemented in different industries such as the textile industry, which is one of the highest polluters of microplastics in the ocean.

In addition, the major recommendation for this plant is in its scalability. According to all previous reports and commercial processes that convert biomass into biofuel, the feedstock needs to be much larger. Most commercial plants generate profits by using more than 10 times the feedstock of the proposed design. The design currently proposed is able to handle a much larger feed input and scale to size accordingly. This will also allow for an increase in the bio-oil yield as higher temperatures can be used increasing quality and profit. This larger feed input can be taken from textiles industries near and around the Toronto harbor. The textile industry is one of the largest polluters of microplastic to the environment. Once a proof of work is established that municipal wastewater can be cleaned and filtered while generating a revenue stream for the City of Toronto and the taxpayers, the next objective will be to target waste-water effluent, screenings/dust and other waste fabric from private textile plants. The incentive for textile plants is to generate less waste, disposal fees, and generate good PR by reducing their environmental damage. By targeting waste outflow from waste-water treatment facilities and textile plants along the Lake Ontario shore, the proposed design can effectively remove around 70-80% of the microplastics currently entering Lake Ontario every year, as well as generate vast amounts of biofuel which can be used within the local economy for heating, electricity and transportation.

14. References

Anderson, J. C., Park, B. J., & Palace, V. P. (2016). Microplastics in aquatic environments: Implications for Canadian ecosystems. *Environmental Pollution (1987), 218*, 269-280. doi:10.1016/j.envpol.2016.06.074

Ashbridges Bay Landform Project - Toronto and Region Conservation Authority (TRCA). (2021). from https://trca.ca/conservation/green-infrastructure/ashbridges-bay-erosion-sediment-control-project/

Barillon, Bruno et al. *Characterization Of Screenings From Three Municipal Wastewater Treatment Plants InTheRegionRhone-Alpes*.IWAPublishing,2009, https://www.researchgate.net/publication/26696486_Characterization_of_Screenings_from_Three_Municipal_Wastewater_Treatment_Plants_in_the_Region_Rhone-Alpes. Accessed 21 Mar 2021.

Barttfeld, M., Aguirre, P., & Grossmann, I. (2005). Optimal synthesis of complex distillation columns using rigorous models. *Computers&Chemical Engineering*. doi:https://doi.org/10.1016/j.compchemeng.2005.02.030

Bhatia, A. (2016). Process Piping Fundamentals, Codes and Standards. Retrieved 2021, from https://www.cedengineering.com/userfiles/Process%20Piping%20Fundamentals,%20Codes%20and%20Standards%20%20-%20Module%201.pdf

Biomass explained - U.S. Energy Information Administration (EIA). (2020). from https://www.eia.gov/energyexplained/biomass/

Briain, O., Mendes, A., McCarron, S., Healy, M., & Morrison, L. (2020, June 10). The role of wet wipes and sanitary towels as a source of white microplastic fibres in the marine environment., from https://www.sciencedirect.com/science/article/pii/S0043135420305583?fbclid=IwAR3Xkx9Lv9NzR0Q6P0fIH6WGMOSxJFz2L7-wao9q0cqeil49VC4cudZ7wos

Brown, T. R., Thilakaratne, R., Brown, R. C., & Hu, G. (2013). Regional differences in the economic feasibility of advanced biorefineries: Fast pyrolysis and hydroprocessing. *Energy Policy*, *57* (Complete), 234–243. https://doi.org/10.1016/j.enpol.2013.01.058

Cadwallader, L. (1998). Selected component failure rate values from fusion safety assessment tasks. Retrieved March 23, 2021, from https://www.osti.gov/biblio/752571

City of Toronto. (2019). *Ash bridges Bay Annual Report 2019.* Toronto. https://www.toronto.ca

Cooper, C. D., & Alley, F. C. (2011). *Air pollution control: A design approach* (4th ed.). Long Grove, IL: Waveland Press

Costello, J. D. (2020). *Microplastic pollutants in the coastal dunes of lake erie and lake ontario* International Association for Great Lakes Research. doi:10.1016/j.jglr.2020.08.001

Crowl, D. A., & Louvar, J. F. (2002). *Chemical process safety: Fundamentals with applications* (2nd ed.). Boston: Pearson Education

Danish, M., Mubashshir, M., & Zaidi, S. (2017). An Improved Restarted Adomian-based Solution for the Minimum Reflux Ratio of Multicomponent Distillation Columns. *Chemical Engineering India*. doi:https://doi.org/10.1080/00194506.2017.1301225

Dau, J. (2014, April 27). The Great Lakes have some of world's most concentrated plastic pollution. from https://greatlakesecho.org/2012/10/29/the-great-lakes-have-some-of-the-worlds-greatest-concentrations-of-plastic-pollution/

Disc Filter. 1st ed., IN-ENKO Team, 2018, pp. 39-49, https://www.in-ekoteam.ru/wp-content/uploads//2018/07/fd_en.pdf. Accessed 21 Mar 2021.

(EESI), E., 2021. *Fact Sheet | Biogas: Converting Waste to Energy | White Papers | EESI*. [online] Eesi.org. Available at: <https://www.eesi.org/papers/view/fact-sheet-biogasconverting-waste-to-energy>

Fogler, H. Scott. *Elements Of Chemical Reaction Engineering*. 4th ed., Pearson Education Inc, 2005.

Grbić, J., Helm, P., Athey, S., & Rochman, C. M. (2020, February 15). Microplastics entering northwestern Lake Ontario are diverse and linked to urban sources. Retrieved from https://www.sciencedirect.com/science/article/abs/pii/S0043135420301597

Haas, M., McAloon, A., Yee, W. and Foglia, T., 2006. *A Process Model to Estimate Biodiesel Production Costs*. [online] Webservices.itcs.umich.edu. Available at: <http://webservices.itcs.umich.edu/mediawiki/algaebiofuel/sites/algaebiofuel/uploads/d/df/Haas_Biodiesel_Process.pdf>

Huber Technology waste water solutions. (2014). HUBER Disc Filter RoDisc® [Ebook] (pp. 1-4) Berching. Retrieved from https://www.huber.de/products/micro-screeningfiltration/microscreens/huber-disc-filter-rodiscr.html

Hyaric, R., Gourdon, R., Canler, J., Barillon, B., & Naquin, P. (2009). Characterization of Screenings from Three Municipal Wastewater Treatment Plants in the Region Rhone-Alpes., from https://www.researchgate.net/publication/26696486_Characterization_of_Screenings_from_Three_Municipal_Wastewater_Treatment_Plants_in_the_Region_RhoneAlpes?fbclid=IwAR30Fmw_0U8eV20toI11C7OiKKcrBAVFWvjSW6jxHotrgQoKqzEFd1uvJck

Jahirul, Mohammad et al. "Biofuels Production Through Biomass Pyrolysis —A Technological Review". *Energies*, vol 5, no. 12, 2012, pp. 4952-5001. *MDPI AG*, doi:10.3390/en5124952. Accessed 22 Mar 2021.

John Rumble, Daniel et al. "Handbook Of Chemistry And Physics 101St Edition". *Hbcponline.Com*, 2021, http://hbcponline.com/faces/contents/ContentsSearch.xhtml. Accessed 21 Mar 2021.

Karapanagioti, H. K., & Kalavrouziotis, I. K. (2019). *Microplastics in water and wastewater*. Ashland: IWA Publishing

Kay, P., Hiscoe, R., Moberley, I. *et al*. Wastewater treatment plants as a source of microplastics in river catchments. *Environ Sci Pollut Res* 25, 20264–20267 (2018). https://doi.org/10.1007/s11356-018-2070-7

Kister, H. Z. (1992). *Distillation Design*. N.p.: Mc-Graw Hill Inc.

Litchfield, S. G. (2020). *The influence of plastic pollution and ocean change on detrital decomposition* Elsevier. doi:10.1016/j.marpolbul.2020.111354

Liu, J. (2012). Predicting the Products of Crude Oil Distillation Columns. *School of Chemical Engineering and Analytical Science*. Retrieved from http://www.manchester.ac.uk/escholar/uk-ac-man-scw:159595

Love, J. (2007). *Process Automation Handbook: A Guide to Theory and Practice* (2nd ed.) Springer London.

Ludwig, E. E. (1997). *Applied Process Design for Chemical and Petrochemical Plants* (3rd ed., Vol. 2). N.p.: Gulf Professional Publishing.

Maget, N., Berdouzi, F., Murillo, C., & Gabas, N. (2019). Quantitative Risk Analysis using Dynamic Simulation: Deviation Propagation along Propylene Glycol Process. CHEMICAL ENGINEERING TRANSACTIONS, 77. doi:10.1021/ci60018a602

Marzouk, O. A. (2017). Thermo physical chemical properties of fluids using the free nist chemistry webbook database. *Fluid Mechanics Research International Journal, 1*(1). doi:10.15406/fmrij.2017.01.00003

Pagliuso, J., 2010. *Biogasoline - an overview*. [online] Sciencedirect.com. Available at: <https://www.sciencedirect.com/topics/engineering/biogasoline>

Perry, R. H., Green, D. W., & Maloney, J. O. (1997). Perry Handbook Seventh Edition (7th ed.). United States: McGraw-Hill

Pyrolysis [Ebook]. Milano: ACS Publications. Retrieved from

Ragaert, K. (2017). *Mechanical and chemical recycling of solid plastic waste* Elsevier. doi:10.1016/j.wasman.2017.07.044

Ranzi, E., Cuoci, A., Faravelli, T., & Frassoldati, A. (2008). Chemical Kinetics of Biomass

"Regulations Limiting Carbon Dioxide Emissions From Natural Gas-Fired Generation Of Electricity". *Laws-Lois.Justice.Gc.Ca*, 2015, https://laws-lois.justice.gc.ca/eng/regulations/SOR-2018-261/FullText.html.

Toronto Water. (2018). Sewers and Water Supply By-laws 2017 Compliance and Enforcement Annual Report. Retrieved February 25, 2021, from https://www.toronto.ca/legdocs/mmis/2018/pw/bgrd/backgroundfile-117623.pdf

Towler et al., G., & Sinnott, R. (2013). *CHEMICAL ENGINEERING DESIGN: Principles, practice and economics of plant and process design* (2nd ed.). S.l.: Butterworth-Heinemann

Treese, S. A., Pujado, P. R., & Jones, D. S. (2015). *Handbook of Petroleum Processing* (2nd ed.). N.p.: Springer.

United States, Congress, Federal, *Canadian Environmental Protection Act*. Vol 44, Canada Gazette, 1999.

Watkins, R. N. (1979). *Petroleum Refinery Disillation* (2nd ed.). N.p.: Gulf Pub Co.

Watzdorf, R., Bausa, J., & Marquardt, W. (2004). Shortcut methods for nonideal multicomponent distillation: 2. Complex columns. *AIChE*, *48*(8). doi:https://doi.org/10.1002/aic.690450803

Weast, Robert C, Melvin J. Astle, and William H. Beyer. *Crc Handbook of Chemistry and Physics: A Ready-Reference Book of Chemical and Physical Data*. Boca Raton, Fla: CRC Press, 1984. Print.

Weeks, C. (2016). Breaking down canada's move to ban microbeads.(life & arts). *Globe and Mail*

Wright, M., Daugaard, D. and Hsu, D., 2007. *Techno-Economic Analysis of Biomass Fast Pyrolysis to Transportation Fuels*. [online] Nrel.gov. Available at: <https://www.nrel.gov/docs/fy11osti/46586.pdf>

15. Appendix

15.1 Elementary Calculation Sample for Stream 25

15.1 Mass Balance for Stream

A sample of the mass balance calculation on each stream was based on the percentage of the components in that stream, for the sample Line 25 will be used. The Line is comprised of 6% Gasoline and 94% Naphtha.

$$M_{Line\ 25\ in} = M_{Line\ 25\ out}$$

$$M_{Line\ 25\ in} = M_{gasoline} + M_{Naphtha} = 95.13\frac{kg}{day}$$

$$M_{Line\ 25\ in} = (0.06)M_{Line\ 25\ in} + (0.94)M_{Line\ 25\ in}$$

$$M_{Line\ 25\ in} = (0.06 \times 95.13) + (0.94 \times 95.13) = (5.707\frac{kg}{day} + 89.422\frac{kg}{day})$$

$$M_{Line\ 25\ out} = 95.13\frac{kg}{day}$$

15.1.2 Energy Balance Calculation for Stream

A sample of the energy balance calculation on each stream was based on the percentage of the components in that stream, for the sample Line 25 will be used. The Line is comprised of 6% Gasoline and 94% Naphtha. The C_p values and the respective correction needed for the fuel products are found in for the product composition was found in Fig 46 and using Perry's Handbook.

$$\sum \boldsymbol{Hin} = \sum \boldsymbol{Hout}$$

$$\sum Hin = m_{gasoline_{in}} \cdot \boldsymbol{c_{pgasoline}} \times \boldsymbol{c_{correction}} \cdot (T_{in} - T_{ref}) + m_{naptha_{in}} \cdot \boldsymbol{c_{pnaptha}} \times \boldsymbol{c_{correction}} \cdot (T_{in} - T_{ref})$$

$$\sum Hin = \left(5.707\frac{kg}{day} \times 2.0204\frac{lb}{kg}\right) \times 0.56\ \frac{Btu}{lb°\mathrm{F}} \times 1.06 \times (334.99°\mathrm{F} - 69.8°\mathrm{F}) + \left(89.422\frac{kg}{day} \times 2.0204\frac{lb}{kg}\right) \times 0.55\ \frac{Btu}{lb°\mathrm{F}} \times 1.06 \times (334.99°\mathrm{F} - 69.8°\mathrm{F})$$

$$\sum \boldsymbol{Hin} = \boldsymbol{32460.63\frac{kJ}{day}}$$

15.2 Elementary Calculations for Fluidized Bed Reactor

15.2.1 Mass Balance Fluidized Bed Reactor

$$M_{Biomass,IN} + M_{Nitrogen+steam\ in} = M_{Biocrude\ oil\ OUT} + M_{Gas\ out} + M_{Char,out} + M_{Nitrogen+steam\ out}$$

$$M_{Biomass,IN} = 2197.37 kg/day$$

The feed of steam and nitrogen is calculated using the fluidizing gas volume used in the reactor by multiplying it with density

$$M_{Nitrogen+Steam,IN} = 0.0162 \frac{m^3}{s} * 60 * 60 * 24 * 0.599 \frac{kg}{m^3} = 839.76 kg/day$$

The composition of Product was based of report from the pyrolysis of biomass in a cellulose thermal decomposition reaction. The product was represented in biocrude oil form to easily process it in the distillation column. (Jahirul, Mohammad et al, 2012)

$$M_{Biocrude\ oil\ OUT} = 2197.37 * 0.769 = 1689.78 kg/day$$

$$M_{Syngas,OUT} = 2197.37 * 0.1975 = 433.98 kg/day$$

$$M_{Char\ OUT} = 2197.37 * 0.0366 = 73.61 kg/day$$

15.2.2 Energy Balance Fluidized Bed Reactor

Energy in the System= ΣHs+ΣHL+ ΣHR

Where H_s is the sensible heat of system, H_L is the latent heat of the system and H_r is the heat of reaction in pyrolysis (Ranzi,2008)

$$Q = H$$

$$Q_{BFBR} = \Sigma H_{sensible} + \Sigma H_{Latent} + \Sigma H_{Reaction}$$

$\Sigma H_s = H_{polyester} + H_{cellulose}$ = 2197.37 *(0.9*1350 (790-296)) + (0.1*1300 (790-296)) = 1.4x10^9 KJ/day

$$H_{Latent\ of\ cellulose,polyester\ and\ water} = m_{water}\lambda_{water} + m_{cellulose}\lambda_{cellulose} + m_{polyester}\lambda_{polyester}$$

$$\boldsymbol{\Sigma H_L = 6.52 * 10^6\ kJ/day}$$

$$\Sigma H_R = H_{polyester} + H_{cellulose} + H_{methane}$$

$$\boldsymbol{\Sigma H_{Reaction} = -84570.05\ kJ/day}$$

$$\boldsymbol{Total\ Q_{BFBR} = 1.406 \times 10^9\ kJ/day}$$

The total amount of heat generated by the reactor is cooled down using the cooling jacket and steam. Since it is exothermic additional pipe could be inserted for direct cooling from inside the reactor if needed.

15.3 Elementary Calculations for Distillation Column

15.3.1 Mass Balance for Distillation Column

$$M_{BioCrude\ Oil\ in} + M_{SynGasin} + M_{Steam} = M_{out,syngas} + M_{gasoline} + M_{Naptha} + M_{Kerosene} + M_{Gas\ oil} + M_{RC} + M_{Steam\ out}$$

$$M_{gasoline} = \left(\frac{1689.78 kg}{day}\right)(0.268) = 452.86\ kg/day$$

15.3.2 Energy Balance for Distillation Column

In order to, find the specific heat capacities for the enthalpies calculated, these charts in Figure 46 and 47 were used from the Nelson Petroleum Refining Textbook. The correction values for specific heat are used when the stream contains fuel that is not 100% pure. This correction value will help account for the error in the fuel mixture. (Nelson, 1968).

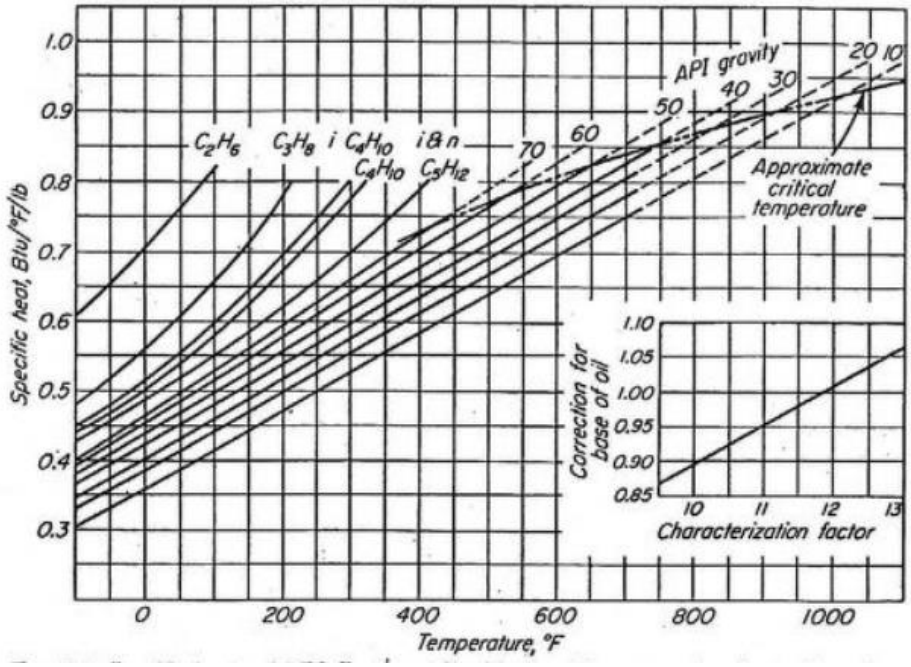

Figure 46 Specific Heat of Different Crude Based on API and Temperature (Nelson, 1968)

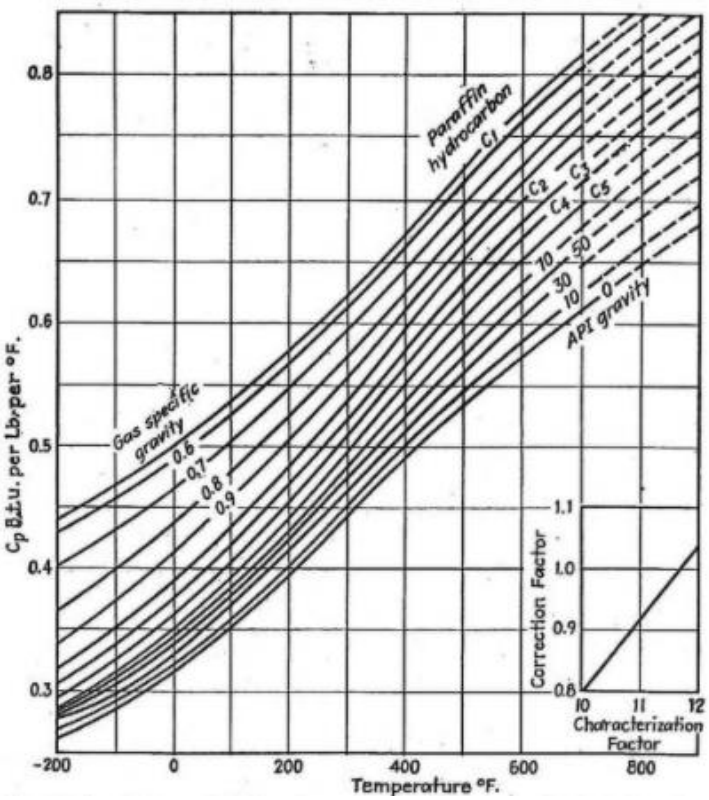

Figure 47 Specific Heat Correction Factors of Hydrocarbon based on Specific Gravity (Nelson, 1968)

Table 57 Specific Heat Values and Correction Values of Fuel Products

	API	Correction Factor	Specific Heat (Cp)	Latent Heat
Crude oil	48.0	1.03	0.77	-
Gasoline	62.8	1.06	0.56	120
Naphtha	52.8	1.06	0.55	113
Kerosene	45.6	1.06	0.57	100
Gas oil	39.4	1.06	0.59	90
Reduced Crude	31.2	1.03	0.72	-

$$Q = H$$

$$Q_{distillation} = \Sigma H_{sensible} + \Sigma H_{Latent} - \Sigma H_{Relfux}$$

$$\Sigma H_s = H_{reduced\ crude} + H_{Gas\ oil} + H_{kerosene} + H_{naphtha} + H_{gasoline} + H_{steam}$$

$$\boldsymbol{H_c = m \times c_p \times c_{correction} \times \Delta T = \left(1377.24 \frac{\text{lb}}{\text{day}} \times 0.72 \frac{btu}{(lb * °\text{F})} \times 1.03 \times (510°\text{F} - 599°\text{F}) \right)}$$

$$\boldsymbol{= -90909.1 \frac{btu}{day} = 95906.16\ kJ/day}$$

$$\boldsymbol{\Sigma H_s = -34177807.5\ kJ/day}$$

$$\Sigma H_L = H_{Naptha} + H_{Kerosene} + H_{gas\ oil}$$

$$H_{Latent\ of\ gas\ oil} = m \times \lambda = 209.73\frac{\text{lb}}{\text{day}} \times 113 = 23699\frac{\text{btu}}{\text{day}} = \frac{25002.43\ \text{kJ}}{\text{day}}$$

$$\boldsymbol{\Sigma H_L = 14100.5\ kJ/day}$$

$$\Sigma H_{Reflux} = H_{Reflux\ of\ gas\ oil\ stripping} + H_{Reflux\ of\ kerosene\ stripping} + H_{Reflux\ of\ naphtha\ stripping} + H_{Reflux\ from\ condenser}$$

$$\boldsymbol{\Sigma H_{Reflux} = -314966.9\ kJ/day}$$

$$\boldsymbol{Total\ Needed\ Q_{distillation} = 3.4146 \times 10^6\ kJ/day}$$

15.4 Elementary Calculations for Stripping Towers

15.4.1 Mass Balance for Stripping Towers

$$M_{Gas\ Oil\ IN} + M_{steam\ in} = M_{Gas\ Oil\ OUT} + M_{steam\ out}$$

$$M_{Gas\ Oil\ IN} = 179.11 kg/day$$

Assume that 2% of Gas Oil leaving distillation column is Kerosene Vapor and this is the vapor that sent back in the reflux stream.

$$M_{Gas\ Oil\ OUT} = 179.11 \times 0.98 = \boldsymbol{175.53\ kg/day}$$

$$M_{steam\ out} = M_{kerosene} + M_{steam\ in}$$

$$M_{kerosene} = (179.11 \times 0.02) = \frac{3.58kg}{day} of\ kerosene\ in\ relux = 7.90\frac{lb}{day}$$

$$M_{steam\ in} = (F\ C_p\ C_{correction}(T_2 - T_1))/H$$

$$M_{steam\ in} = (7.90\frac{lb}{day}) \times 0.56 \times 1.06\ (510 - 469))/(0.5 \times (469 - 444) = 15.38\frac{lb}{day} = \boldsymbol{\frac{6.97kg}{day}}$$

$$M_{steam\ out} = M_{kerosene} + M_{steam\ in}$$

$$M_{steam\ out} = 3.58\frac{kg}{day} + \frac{6.97kg}{day} = \boldsymbol{\frac{10.56kg}{day}}$$

15.4.2 Energy Balance for Stripping Towers

$$Q_{Gas\ oil\ Stripping\ tower} = H_{Gasoil} + H_{Kerosene} + H_{steam}$$

$$H_{Reflux} = H_{Kerosene} + H_{steam}$$

$$H_{kerrosene} = m * c_p * C_{corr} * \Delta T = \left(7.90\ \text{lb/day} \times 0.57\frac{btu}{(lb * °\text{F})} \times 1.06 \times (469°\text{F} - 510°\text{F})\right) = -195.64\frac{btu}{day}$$

$$H_{steam} = m * c * \Delta T = \left(15.38\frac{lb}{day} \times 0.5\frac{btu}{(lb * °\text{F})} \times (469°\text{F} - 510°\text{F})\right) = -315.29\frac{btu}{day}$$

$$\boldsymbol{H_{Reflux}} = -195.64\frac{btu}{day} + -315.29\frac{btu}{day} = -510.93\frac{btu}{day} = \boldsymbol{-539.06\frac{kJ}{day}}$$

$$H_{Gasoil} = m * c * \Delta T = (389.97\frac{lb}{day} \times 0.59\ \frac{btu}{(lb*°F)} \times (486°F - 510°F) = -5479.32\frac{btu}{day} = \mathbf{-5781.23\frac{kJ}{day}}$$

$$\boldsymbol{Q = -5792.73}$$

15.5 Elementary Calculations for Venturi Scrubber

15.5.1 Mass Balance for Venturi Scrubber

$$M_{in,syngas} + M_{in,liquid\ scrubbing} = M_{out,syngas} + M_{out,liquid\ scrubbing+Tar}$$

$$M_{in,syngas} = \frac{433.99\ kg}{day} * 0.23\ (Tar) + \frac{433.99\ kg}{day} * 0.77\ (CO, CO2, H2, CH4)$$

$$M_{out,syngas} = \frac{99.82\ kg}{day} * 0.05\ (Tar\ remaining) + \frac{334.17\ kg}{day}(CO, CO2, H2, CH4) = 339.16\frac{kg}{day}$$

A L/G ratio of 5 gal/1000ft^3 and the known inlet gas flowrate was used to determine the unknown liquid flowrate required for efficient scrubbing which came to 305 L/day.

$$\frac{L}{G}ratio = \frac{5\frac{gal}{min}}{1000\frac{ft^3}{min}} = \frac{5\frac{gal}{min}}{7480\frac{gal}{min}} * \frac{433.99\frac{kg}{day} * \frac{1day}{1440\ min}}{0.95\frac{kg}{m3} * \frac{1m3}{264.17gal}} = 0.056\frac{gal}{min} * 5450.99 = \frac{305\ L}{day}$$

$$M_{in,liquid\ scrubbing} = \frac{305\ L}{day} * \frac{997kg}{m3} * \frac{1m3}{1000L} = \frac{304.09\ kg}{day}$$

The removal efficiency is 95% which means that the gas has a tar concentration of only 5% in the outlet stream. The removed tar is added to the liquid water stream leaving the scrubber to give a total mass of the wastewater stream to be 398.92 kg/day.

$$M_{out,liquid\ scrubbing+Tar} = \frac{304.09\ kg}{day} + \frac{99.82\ kg}{day} * 0.95\ (Tar\ removed) = \frac{398.92\ kg}{day}$$

15.5.2 Energy Balance for Venturi Scrubber

$$\sum Hin = m_{water_{in}} \cdot Cp_{H2O} \cdot (T_{in} - T_{ref}) + m_{gas_{in}} \cdot Cp_{gas\ mix} \cdot (T_{in} - T_{ref})$$

The specific heat of the gas mixture was calculated by multiplying the specific hear of each component at the inlet temperature with its fraction in the gas mixture to find the accurate specific heat of the mixture.

$$Cp_{gas\ mix} = \left(\frac{m1}{mgas}\right) \cdot Cp_1 + \left(\frac{m2}{mgas}\right) \cdot Cp_2 + \left(\frac{m3}{mgas}\right) \cdot Cp_3 + \left(\frac{m4}{mgas}\right) \cdot Cp_4 + \left(\frac{m5}{mgas}\right) \cdot Cp_5$$

$$Cp_{gas\ mix} = 6.093\frac{kJ}{kg\ K}$$

$$\sum Hin = \left(304.09\frac{kg}{day}\right)\left(4.1856\frac{kJ}{kg \cdot K}\right) \cdot (288K - 298K) + \left(\frac{433.99\ kg}{day}\right)6.093\frac{kJ}{kg\ K} \cdot (333 - 298)$$

$$= 79826.31\frac{kJ}{day}$$

The difference in sensible heat produces a negative value which confirms that the process is an exothermic one.

$$\sum \boldsymbol{Hout} - \sum \boldsymbol{Hin} = \mathbf{47801.8 - 79826.31} = \frac{\mathbf{-32024.51\ kJ}}{\boldsymbol{day}}$$

Since there is a phase change of tar (toluene) from gas to liquid, the latent heat of vaporization is calculated

$$\boldsymbol{H_{Latent}} = n \times \lambda$$

$$\boldsymbol{H_{Latent}} = \frac{433.99\frac{kg}{day}}{0.03436\frac{kg}{mol}} \times 35.4\frac{kJ}{mol} = 446106\frac{kJ}{day}$$

15.6 Condenser Energy Calculations

$$Q_{condenser} = H_{gasoline} - H_{vaporization}$$

$$Q_{condenser} = \left(\left(\frac{998.34\text{lb}}{\text{day}} \times 0.56\frac{btu}{(lb * °\text{F})} \times (80°\text{F} - 285.8°\text{F})\right) - 120\text{btu/day}\right) = \frac{-114724.84\text{ btu}}{\text{day}} = 121041.11\text{ kJ/day}$$

$$M_{water\ in\ condenser} = \left(\frac{998.34\text{lb}}{\text{day}} \times 0.56\frac{btu}{(lb * °\text{F})} \times (80°\text{F} - 285.8°\text{F})\right) / (0.9994\ \frac{btu}{(lb * °\text{F})} \times (176°\text{F} - 59°\text{F}) = \frac{984.04lb}{day}$$

$$= 446.35\ kg/day$$

Assume reflux ratio of condenser is 20%

$$\boldsymbol{H_{gasoline\ reflux\ from\ condenser}} = \mathbf{-1275.71\ kJ/day}$$

15.7 Heat Exchanger Energy Calculations

For the Heat exchangers that have crude products the correction value for the Cp will be dismissed because the assumption is that the hydrocarbon product is pure. The crude oil will have the correction factor as the composition varies based on the hydrocarbon components in the mixture.

$$Q_{heat\ exchanger} = H_{heat\ exchanger} + H_{Latent\ Heat}$$

$$H_{heat\ exchanger\ for\ gas\ oil} = \boldsymbol{m \times c_p \times \times\ \Delta T}\left((386.97\ lb/day\ \times 0.59\frac{btu}{(lb * °\text{F})} \times (486°\text{F} - 122°\text{F}\right)$$

$$= \mathbf{-83015.8}\frac{\boldsymbol{Btu}}{\boldsymbol{day}} = \mathbf{-87586.7\ kJ/day}$$

$$\boldsymbol{H_{Latent}} = n \times \lambda$$

$$H_{Latent} = \frac{386.7\frac{lb}{day}}{240\frac{lb}{mol}} \times -90\frac{btu}{1b} \times 1.055\frac{kJ}{btu} = -297.65\frac{kJ}{day}$$

$$H_{heat\ exchanger} + H_{Latent\ Heat} = -\ 87900.7\ kJ/day$$

$$H_{heat\ exchanger\ for\ kerosene} = -44778.75\ kJ/day$$

$$H_{heat\ exchanger\ for\ naptha} = -7902.6\ kJ/day$$

$$H_{heat\ exchanger\ for\ distillation} = \left((4682.08\ lb/day\ \times 0.7743\ \frac{btu}{(lb * °F)} \times 1.06\ \times (600°F - 932°F)\right)$$
$$= -\frac{1275827.73lb}{day} = -578705.72\ kJ/day$$
$$C_p = -1.39 * 10^{-6} * T + 1.847 * 10^{-3})x\ API + (6.312 * 10^{-4})xT + 0.352$$
$$C_p = (-1.39 * 10^{-6} * (600°F) + 1.847 * 10^{-3})x\ 43.0 + (6.312 * 10^{-4})x\ 600°F + 0.352$$
$$C_p = 0.0436 + 0.7307 = \mathbf{0.7743}$$

15.8 Screw Conveyor Power Consumption Calculation

The power consumption of a screw conveyor can be correlated using the following equation:

$$p = 0.038 + 0.0072mL_c{}^{0.8} \tag{5}$$

$$p = 0.038 + 0.0072\left(\frac{0.19\ tonnes}{hr}\right)(65.6ft)^{0.8} = 0.077\ hp$$

15.9 Piping and Pump Design Sample Calculation

A sample calculation for stream number 2 for the water leaving the disc filters is shown. The volumetric flowrate was first converted from 1500000 kg/day to 0.01736 m3/s using the density of the fluid. Then the velocity was assumed based on the type of fluid, whether it was liquid or gas. For liquid water, the velocity was assumed to be 2m/s.

To find the inner diameter of the pipes:

$$D = \sqrt{\frac{4\left(\frac{0.01736m3}{s}\right)}{\pi\left(\frac{2m}{s}\right)}} = 0.105m \tag{42}$$

The Reynolds number can be calculated using the following equation:

$$Re = \frac{\rho * u * di}{\mu} \tag{43}$$

Where, μ is the fluid viscosity in units of pa*s

$$Re = \frac{\left(\frac{1000kg}{m3}\right) * \left(\frac{2m}{s}\right) * (0.105m)}{0.000931\ Pa.s} = 225837.07$$

The absolute surface roughness of commercial steel pipe was 0.046mm that was used throughout the piping system. To find the relative roughness of the pipe in stream 2, the absolute roughness was divided by the inside pipe diameter using the equation below.

$$relative\ roughness, e = \frac{absolute\ roughness}{inside\ pipe\ diameter} = \frac{0.046mm}{105mm} = 0.00044 \qquad (44)$$

The friction factor can be found using the friction factor chart as in figure 48 using the calculated Reynolds number and relative roughness value. The friction factor was found to be around 0.018 and a length of 20 m was assumed from the 3D model.

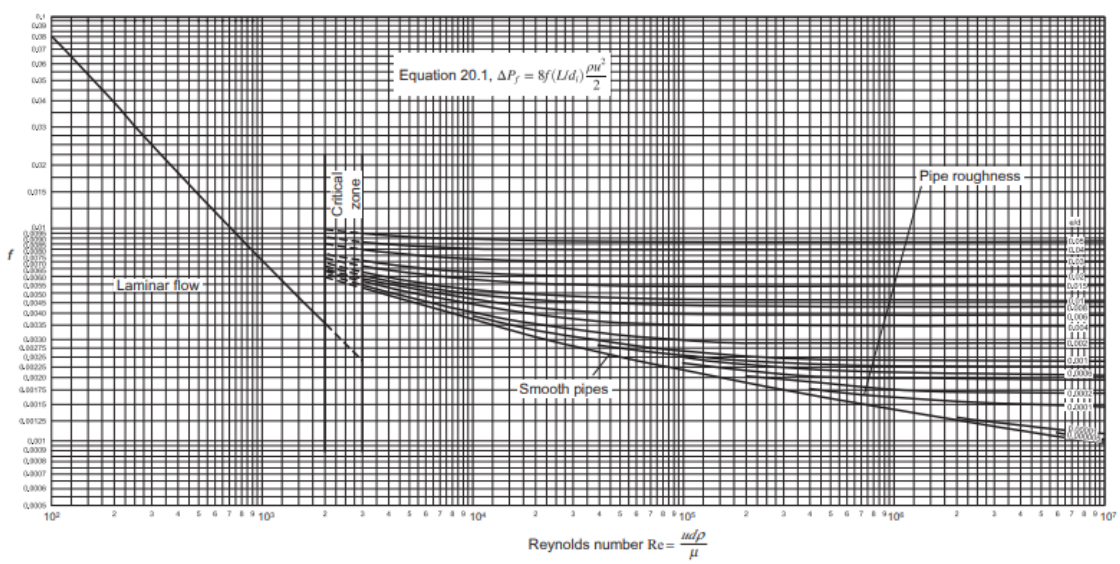

FIGURE 20.5

Pipe friction versus Reynolds number and relative roughness.

Figure 488 Pipe frction versus Reynolds number and relative roughness (Nelson, 1968)

$$Total\ equivalent\ pipe\ diameters = [(30x3) + 450 + 20]x0.105 = 58.87m$$
$$Total\ in\ pressure\ loss = (58.87m)x(0.105m) = 6.181$$
$$Total\ length\ for\ delta\ P = 6.181 + 20m = 26.18m$$

Now that the actual length of the pipe was calculates, the pressure drop can be found using the following calculations:

$$\Delta P_f = 4(0.018)\left(\frac{26.18\,m}{0.105m}\right)\left(\frac{1000kg}{m3}\right)\left(\frac{2m}{s}\right)^2 = 163788.8\frac{N}{m2} = 163kPa \tag{41}$$

$$W = g\Delta z + \frac{\Delta P}{\rho} - \frac{\Delta P_{total}}{\rho} \tag{45}$$

$$W = \left(\frac{9.8m}{s2}\right)(5m) + 0 - \frac{163788.8\frac{N}{m2}}{\frac{1000kg}{m3}} = -114.8\,J/kg$$

Since the stream is water, a pump is used for liquids. The power of the pump required is calculated as follows:

$$P = \frac{W\ x\ Q}{\eta} \tag{46}$$

$$P = \frac{-114.8\,J/kg\ x\ 17.36\,kg/s}{0.7} = 2847.04\,Watts = 3.8\,hp$$

15.10 Compressor Design Sample Calculation

$$-W = Z\frac{RT_1}{M_W}\left(\frac{n}{n-1}\right)\left[\left(\frac{P2}{P1}\right)^{\frac{(n-1)}{n}} - 1\right] \tag{47}$$

$$n = \frac{1}{1-m} \tag{48}$$

$m = \frac{\gamma-1}{\gamma E_p}$ for compression

$m = \frac{(\gamma-1)E_p}{\gamma}$ for expansion

E_p= polytropic efficiency which can be obtained from the figure below.

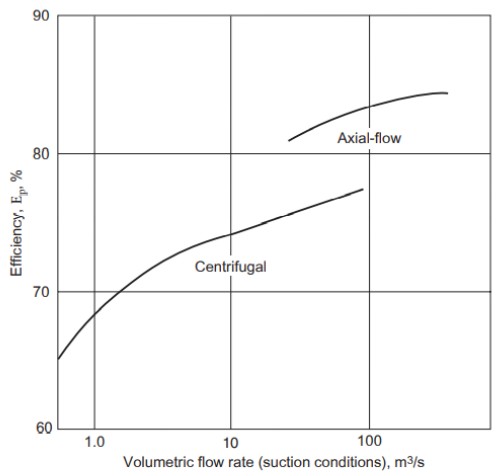

FIGURE 20.8

Approximate polytropic efficiencies of centrifugal and axial-flow compressors.

Figure 49 Approximate Polytropic Efficiency (Towler et al., 2013)

To find the compressibility factor, the reduced pressure and reduced temperature values must be calculated. Sample calculations were prepared for stream 17 (steam entering the distillation column). To find the polytropic coefficient for a gas experiencing compression using the ratio of specific heat of steam is 1.3, the calculations are as shown below. The efficiency (E_p) was 0.69 for a volumetric flowrate of 0.475 m^3/s.

$$m = \frac{1.3 - 1}{1.3(0.67)} = 0.344$$

$$n = \frac{1}{1 - 0.344} = 1.52 \qquad (48)$$

The critical temperature and pressure of steam are 647.14K and 218.31atm, respectively (source). The ratio of specific heat of steam is 1.3 (Perry et al., 1997)). The operating temperature of steam is 552.4K with a pressure of 9.8atm. The reduced temperature and pressure are calculated as follows:

$$T_R = \frac{T}{T_c} = \frac{552.4K}{647.14K} = 0.85 \qquad (52)$$

$$P_R = \frac{P}{P_c} = \frac{6.9\ atm}{218.31\ atm} = 0.03 \qquad (53)$$

Now that the reduced temperature and pressure are known, figure 44 can be used to find the compressibility factor.

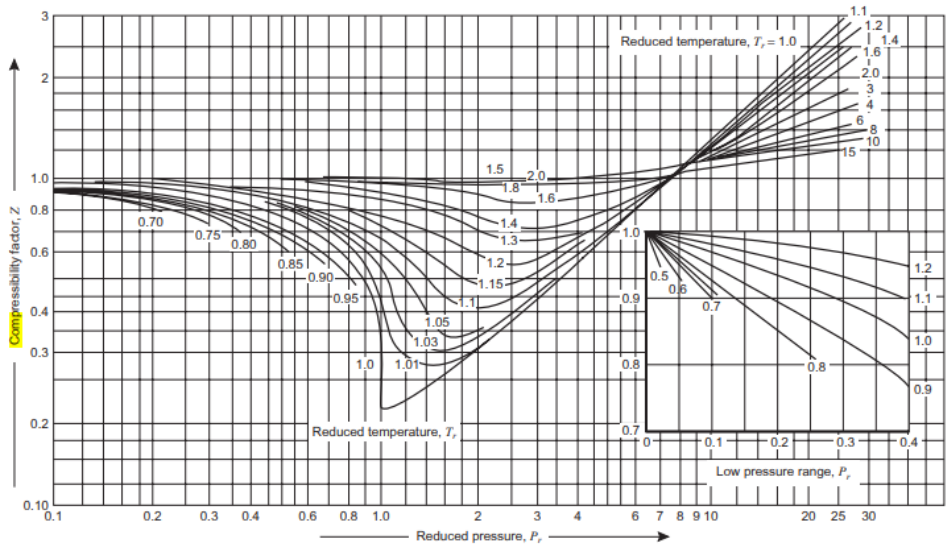

Figure 50 Compressibility of Gases and Vapors (Towler et al., 2013)

From figure 49, the compressibility factor is 1. The work can now be calculated since all parameters are known. The work results are as shown below.

$$-W\ (polytropic) = (1)\frac{\left(\frac{8314\,J}{kmol\ K}\right)(552.4K)}{18\frac{kg}{kmol}}\left(\frac{1.52}{1.52-1}\right)\left[\left(\frac{9.8}{6.9}\right)^{\frac{(1.52-1)}{1.52}}-1\right] = 95115.5\frac{J}{kg} = 95.11KJ/kg \tag{47}$$

$$Actual\ work\ required = \frac{polytropic\ work}{\mathrm{E}_p} = \frac{\frac{95.11kJ}{kg}}{0.67} = 141.96\frac{kJ}{kg} \tag{54}$$

$$Power = 141.96\frac{kJ}{kg}x\ 116524\frac{kg}{day}\ x\ \frac{1\ day}{86400\ sec} = \frac{191.451kJ}{s} = 191.45kW \tag{55}$$

15.11 Fluidized Bed Design Sample Calculations

Thickness for the Hoop Stress,

$$t = \frac{P_i * D_i}{2SE - 1.2P_i} \quad (6)$$

Where,

Maximum allowable Pressure (P_i) = $1*10^6$ N/m^2

Reactor Diameter (D_i) = 0.5m

Join Efficiency (E) = 0.85

Maximum allowable stress for stainless steel (S)= $\frac{Stress}{safety\ factor} = \frac{210*10^6}{3.5} = 6 * 10^7\ N/m^2$ (56)

Hoop wall thickness = $\frac{1*10^6*0.5}{2*6*10^7*0.85-1.2*1*10^6} = 0.00496\ m = 4.96\ mm$ (6)

Thickness for the Longitudinal Stress,

$$t = \frac{P_i * D_i}{4SE + 0.8P_i} \quad (7)$$

Longitudinal wall thickness = $\frac{1*10^6*0.5}{4*6*10^7*0.85-0.8*1*10^6} = 0.00244\ m = 2.44\ mm$

Minimum Wall thickness = Hoop wall thickness + Longitudinal wall thickness (57)

Minimum Wall thickness = (4.96 + 2.44) mm = 7.4 mm

7.3.2 Design of Distributor Plate

Density of the sand and biomass particle(ρ_c)= (1500+1560)/2 = 1530 Kg/m^3

Steam Density (ρ_g)= 1.225 kg/m^3

Coarse sand diameter (d_p)= 0.00025 m

Voidage(ψ) = 0.5

Acceleration due to gravity (g) = 9.8 m/s^2

Viscosity of fluid (u) = 0.000034 kg/m.s

Gravitational term (n) = $g(\rho_c - \rho_g)$ = 9.8(1530-1.225) = 14687.99

Porosity of bed at minimum fluidization

$$(\varepsilon_{mf}) = 0.586\ \psi^{-0.72}\left(\frac{\mu^2}{\rho g * n * dp^3}\right)^{0.029}\left(\frac{\rho g}{\rho c}\right)^{0.021} \quad (9)$$

$$(\varepsilon mf) = 0.586\ 0.5^{-0.72}\left(\frac{\mu^2}{\rho g * n * dp^3}\right)^{0.029}\left(\frac{\rho g}{\rho c}\right)^{0.021}$$

$$(\varepsilon_{mf}) = 0.709$$

Gas velocity at minimum fluidization

$$(u_{mf}) = \frac{(\psi * d_p)^2}{150u} g(\rho c - \rho g)\left(\frac{\varepsilon mf^3}{1-\varepsilon mf}\right) \quad (10)$$

$$(u_{mf}) == \frac{(0.5*0.00025)^2}{150*0.000034} * 14687.99 * \left(\frac{0.709^3}{1-0.709}\right)$$

$$(u_{mf}) == 0.05508 \text{ m/s}$$

7.3.4 Superficial velocity(u_s)

Terminal velocity for the bed reactor = $\frac{g(\rho c - \rho g)\ \ d_p^2}{18u}$ (11)

$$= \frac{9.8(1530 - 1.225)\ \ 0.00025^2}{18*0.000034}$$

=1.5 m/s

Initial bubble size (d_o) = $0.00376(u_o-u_{mt})^2$ = 0.00376 *$(0.0550-0.119)^2$ = $1.78*10^{-5}$ m (12)

Assumed bubble size (d_b) = 0.001 (13)

bubble size at the bottom (d_{bm}) = $0.652[A_o(u_o-u_{mt})]^{0.4}$=0.652[0.0078*(0.0550-0.119)]$^{0.4}$=0.03139 m (14)

$d_{bavg}=d_{bm}-(d_{bm}-d_{b0})\ e^{-0.3h/D_t} = 0.03139 -(0.03139 -1.78*10^{-5})\ e^{-0.3*25/0.1} = 0.031396$ m (15)

Height of freeboard space

$$d_b = \frac{0.54(u-u_{mb})^{0.4}\left(h+4\sqrt{A}\right)^{0.8}}{g^{0.2}} \quad (16)$$

$$h = \sqrt[0.8]{\left(\frac{d_b\ g^{0.2}}{0.54(u-u_{mb})^{0.4}}\right)} - 4\sqrt{A} \quad (58)$$

$$h = \sqrt[0.8]{\left(\frac{0.031396*\ 9.8^{0.2}}{0.54(0.1-0.05508)^{0.4}}\right)} - 4\sqrt{0.196} = 0.565 \text{ m}$$

7.4.5 Bed Pressure Drop

$\Delta p = hp(1-\mathcal{E})\ g(\rho_c - \rho_g) = 0.8*(1-0.5)*9.8*(1580-1.225) = 5654.8\ N/m^2$ (17)

Distributor plate pressure drop

$$(\Delta p_d) = 0.3*\ \Delta p = 0.3*5654.8 = 1696.46\ N/m^2 \quad (59)$$

Gas velocity through orifices:

$$u_0 = C_D * \frac{[2*\Delta p_D]^2}{\rho} = 0.8 * \frac{[2*1696.46]^2}{1.2} = 42.1 \text{ m/s} \quad (18)$$

Triangular pitch

$$P = \sqrt{\left(\frac{2}{N\sqrt{3}}\right)} \quad (19)$$

$$P = \sqrt{\left(\frac{2}{336\sqrt{3}}\right)} = 58.66 \text{ mm}$$

$$d_n > \sqrt{n * d_0} \quad (20)$$

$$d_n > \sqrt{0.003 * 3} = 5.19 \text{ mm}$$

The nozzle diameter was calculated to be higher than 5.19 mm, so a safe 10 mm diameter nozzle was selected to distribute the fluidizing gas for the bed. The thickness of the distributor plate was decided with the corrosion allowance of 63% of the total thickness used in the reactor. The distributor plate nozzle thickness is about 0.2mm to withstand the hoop and longitudinal stress from the velocity of the fluidizing gas.

7.4.6 Diffusion and Mass Transfer Analysis

The mass transfer and reaction parameters somewhat show the process in the fluidized bed reactor using the following equation:

$$K_{bc} = 4.5\left(\frac{u_{mf}}{d_b}\right) + \left(\frac{5.85\left(D_{AB}^{\frac{1}{2}} g^{\frac{1}{4}}\right)}{d_b^{\frac{5}{4}}}\right)$$

$$K_{bc} = 4.5\left(\frac{0.055}{0.03}\right) + \left(\frac{5.85\left(0.00000006^{\frac{1}{2}} * 9.8^{\frac{1}{4}}\right)}{0.03^{\frac{5}{4}}}\right) = 8.08 \text{ s}^{-1}$$

$$K_{ce} = 6.78\left(\frac{E_{mf} D_{AB} u_b}{d_b^3}\right)^{\frac{1}{2}}$$

$$K_{ce} = 6.78\left(\frac{0.708 * 0.0000006 * 0.4586}{0.0314^{0.5}}\right)^{\frac{1}{2}} = 0.17 \text{ s}^{-1}$$

To find the overall mass transfer coefficient in the bubbling fluidized reactor, the mass transfer coefficient between the bubble-cloud and cloud-emulsion was calculated. These values help determine the overall mass transfer coefficient to be 1.18.

Table 58 Assumptions Used for Reactor Design Calculations

Parameter	Value
Diameter of the reactor, D (Assumed)	0.5m
Initial Height of the sand	0.1 m
Initial Height of the sand	0.67m
Initial Height of the particle	0.77m
Density of the gas	1.225m
Density of the Sand	1500 kg/m^3
Density of the particles (Sand + biomass)	1530 kg/m^3
Diameter of particle coarse sand	0.00025 m
Acceleration due to gravity	9.81 kg/m^3
Dynamic viscosity	$3.4*10^{-5}$ kg/ms
Natural porosity of sand	0.5

Table 59 Calculated Values for Reactor Design

Parameter	Value
Diameter of the reactor	0.5m
Height of reactor	2.411 m
Residence time	10 sec
Bed Pressure Drop	5654.87 N/m^2
Superficial velocity	0.1 m/s
Number of orifices	13
Reactor vessel thickness	7.4 mm
Distributor plate thickness	7.48mm
Jet height for the orifice	20.93 mm
Minimum nozzle height	0.072 m
Distributor plate nozzle thickness (Safe resistant)	1.79 mm
Overall transport coefficient	1.18
Conversion	0.99

15.12 Distillation and Stripping Design Sample Calculations

$Crude\ Oil = 1690.5 \frac{kg}{day}$

$Bio\ Gas = 433.27 \frac{kg}{day}$

$Bottoms\ Product\ (Reduced\ Crude) = 624.71 \frac{kg}{day}$

$Distillate\ Product: Gasolone\ = 452.86 \frac{kg}{day}$

$Distillate\ Product: Naptha = 95.13 \frac{kg}{day}$

$Distillate\ Product: Kerosene\ = 337.96 \frac{kg}{day}$

$Distillate\ Product: Gas\ Oil\ = 179.11 \frac{kg}{day}$

$Number\ of\ Trays = 29$

$Relux\ Rate\ = 1.2$

Vapor and Liquid Flow Rate Calculations (Towler et al., 2013)

$$\boldsymbol{Overall\ Mass\ Balance = F = B + D}$$

Above Feed

$$Vapor\ Rate = (Total\ Distillate)(1 + Reflux\ Ratio) \tag{60}$$

$$Vapor\ Rate = (1065.06\ kg/day)(1 + 1.2)$$
$$Vapor\ Rate = 2343.132\ kg/day$$

$$Liquid\ Rate\ Above\ Feed = (Total\ Distillate)(Reflux\ Ratio) \tag{61}$$

$$Liquid\ Rate = (1065.06)(1.2)$$
$$Liquid\ Rate = 1278.072 kg/day$$

Below Feed

$$Liquid\ Rate\ Below\ Feed = (\ Crude\ Oil + Liquid\ Rate\ Above\ Feed) \tag{62}$$

$$Liquid\ Rate = \left(1690.5 \frac{kg}{day} + 1278.072 \frac{kg}{day}\right) = 2968.572 \frac{kg}{day}$$

$$Vapor\ Rate\ = (\ Liquid\ Rate\ Below\ Feed -\ Bottom\ Product) \tag{63}$$

$$Vapor\ Rate\ = \left(2968.572\frac{kg}{day} - 624.71\frac{kg}{day}\right) = 2968.572\frac{kg}{day}$$

<u>Sizing Column</u>

$Efficency = 0.6$
$Number\ of\ Stages\ = 29$

Bottoms Product (Nelson, 1968)
$\rho_v = 2.5\ kg/m^3$
$\rho_l = 800\ kg/m^3$
$MW_B = 228\ g/mol$
$\xi_B = d = 34\ dynes/cm$

Average Top Product Properties (Nelson, 1968)
$\rho_v = 3.9\ kg/m^3$
$\rho_l = 711\ kg/m^3$
$MW_B = 114\ g/mol$
$\xi_B = 26\ dynes/cm$

Find Liquid Vapor Flow Factor:

$$F_{LV} = \frac{L_w}{V_w}\sqrt{\frac{\rho_v}{\rho_L}} \tag{64}$$

Where:

F_{LV}- Liquid Vapor Flow Factor, L_w = Liquid mass flow Rate kg/day, V_w- Vapor mass flow rate kg/day, ρ_v Density of Vapor, ρ_L Density of Liquid

$$F_{LV\ Bottom} = \frac{2343.862}{2968.572}\sqrt{\frac{2.5}{800}}$$
$$F_{LV\ Bottom} = 0.07081$$
$$F_{LV\ Top} = \frac{1278.072}{2343.132}\sqrt{\frac{3.9}{700}}$$
$$F_{LV\ Top} = 0.04039$$

Refer to Fig 50

$$Plate\ Spacing = 0.5m$$
$$Bottom\ K1 = 0.06$$
$$Top\ K1 = 0.08$$
$$Correction\ of\ K1 = \left(\frac{\sigma}{20}\right)^{0.2} \times K1$$

$$Correction\ of\ K1\ Bottom = \left(\frac{34}{20}\right)^{0.2} \times 0.06 = 0.026$$

$$Correction\ of\ K1\ Top = \left(\frac{26}{20}\right)^{0.2} \times 0.08 = 0.0335$$

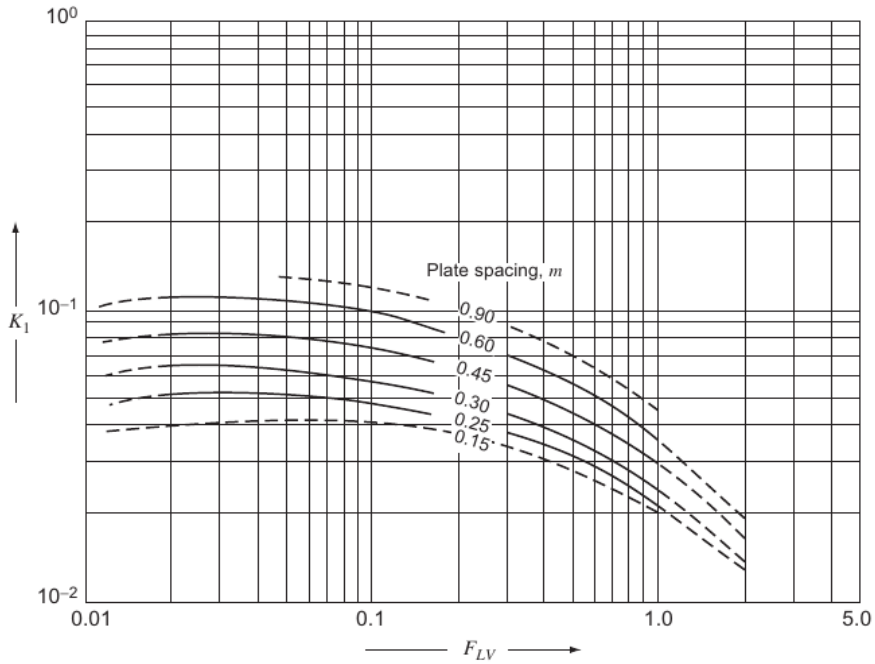

Figure 51 The K1 Values Based on Plate Spacing and Flv (Towler et al., 2013)

Calculate Flooding Velocity:

$$u_f = K_1 \sqrt{\frac{\rho_L - \rho_V}{\rho_V}} \tag{29}$$

K_1 Constant obtained from graph in Figure 51.

$$u_{f\ Bottom} = 0.026 \sqrt{\frac{800 - 2.5}{2.5}} = \mathbf{0.474\ m/s}$$

$$u_{f\ Top} = 0.0335 \sqrt{\frac{711 - 3.9}{3.9}} = \mathbf{0.4519\ m/s}$$

Assume 85% Flooding Velocity of Maximum Flow Rate:

$$u_{f\ Bottom} = 0.474 \frac{m}{s} \times 0.85 = 0.403 \frac{m}{s}$$

$$u_{f\ Top} = 0.4519\frac{m}{s} \times 0.85 = 0.38415\frac{m}{s}$$

Maximum Flow Rate:

$$V_{flowrate} = \frac{Mass\ Flow\ Rate}{Density}$$

$$V_{flowrate\ top} = 0.06779\frac{m^3}{s}$$

$$V_{flowrate\ bottom} = 0.5762\frac{m^3}{s}$$

Required Area:

$$Area = \frac{V_{flowrate}}{u_f} \tag{65}$$

$$Area_{bottom} = \frac{0.06779}{0.403} = 0.1681\ m^2$$

$$Area_{top} = \frac{0.5762}{0.38415} = 1.6550\ m^2$$

First Trial of Downcomer take as 12% of Total Area

$$Bottom = \frac{0.1681}{0.88} = 0.19106\ m^2$$

$$Top = \frac{1.655}{0.88} = 1.8806 m^2$$

Column Diameter

$$D = \sqrt{\frac{(A \times 4)}{\pi}} \tag{31}$$

$$D_{bottom} = \sqrt{\frac{(0.041 \times 4)}{\pi}} = 0.22m$$

$$D_{Top} = \sqrt{\frac{(1.8806 \times 4)}{\pi}} = \mathbf{1.5474m}$$

Chosen Diameter will be targeted to cater to the top of the column with a diameter of around 1.547m.

<u>Provisional Plate Design</u>

$$Chosen\ Diameter\ (D_c) = 1.5474m$$
$$Column\ Area\ \ (A_c) = 1.8806\ m^2$$

$$Downcomer\ Area\ (A_d) = 1.8806\ \times 0.12 = 0.2256\ m^2 \tag{66}$$

$$Net\ Area\ (A_n) = A_c - A_d \tag{67}$$

$$Net\ Area\ (A_n) = 1.8806 - 0.2256 = 1.6549\ m^2$$

$$Active\ Area\ (A_a) = A_c - 2A_d \tag{68}$$

$$Active\ Area\ (A_a) = 1.8806 - (2 \times 0.2256) = 1.4292\ m^2$$

For Trial 1, Take Hole Area 10%

$$Hole\ Area\ (A_h) = (A_a \times 0.1) = 0.142\ m^2 \tag{69}$$

Weir Length

$$\frac{(A_d)}{(A_c)} = \frac{0.22568}{1.8806} \times 100\% = 12\ \% \tag{70}$$

Refer to Fig 52 (Towler et al., 2013)

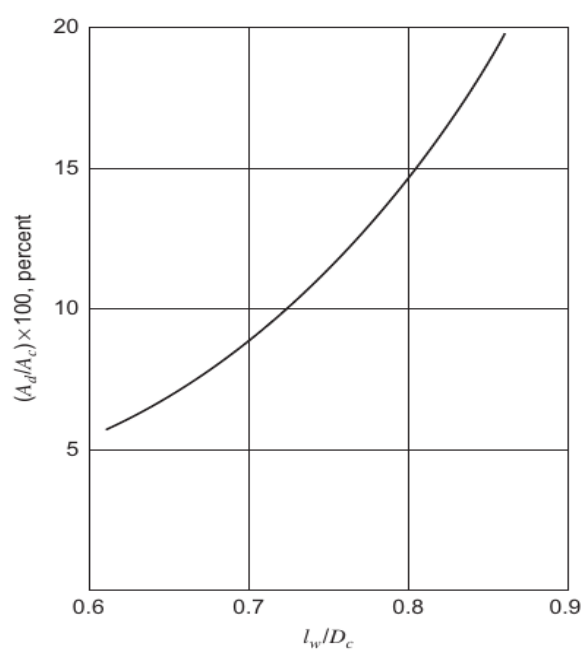

Figure 52 Weir Length to Column Diameter Ratio Based on Area % (Towler et al., 2013)

$$\frac{I_w}{D_c} = 0.76$$

$$Weir\ Length\ (I_W) = D_c \times \frac{I_w}{D_c} = 1.5474m\ \times 0.76 = 1.176\ m \tag{71}$$

$$Weir\ Width\ (I_{wi}) = 0.005\ m$$
$$Plate\ Thickness\ (P_t) = 0.005\ m$$
$$Weir\ Height\ (I_H) = 0.05\ m$$

<u>Check for Weeping</u>

$$Maximum\ Liquid\ Feed\ Rate = Mass\ Flow\ Rate\ of\ Liquid\ at\ Bottom \tag{72}$$
$$Maximum\ Liquid\ Feed\ Rate = 0.03435\frac{kg}{s}$$

Minimum liquid rate at 70% Turndown

$$Minimum\ Liquid\ Feed\ Rate = 0.03435 \times 0.7 = 0.024\frac{kg}{s}$$
$$h_{ow} = 750\ \frac{L_w}{\rho_L I_W}^{2/3} \tag{33}$$

$$h_{ow\ maximum} = 750\ \frac{0.3435\frac{kg}{s}}{800 \times 1.176\ m}^{2/3} = 8.2541\ mm\ Liquid$$
$$h_{ow\ minimum} = 750\ \frac{0.024\frac{kg}{s}}{800 \times 1.176\ m}^{2/3} = 6.5076\ mm\ Liquid$$

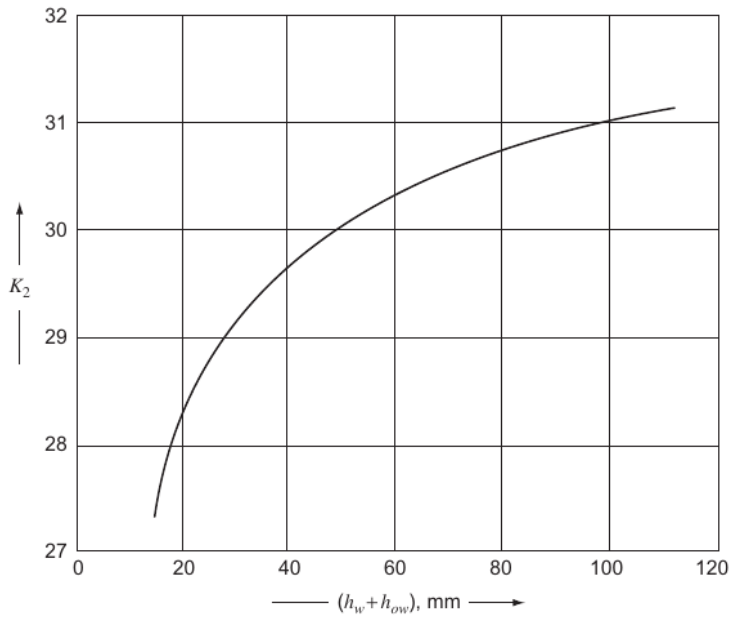

Figure 53 K2 Value for Weeping Based on Weir Length (Towler et al., 2013)

$$At\ Minimum\ Rate = h_{ow\ minimum} + I_H = 6.5076 + 50 = \mathbf{56.073mm\ Liquid}$$

$$K_2 = 32$$

$$u_h = \frac{(K_2 - 0.90\ (25.4 - d_h))}{\rho_v{}^{1/2}} \tag{32}$$

$$u_h = \frac{\left(32 - 0.90\ (25.4 - 5)\right)}{2.5^{\frac{1}{2}}} = \mathbf{8.6266}\frac{\boldsymbol{m}}{\boldsymbol{s}}$$

Reduce the hole to 7% of active area:

$$Active\ Area\ (A_a) = (A_a \times 0.07) = \mathbf{0.0265\ m^2} \tag{73}$$

$$New\ Actual\ Minimum\ Vapor\ Velocity = \frac{Minimum\ Liquid\ Rate\ \times Minimum\ vapor\ Flow\ Rate}{Active\ Area} \tag{74}$$

$$New\ Actual\ Minimum\ Vapor\ Velocity = \mathbf{0.4743}\frac{\boldsymbol{m}}{\boldsymbol{s}}$$

<u>Plate Pressure Drop</u>

Maximum Vapor Velocity through Holes:

$$u_{h\ max} = \frac{u_{f\ Bottom}}{A_a} = 0.6776\ \frac{m}{s} \tag{75}$$

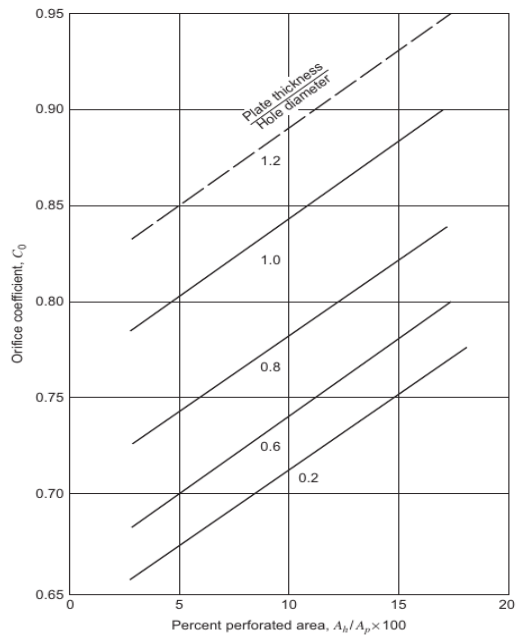

Figure 54 Orifice Coefficient Based on Percent Perforated Area (Towler et al., 2013)

With Percent Perforated Area being 7% and the plate thickness/hole diameter being 1, refer to FIG 53

$$C_0 = 0.82$$

Dry Plate Drop

$$h_d = 51\ \frac{{u_h}^2}{C_0}\ \frac{\rho_V}{\rho_L} \tag{76}$$

Where the h_d is dry plate drop,

$$h_d = 51\ \frac{0.6776^{\ 2}}{0.82}\ \frac{2.5}{800}$$
$$h_d = 0.108848\ mm$$

Residual Head

$$h_r = 12.5 \times 10^3\ \frac{{u_h}^2}{C_0}\ \frac{\rho_V}{\rho_L} \tag{77}$$

$$h_r = 12.5 \times 10^3 \frac{0.6776}{0.82}^2 \frac{2.5}{800} = 21.876mm$$

Total Head

$$h_t = h_d + h_r + h_{ow\ maximum} + I_H \tag{78}$$

$$\boldsymbol{h_t = 80.23mm}$$

<u>Downcomer Liquid Backup</u>

Area under apron

$$A_{ap} = I_{wi} \times h_{ap} = 0.04m \times 1.176m = 0.04725m^2 \tag{79}$$

Downcomer Head Loss

$$h_{dc} = 166 \left(\frac{L_{wd}}{\rho_L A_w}\right)^2 = 166 \left(\frac{0.0342}{800 \times 0.04725}\right)^2 = 0.00138mm \tag{80}$$

$$h_{bc} = (h_w + h_{ow\ maximum}) + h_t + h_{dc} = \boldsymbol{138.49mm} \tag{81}$$

Residence Time

$$t_r = \left(\frac{A_d h_{bc}\, \rho_L}{L_{wd}}\right) = 727.7\ s \tag{82}$$

<u>Check Entertainment</u>

$$u_v = \frac{V_{flowrate\ top}}{A_{net}} = 0.0409 \frac{m}{s} \tag{83}$$

$$\%\ Flooding = \frac{u_v}{u_f} = \boldsymbol{52.3\%} \tag{84}$$

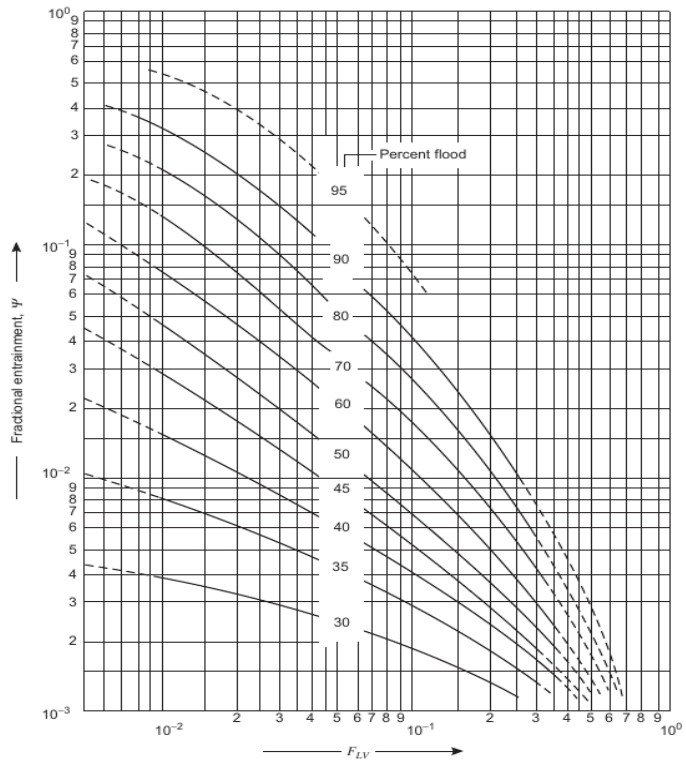

Figure 55 Fractional Entrainment Based on Flv (Towler et al., 2013)

Refer to Fig 55 $\boldsymbol{Entrainment\ \psi = 0.004}$

<u>Number of Holes</u>

Area of one Hole

$$A_H = \frac{\pi d^2}{4} = 1.96 \times 10^{-5}\ m^2 \tag{85}$$

Number of Holes:

$$Number\ of\ Holes = \frac{A_a}{A_H} = \mathbf{5097.9\ Holes} \tag{86}$$

15.13 Condenser Design Sample Calculations

Heat Transferred from Vapor

$$H = \frac{Condensate\ Flow\ Rate}{3600}(H_{Gasoline} - H_{water}) \tag{87}$$

$$H = \frac{15.09\frac{kg}{hr}}{3600}\left(452.8\frac{kJ}{kg} - 120\frac{kJ}{kg}\right) = 13949\ W$$

$$Cooling\ Water\ Flow = \frac{Heat\ Duty\ Removed}{(T_2 - T_1)}\left(\frac{1}{C_{p\ water}}\right) \tag{88}$$

$$Cooling\ Water\ Flow = \frac{139494W}{(80°C - 15°C)}\left(\frac{1}{4.18\frac{kJ}{kgK}}\right) = 18.46\frac{kg}{hr}$$

<u>The mean Temperature Difference:</u>

$$\Delta T_{LM} = \frac{(T_1 - t_2) - (T_2 - t_1)}{In\ \frac{(T_1 - t_2)}{(T_2 - t_1)}} \tag{89}$$

Where ΔT_{LM} is the log mean temperature, T_1 and T_2 is the hot fluid inlet and outlet temperature respectively and t_1 and t_2 is the cold fluid inlet and out temperature respectively

$$\Delta T_{LM} = \frac{(141°C - 80°C) - (26°C - 15°C)}{In\ \frac{(141°C - 80°C)}{(26°C - 15°C)}} = \mathbf{26.85}\ °C$$

The Overall Heat Transfer Coefficient that is Assumed $U_{assumed}$ for this water to gasoline transfer is found to be around 20-88 Btu/hrft^2°F (Nelson, 1968), after a few trial-and-error calculations the assumed heat transfer coefficient was around 22 Btu/hrft^2°F, which is around 110 W/m^2°C

$$Required\ Area = \frac{Heat\ Removed}{\Delta T_{LM}} \times \frac{1}{U_{assumed}} \tag{90}$$

$$Required\ Area = \frac{13949W}{26.85} \times \frac{1}{110W/m^2°C} = 5.197\ m^2$$

<u>The Surface Area of One Tube</u>

Where the d_o of one tube is 20mm and the L is 4.88m. (Towler et al., 2013)

$$SA_{tube} = \pi \times d_o \times L \tag{91}$$

$$SA_{tube} = \pi \times 0.02m \times 4.88m = 0.306\ m^2$$

$$Number\ of\ Tubes\ = \frac{Required\ Area}{SA_{tube}} \tag{92}$$

$$Number\ of\ Tubes = \frac{5.197}{0.306} = \mathbf{16.950\ \ tubes}$$

Finding the Square Pitch on Figure 56 (Towler et al., 2013)

Triangular Pitch, $p_t = 1.25d_o$					
No. Passes	**1**	**2**	**4**	**6**	**8**
K_1	0.319	0.249	0.175	0.0743	0.0365
n_1	2.142	2.207	2.285	2.499	2.675
Square Pitch, $p_t = 1.25d_o$					
No. Passes	**1**	**2**	**4**	**6**	**8**
K_1	0.215	0.156	0.158	0.0402	0.0331
n_1	2.207	2.291	2.263	2.617	2.643

Figure 56 Pitch Values Based on Number of Passes in Condenser

$$Square\ Pitch = 1.25\ \times d_o \tag{93}$$

$$Square\ Pitch = 1.25\ \times 20mm = 25mm = 0.025m$$

Finding the Bundle Diameter D_b, Use the square pitch 2 number of passes.

$$D_b = \ d_o \times \left(\frac{Number\ of\ Tubes}{K1}\right)^{\frac{1}{n1}} \tag{34}$$

$$D_b = \ 20mm \times \left(\frac{16.90}{0.156}\right)^{\frac{1}{2.291}} = \ \mathbf{154mm}$$

Number of Tubes in the Center Row N_c

$$N_c = \frac{D_b}{square\ pitch} \tag{94}$$

$$N_c = \frac{0.154}{0.025} = \mathbf{6.191}$$

Find the Shell Side Heat Transfer Coefficient

Physical Properties:

$$\mu = 0.5\ mNs/m^2$$
$$\rho = 700\ kg/m^3$$
$$\kappa = 0.03\ W/m^2{}^\circ\mathrm{C}$$
$$Mean\ Vapor\ Tempreature\ = \mathbf{83.75}\ ^\circ\mathrm{C}$$

Vapor Density at Mean Temperature of 141℃ was found to be around 0.2 kg/m^3

$$\Gamma = \frac{\frac{MassFlowRate\ of\ Vapor}{Lenth\ of\ Tube\ \times 3600}}{Number\ of\ Tubes} \tag{95}$$

$$\Gamma = \frac{\frac{\frac{452.86kg}{day}}{4.88m \times 86400}}{Number\ of\ Tubes} = 5.31 \times 10^{-4}\frac{kg}{sm}$$

$$\mathrm{N}_r = \frac{2 \times N_c}{3} \tag{96}$$

$$\mathrm{N}_r = \frac{2 \times 6.191}{3} = 4.127$$

$$\mathrm{hc} = (0.95 \times \mathrm{N}_r)^{-1/6} \times \kappa \times \left(\frac{\rho_l(\rho_l - \rho_g) \times g}{\mu_l \Gamma}\right)^{1/3} \mathrm{N}_r{}^{-1/6} \tag{97}$$

$$\mathrm{hc} = (0.95 \times 4.127)^{-1/6} \times 0.03\ W/m^2{}^\circ\mathrm{C} \times \left(\frac{700\ kg/m^3(700\ kg/m^3 - 0.2\ kg/m^3) \times 9.81m/s^2}{0.5\ mNs/m^2\Gamma}\right)^{1/3} 4.127^{-1/6}$$

$$\mathrm{hc} = \mathbf{1316.38\ W/m^2}{}^\circ\mathrm{C}$$

Finding the Tube Side Heat Transfer Coefficient

Tube Cross Sectional Area

$$CA_{tube} = \frac{\pi \times {d_i}^2}{4} \times \frac{Number\ of\ Tubes}{Number\ of\ Passes} \tag{98}$$

$$CA_{tube} = \frac{\pi \times 0.0168m^2}{4} \times \frac{16.950}{2} = 9.3 \times 10^{-3}m^2$$

Density of Water at 15℃ is 989 kg/m^3

$$v_{tube} = \frac{\frac{Cooling\ water\ Flow}{\rho_{water} at\ 15℃}}{CA_{tube}} \tag{99}$$

$$v_{tube} = \frac{\frac{18.46\ kg/hr}{989\ kg/m^3}}{9.3 \times 10^{-3}m^2} = 0.0553\ m/s$$

$$\text{hi} = \left(\frac{4200 \times (1.35 + 0.02t)\ {v_t}^{0.8}}{{d_i}^{0.2}}\right) \tag{100}$$

$$\text{hi} = \left(\frac{4200 \times (1.35 + 0.02(47.5℃))0.0533m/s^{0.8}}{0.0168m^{0.2}}\right) = \mathbf{178.89\ W/m^2℃}$$

The Fouling Heat Transfer Coefficient will be 6000W/m^2℃ and the Thermal Conductivity of water will be 50 W/m^2℃ (Towler et al., 2013)

$$\frac{1}{U_0} = \frac{1}{h_0} + \frac{1}{h_{0d}} + \frac{d_o ln\left(\frac{d_o}{d_i}\right)}{2k_w} + \frac{d_o}{d_i} \times \frac{1}{h_{id}} + \frac{d_o}{d_i} \times \frac{1}{h_i} \tag{36}$$

$$\frac{1}{U_0} = \frac{1}{1316W/m^2℃} + \frac{1}{178.89W/m^2℃} + \frac{0.02ln\left(\frac{0.02}{0.0168}\right)}{2 \times 50\ W/m^2℃} + \frac{0.02m}{0.01668m} \times \frac{1}{6000W/m^2℃} + \frac{0.02m}{0.01668m} \times \frac{1}{178.89\ W/m^2℃}$$

$$\frac{1}{U_0} = \frac{0.00791}{\frac{W}{m^2℃}}$$

$$\boldsymbol{U_0 = 127.3\ /m^2℃}$$

Therefore, the calculated Overall Heat Transfer Coefficient from water to gasoline for cooling is found to be **127 W/m^2℃** which is very close to the estimated value. Thus, Calculated values are valid.

Finding the Shell Side Pressure Drop

Use A pull-through Floating Head

Selected Baffle Cut is 45% and Clearance Space is 0.095m (Towler et al., 2013)

$$Shell\ inner\ Diamter = D_b + 0.095m \tag{35}$$

$$Shell\ inner\ Diamter = 0.154m + 0.095m = 0.249m$$

$$\text{Cross Flow Area } A_s = \frac{(Square\ Pitch - outer\ Diameter) \times Shell\ inner\ Diamter \times bafflespacing}{square\ pitch} \tag{101}$$

$$\text{Cross Flow Area } A_s = \frac{(0.025 - 0.02) \times 0.249845 \times 0.249845}{0.025} = \mathbf{0.0574\ m^2}$$

Mass Flux

$$G_s = \frac{(Mass\ Vapor\ Flow)}{Cross\ Flow\ Area} = \frac{\frac{452.86kg}{day}}{0.0574\ m^2} = \frac{\mathbf{0.091kg}}{\mathbf{s\ \ m^2}} \tag{102}$$

Equivalent Diameter

Where p_t is the tube pitch

$$d_e = \frac{(127)}{d_o}({p_t}^2 - 0.785{d_0}^2) \tag{103}$$

$$d_e = \mathbf{19.74mm}$$

Vapor Viscosity is 9.65 x 10^{-7} kg/ms (Nelson, 1968)

$$Re = \frac{\rho v L}{\mu} = \frac{G_s}{d_e \mu} \tag{104}$$

$$Re = \frac{0.091kg/s}{0.01974m\ \times 9.65 \times 10^{-7}kg/ms} = 1802.53$$

Looking at Figure 56 J_h is around 0.06

$$v_{vapour} = \frac{G_s}{\text{Cross Flow Area } A_s} = 0.455 m/s \tag{105}$$

<u>Shell Side Pressure Drop</u>

$$Shell\ Side\ \Delta P = \left(\frac{\frac{8\ \times j_h \times Shell\ inner\ Diameter \times L}{d_e}}{\frac{baffle\ spacing}{2 \times {v_{vapour}}^2 \times \rho_{vapour}}} \right) \times \frac{0.5}{1000} \tag{106}$$

$$Shell\ Side\ \Delta P = \frac{\frac{8\ \times 0.06 \times 0.249m \times 4.88m}{0.0194\text{m}}}{\frac{0.249845}{2 \times 0.455^2 \times 0.2 kg/mm^3}} \times \frac{0.5}{1000} = \mathbf{11.85\ kPa}$$

<u>Tube Side Pressure Drop</u>

$$Re = \frac{\rho v d_i}{\mu}$$

$$Re = \frac{989 \frac{kg}{m^3} \times 0.0553\ m/s \times 0.0168m}{0.0006 kg/ms} = 1531.36$$

Looking at Figure 56 J_h is around 0.065

$$Tube\ Side\ \ \Delta P = \left(2 \times \frac{8\ \times j_h \times L}{d_e + 2.5} \times \rho \times v\right) \times \frac{1}{1000} \tag{107}$$

$$Tube\ Side\ \ \Delta P = \frac{2 \times 8\ \times 0.065 \times 4.88m \times 989 \frac{kg}{m^3} \times 0.0553\ m/s}{0.0194\text{m} + 2.5} \times \frac{1}{1000} = \mathbf{1.03\ kPa}$$

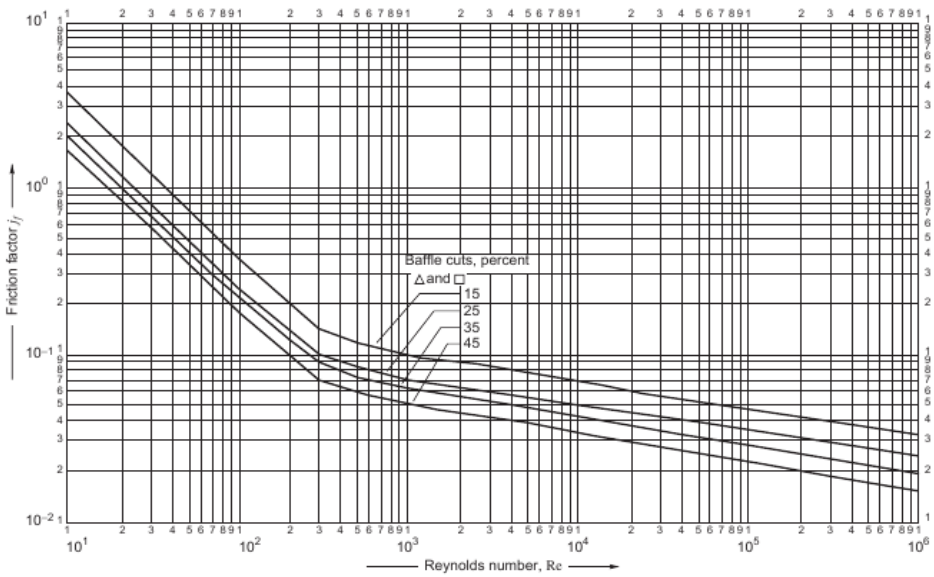

Figure 57 Friction Factor Based Re Number and Baffle Cut for Condenser (Towler et al., 2013)

15.14 Storage Tank Design Sample Calculation

To find the volume of the tank, the volumetric flowrate must be calculated. Using the mass flowrate and the density, the volumetric flowrate is found for Tank-5 that contains gasoline as follows:

$$V = \frac{m}{\rho} = \frac{362.33\ kg/day}{700\ kg/m^3} = 0.518\,\frac{m^3}{day} \tag{108}$$

Volume of a tank is calculated as follows:

$$V = 0.518\,\frac{m^3}{day} * 60\ days = 31.08\ m^3\ (bi - monthly) \tag{109}$$

Now to find the volume of the tank with overcapacity. Assuming the overcapacity is 20%, the new volume of the tank is as follows:

$$V = 31.08\ m^3 * 1.2 = 37.27\ m^3 \tag{110}$$

Assuming the height is the same as the diameter, the height and diameter of the tank can be found if the tank shape is a cylinder using the following equation.

$$V = \pi r^2 h = \frac{\pi d^2 h}{4} = \frac{\pi h^3}{4} \quad (111)$$

$$h = \left(\frac{4 * V}{\pi}\right)^{1/3} = \left(\frac{4 * 37.27\ m^3}{\pi}\right)^{1/3} = 13.19\ m \quad (112)$$

15.15 Toxic Dispersion Sample Calculation

Evaporation rate (Q_m) = $\frac{MKAP^{sat}}{R*T}$

= $\frac{0.000003*400*78.11*13998.9}{8.314*353.24}$ = 0.446788 kg/s = 446.788 g/s

mg/m^3 = C_{ppm}/0.3214 = 31.21 mg/m^3

$$\frac{mg}{m^3} = \frac{Q_m}{pi * \sigma_y \sigma_z} \qquad \frac{mg}{m^3} = \frac{Q_m}{pi() * \sigma_y \sigma_z} \quad (49)$$

$$\sigma_y \sigma_z = \frac{446.788}{pi(\quad) * 4.02 * 0.0311} = 200\ m^2$$

Using trial and error the downward wind was calculated to be 165 m

15.15 Risk Assessment Sample Probability Calculations

To find the total probabilities of each result in Event Tree 1 (Figure 37), the following calculations were made.

Continuous Operation= 0.855+ 0.0338 + 0.001125 = 0.8899 * 10^{-5} = 8.89x10^{-6} occurrences/year (51)

Shutdown= 0.094+ 0.00375 + 0.00125 = 0.099*10^{-5} = 9.9x10^{-7} occurrences/year

Gas Leakage to the Atmosphere= 0.00095+ 0.0000375 +0.00000125 = 0.0009888*10^{-5} = 9.9x10^{-9} occurrences/year

15.16 Economic Evaluation Sample Calculations

(113)

$$Total\ Loans\ Required = Total\ Capital\ Cost + Total\ Installation, shipping, and\ working\ capital + Total\ taxes\ and\ insurace$$

$$Total\ Loans\ Required = \$2{,}085{,}945 + 0.05(\$2{,}085{,}945) + 0.015(\$2{,}085{,}945)$$
$$Total\ Loans\ Required = \$2{,}223{,}096$$

$$Total\ Payment\ on\ Loan = \frac{a}{\frac{\{[(1+r)^n]-1\}}{[r(1+r)^n]}} \tag{114}$$

$$Total\ Payment\ on\ Loan = \frac{\$2{,}223{,}096}{\frac{\{[(1+0.0245)^{10}]-1\}}{[0.0245(1+0.0245)^{10}]}}$$
$$Total\ Payment\ on\ Loan = \$253{,}352.37$$

15.17 Quantification of Microplastics Calculation

Ashbridge Bay WWTP Mass Balance:

Average Daily Influent Flow rate in 2018:563.7 ML/day + 0.46 ML/day (transfer from North Toronto TP)

Total Solids Removed (2018): Grit Removal: 4.9 tonnes/day = 0.0049897 ML/day

Primary sludge: 5980 m^3/day = 5.98 ML/day

Total Daily Effluent after solids removal: 558.175 ML/day = 558175 m^3/day
(Ashbridges Bay Final Report, 2019)

Microplastics found in WWTP Effluent in Ontario: 13.3 particles/L =13300 particles/m^3
(Grbic et al., 2020)

Average Density of Microplastics: *1.078 g/cm^3 = 1078 kg/m^3*
(Everaert et al., 2018)

Volume of a cylinder (40% void fraction):
(Simon et al., 2018)

Average length of MP in effluent :1.2mm = 0.0012m
Average width of MP in effluent : 0.07mm = 0.00007m

$$V = \pi r^2 h \tag{115}$$

$$Where\ h = L\ \&\ r = \frac{w}{2},$$
$$V = \pi\ (0.000035m)^2(0.0012m)$$
$$V = 4.618x10^{-12}m^3x\ 0.6 = 2.77x10^{-12}m^3$$

Volume of an ellipsoid:

$$V = \frac{4}{3}\ \pi ab^2 \tag{116}$$

$$V = \frac{4}{3}\pi(0.0012)(0.000035)^2$$
Where a=length/2 and b=width/2
$$V = 6.157x10^{-12}\ m^3$$

Total mass of effluent: (90% microfibers, 10% other)
(Grbic et al., 2020)

$$M = 0.9(2.77x10^{-12})(1078) + 0.1(6.157x10^{-12})(1078) \tag{117}$$

$$M = 3.35x10^{-9}\ kg$$

Total volume of overflow: 15.4 particles/L microplastic contamination**,** 41% fibres, 59% other (Ashbridges Bay Final Report, 2019)

Particle size: avg length = 0.9 mm, avg width = 0.2 mm

$$\boldsymbol{Volume\ of\ cylinder} = \pi\ r^2h$$
$$= \pi\ (0.0009)(0.0001)^2$$
$$= 2.83x10^{-11}\ m^3$$
$$\boldsymbol{Volume\ of\ ellipsoid} = \frac{4}{3}\pi\ ab^2$$
$$= \frac{4}{3}\pi\ (0.0009)(0.0001)^2$$
$$= 3.77x10^{-11}\ m^3$$
$$\textbf{\textit{Total mass of overflow}} = 0.41(2.83x10^{-11})(1078) + 0.59(3.77x1^{-11})(1078)$$
$$= 3.65x10^{-8}\ kg$$

Mass of MP:

$$M(effluent) = (3.35x10^{-9}\ kg)(13300\ particles/m^3) \tag{118}$$
$$= 4.4555x10^{-5}\ kg/m^3$$
$$M(stormwater) = (3.65x10^{-8}\ kg)(15400\ particles/m^3)$$
$$= 5.621x10^{-4}\ kg/m^3$$

Quantity of MP:

$$Mass\ (effluent) = 4.455x10^{-5}\ kg/^{3}\ X\ 558175\ m^{3}/day = 24.87\ kg/day = 9077\ kg/year \quad (119)$$

$$Mass\ (stormwater) = 5.621X10^{-4}\ kg/m^{3}\ X\ 1556000\ m^{3}/year = 874.3\ kg/year$$

Total = 9952 kg/year

15.8 True Boiling Point Graphs for Crude Oil

The TBP charts that were compared in order to determine the number of trays in the distillation column based on the change of composition with temperature was based on Figure 57 and Figure58. Figure 57 displays the TBP data for an API of 43 and Figure 58 displays the TBP Data for an API of 41.7 (Liu, 2012).

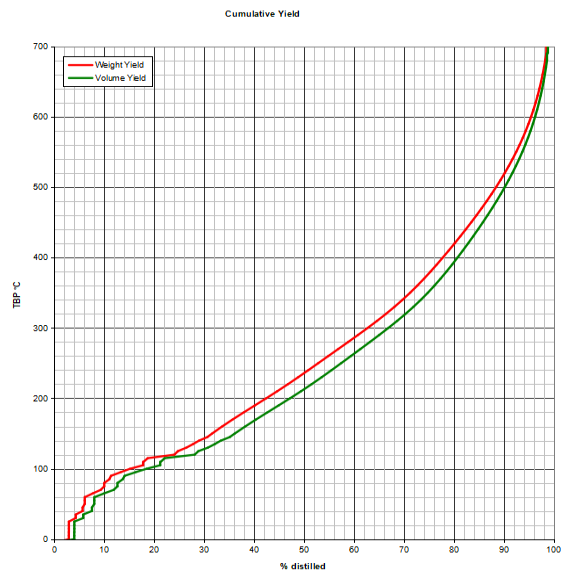

Figure 587 TBP Data Obtained For Crude oil of API 43 (Treese et al., 2015)

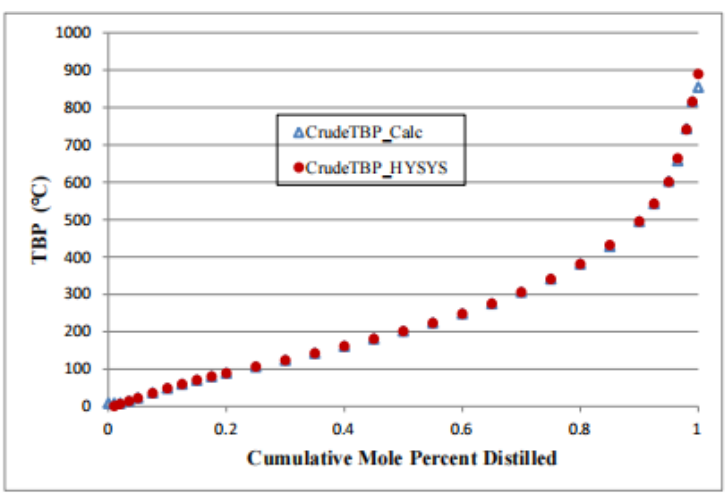

Figure 59 TBP Data For Crude Oil of 41.7 (Liu, 2012).